NORTH-WEST UNIVERSITY
YUNIBESITI YA BOKONE-BOPHIRIMA
NOORDWES-UNIVERSITEIT
POTCHEFSTROOMKAMPUS

The synthesis and evaluation of phenoxymethylcaffeine analogues as inhibitors of monoamine oxidase

Braam Swanepoel

B.Pharm

Dissertation submitted in partial fulfilment of the requirements for the degree Magister Scientiae in Pharmaceutical Chemistry at the North-West University, Potchefstroom Campus

Supervisor: Prof. J.P. Petzer

Co-supervisor: Prof. J.J. Bergh

Potchefstroom

2010

TABLE OF CONTENTS

LIST OF ABBREVIATIONS

6-OHDA	6-hydroxydopamine
ADH	aldehyde dehydrogenase
AOs	amine oxidases
CSC	(E)-8-(3-chlorostyryl)caffeine
DA	dopamine
DAT	dopamine transport system
EDAC	N-(3-dimethylaminopropyl)-N′-ethylcarbodiimide hydrochloride
EI	electron ionization
EIMS	electron impact ionization
FAD	flavine adenine dinucluetide
FDA	food and drug administration
GSH	glutathione
HPLC	high performance liquid chromatograms
HRMS	high resolution mass spectroscopy
IC_{50}	50% inhibitory concentration
LBs	Lewy bodies
MAO	monoamine oxidase
MAOs	monoamine oxidases
$MPDP^+$	1-methyl-4-phenyl-2,3-dihydropyridinium
MPP^+	1-methyl-4-phenylpyridinium
MPPP	1-methyl-4-phenyl-4-propionoxypiperidine

MPTP	1-methyl-4-phenyl-1,2,3,6-tetrahydropyridine
NAD	nicotinamide adenine dinucleotide
NADH	reduced nicotinamide adenine dinucleotide
NSAIDs	non-steroidal anti-inflammatory drugs
PD	Parkinson's disease
ppm	parts per million
QSAR	quantitative structure-activity relationship
ROS	reactive oxygen species
SEM	standard error of the mean
SI	selectivity index
SNpc	substantia nigia pars compacta
SSAOs	semicarbazide sensitive amine oxidases
TLC	thin layer chromatography
TPQ	topa-quinone
UV	Ultraviolet

ABSTRACT

Title

The synthesis and evaluation of phenoxymethylcaffeine analogues as inhibitors of monoamine oxidase.

Key words

Parkinson's disease, monoamine oxidase, substantia nigra, 8-benzyloxycaffeine, 8-(phenoxymethyl)caffeine, safinamide, (E)-8-(3-chlorostyryl)caffeine.

Purpose

Monoamine oxidase (MAO) plays a key role in the treatment of Parkinson's disease (PD), since it is the major enzyme responsible for the catabolism of dopamine in the substantia nigra of the brain. Inhibition of MAO-B may conserve dopamine in the brain and provide symptomatic relief. The MAO-B inhibitors that are currently used for the treatment of PD, are associated with a variety of adverse effects (psychotoxic and cardiovascular effects) along with additional disadvantages such as irreversible inhibition of the enzyme. Irreversible inhibition may be considered a disadvantage, since following treatment with irreversible inhibitors, the rate by which the enzyme activity is recovered may be variable and may require several weeks. In contrast, following the administration of reversible inhibitors, enzyme activity is recovered when the inhibitor is cleared from the tissues. There exists therefore, a need to develop new reversible inhibitors of MAO-B which are considered to be safer than irreversible MAO-B inhibitors.

Rationale

Recently discovered reversible MAO-B inhibitors include safinamide and (E)-8-(3-chlorostyryl)caffeine (CSC). Safinamide has a benzyloxy side chain, which is thought to be important for inhibition of MAO-B. CSC, on the other hand, consists of a caffeine moiety with a styryl substituent at C-8, which is also a critical feature for its inhibitory activity. In a previous study, the caffeine ring and the benzyloxy side chain were combined to produce a series of 8-benzyloxycaffeine analogues which proved to be potent new MAO-B inhibitors. In this study, caffeine was substituted with the phenoxymethyl functional group at C-8, instead of the benzyloxy moiety. The aim of this study was therefore to compare the MAO-B inhibition potencies of selected 8-(phenoxymethyl)caffeine analogues with the previously studied 8-benzyloxycaffeine analogues.

In the current study, 8-(phenoxymethyl)caffeine (**1**) and nine 8-(phenoxymethyl)caffeine analogues (**2**-**10**) were synthesized and evaluated as inhibitors of recombinant human MAO-A and –B. These analogues only differed in substitution on C3 and C4 of the phenoxymethyl phenyl ring. The substituents that were selected were halogens (Cl, F, and Br), the methyl group, the methoxy group and the trifluoromethyl group. These substituents are similar to those selected in a previous study where 8-benzyloxycaffeine analogues were evaluated as MAO inhibitors. This study therefore explores the effect that a variety of substituents on C3 and C4 of the phenoxymethyl phenyl ring will have on the MAO-A and –B inhibition potencies of 8-(phenoxymethyl)caffeine. Based on the results, additional 8-(phenoxymethyl)caffeine analogues with improved MAO-A and –B inhibition potencies will be proposed for investigation in future studies.

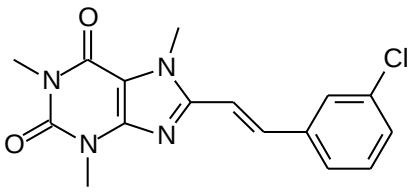

(E)-8-(3-Chlorostyryl)caffeine

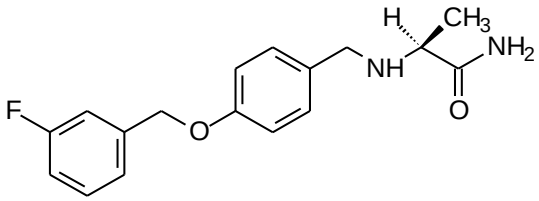

Safinamide

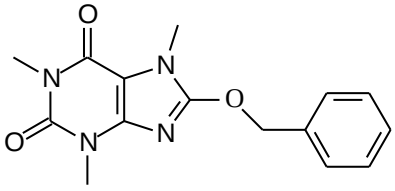

8-Benzyloxycaffeine

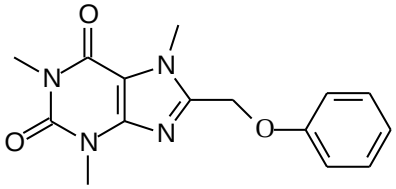

8-(Phenoxymethyl)caffeine

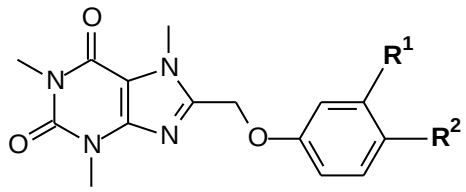

Compound.	R^1	R^2
1	H	H
2	Cl	H
3	Br	H
4	F	H
5	CF_3	H
6	CH_3	H
7	OCH_3	H
8	H	Cl
9	H	Br
10	H	F

Methods

The target, 8-(phenoxymethyl)caffeine, analogues were synthesized by reacting 1,3-dimethyl-5,6-diaminouracil with the appropriately substituted phenoxyacetic acid in the presence of a carbodiimide coupling agent. Ring closure was catalyzed in basic conditions and methylation of the resulting theophyline intermediates at C-7 was carried out with iodomethane. The structures and purities of all the target compounds were verified by NMR, MS and HPLC analysis.

All of the 8-(phenoxymethyl)caffeine analogues were subsequently evaluated as MAO-A and –B inhibitors using the recombinant human enzymes. The inhibition potencies of the analogues were expressed as the IC_{50} values (concentration of the inhibitor that produces 50% inhibition). In addition, the time-dependency of inhibition of both MAO-A and –B was evaluated for two inhibitors in order to determine if these inhibitors interact reversibly or irreversibly with the MAO isozymes. A Hansch-type quantitative structure-activity relationship (QSAR) study was carried out in order to quantify the effect that different substituents on the phenyl ring of the 8-(phenoxymethyl)caffeine analogues have on MAO-B inhibition activity.

Results

The results showed that among the test compounds, several analogues potently inhibited human MAO-B. The most potent inhibitor was 8-(3-bromophenoxymethyl)caffeine with an IC_{50} value of 0.148 µM toward human MAO-B. There were also inhibitors which displayed inhibition activities towards human MAO-A with IC_{50} values ranging from 4.59 µM to 34.0 µM. Compared to the 8-benzyloxycaffeine analogues, that were in general non-selective inhibitors, the 8-(phenoxymethyl)caffeine analogues, evaluated here, were selective for MAO-B. For example, 8-(3-bromophenoxymethyl)caffeine was found to be 141 fold more selective as an inhibitor of MAO-B than of MAO-A. Also, compared to the 8-benzyloxycaffeine analogues, the 8-(phenoxymethyl)caffeine analogues were slightly less potent MAO-B inhibitors. For example, 8-benzyloxycaffeine is reported to have an IC_{50} value of 1.77 µM for the inhibition of human MAO-B while 8-(phenoxymethyl)caffeine was found to have an IC_{50} value of 5.78 µM for the inhibition of human MAO-B. This study also shows that two selected analogues bind reversibly to MAO-A and –B, respectively, and that the mode of MAO-B inhibition is competitive for one representative compound.

Qualitative inspection of the results revealed interesting structure-activity relationships. For the 8-(phenoxymethyl)caffeine analogues, bearing both the C3 and C4 substituents on the phenyl ring, the MAO-B activity significantly increases with halogen substitution. Furthermore, increased MAO-B inhibition was observed with increased electronegativity of the halogen substituent. To quantify these apparent relationships, a Hansch-type QSAR study was carried out. The results showed that the logarithm of the IC_{50} values ($\log IC_{50}$) correlated with Hansch lipophilicity (π) and the Swain-Lupton electronic (F) constants of the substituents at C-3 of the phenoxymethyl ring. The correlation exhibited an R^2 value of 0.87 and a statistical F value of 13.6. From these results it may be concluded that electron-withdrawing substituents at C3 with a high degree of lipophilicity enhance MAO-B inhibition potency. These results are similar to those previously obtained for the series of 8-benzyloxycaffeine analogues. For this series, the MAO-B inhibition potencies correlated with the Hansch lipophilicity (π) and Hammett electronic (σ) constants of the substituents at C-3 of the benzyloxy ring. Similarly to the 8-(phenoxymethyl)caffeine analogues, electron-withdrawing substituents with a high degree of lipophilicity also enhance the MAO-B inhibition potencies of 8-benzyloxycaffeine analogues.

OPSOMMING

Titel

Die sintese en evaluering van fenoksiemetielkafeïenanaloë as inhibeerders van monoamienoksidase.

Kernwoorde

Parkinsonisme, monoamienoksidase, substantia nigra, 8-bensieloksiekafeïen, 8-(fenoksiemetiel)kafeïen, safienamied, (E)-8-(3-chlorosteriel)kafeïen.

Doel

Die ensiem, monoamienoksidase (MAO), speel 'n belangrike rol in die behandeling van Parkinson se siekte omdat dit in 'n groot mate verantwoordelik is vir die metabolisme van dopamien in die substantia nigra van die brein. Inhibisie van MAO-B vertraag dopamienmetabolisme in die brein en lei tot verligting van die simptome van Parkinson se siekte. Die MAO-inhibeerders wat tans gebruik word, veroorsaak ongewenste newe-effekte en veroorsaak ook onomkeerbare inhibisie van die ensiem. Onomkeerbare inhibisie kan as 'n nadeel beskou word, omdat die tempo van herstel van die ensiem baie stadig en wisselvallig kan wees. In teenstelling hiermee, herstel die ensieme sodra die inhibeerder uit die weefsels opgeruim is, in die geval van behandeling met omkeerbare inhibeerders. Om hierdie redes bestaan daar 'n behoefte vir die ontwikkeling van nuwe MAO-B-inhibeerders wat omkeerbaar is en veiliger is as onomkeerbare MAO-B inhibeerders.

Rasionaal

Safienamied en (E)-8-(3-chlorostyryl)kafeïen (CSC) is twee bekende, omkeerbare MAO-B-inhibeerders. Safienamied het 'n bensieloksiesyketting, wat belangrik geag word vir die inhibisie van MAO-B. CSC bestaan uit 'n kafeïenkern wat 'n stirielsyketting aan die C-8-koolstof bevat. Die stirielsyketting word as belangrik beskou vir die inhibisie van MAO-B. In 'n vorige studie is 'n reeks 8-bensieloksiekafeïenanaloë gesintetiseer wat beide die kafeïen- en bensieloksiegroep besit. Daar is vasgestel dat hierdie reeks hoogs potente MAO-B-inhibeerders is. In die huidige studie is die C-8-koolstof van die kafeïenkern met 'n fenoksiemetiel funksionele groep gesubstitueer. Die doel van die studie was dus om die inhibisiepotensie van die 8-(fenoksiemetiel)kafeïenanaloë te vergelyk met diè van die 8-bensieloksiekafeïene.

In die huidige studie is 8-(fenoksiemetiel)kafeïen (**1**) en nege 8-(fenoksiemetiel)kafeïen-analoë (2-10) gesintetiseer en gevalueer as MAO-A- en -B-inhibeerders deur van die

rekombinante menslike ensiem gebruik te maak. Die analoë verskil slegs ten opsigte van substitusie op die C-3 en C-4 van die fenoksiemetielfenielring. Die verskillende substituente waarop besluit is, was die halogene (Cl, F en Br), 'n metiel groep, 'n metoksie groep en 'n trifluorometiel groep. Hierdie substituente is dieselfde as diè wat in die vorige studie gebruikis, waar 8-bensieloksiekafeïenanaloë as MAO-inhibeerders geëvalueer is. Hierdie studie ondersoek dus die invloed wat 'n verskeidenheid substituente, op die C-3- en -4-posisies van die fenoksiemetielfenielring, sal hê, op hul vermoë om MAO-A en -B te inhibeer. Gebaseerop hierdie resultate, sal daar nuwe 8-(fenoksiemetiel)kafeïenanaloë, met beter inhibisie potensie gesintetiseer word in die toekoms.Hierdie resultate mag daartoe lei dat nuwe, 8-(fenoksiemetiel)kafeïenanaloë in die toekoms ondersoek kan word, wat as kragtiger MAO-A en -B-inhibeerders sal optree.

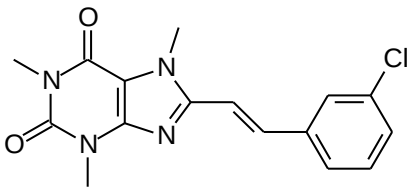

(E)-8-(3-Chlorostiriel)kafeïne

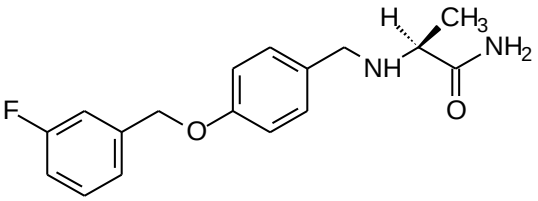

Safinamied

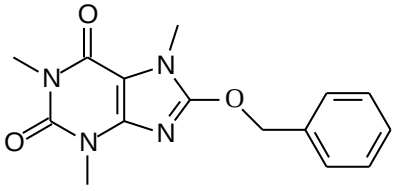

8-Bensieloksiekafeïen

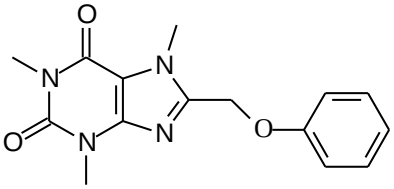

8-(Fenoksiemetiel)kafeïen

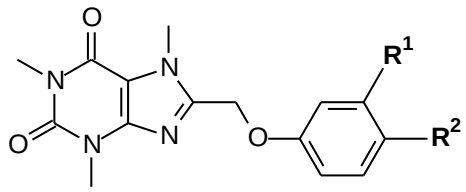

Produk.	R^1	R^2
1	H	H
2	Cl	H
3	Br	H
4	F	H
5	CF_3	H
6	CH_3	H
7	OCH_3	H
8	H	Cl
9	H	Br
10	H	F

Metode

Die 8-(fenoksiemetiel)kafeïenanaloë is gesintetiseer deur 1,3-dimetiel-5,6-diaminourasiel te laat reageer met die toepaslik-gesubstitueerde fenoksieasynsuur in die teenwoordigheid van karbodi-imied-koppelingsreagens. Ringsluiting is onder basiese kondisies bewerkstellig en metilering van die gevormde teofiliënderivate by C-7 is met jodometaan uitgevoer. Die strukture en suiwerheid van al die produkte is met KMR, MS en HPLC geverifieer.

Die 8-(fenoksiemetiel)kafeïenreeks is vervolgens as MAO-A- en -B-inhibeerders geëvalueer deur rekombinante menslike ensiem te gebruik. Die inhibisiepotensie van die analoë is weergegee as IC_{50}-waardes (konsentrasie van 'n inhibeerder wat 50% inhibisie veroorsaak). Hierbenewens is twee van die analoë ook geëvalueer vir tydsafhanklike inhibisie van beide die ensieme, om te bepaal of die analoë omkeerbaar of onomkeerbaar bind aan die MAO iso-ensiem. 'n Hansch-tipe kwantitatiewe struktuur-aktiwiteitsverwantskap-studie (QSAV) is gedoen om die effek van die verskillende substituente op die fenielring van die 8-(fenoksiemetiel)kafeïenanaloë te kwantifiseer ten opsigte van die MAO-B inhibisie aktiwiteit.

Resultate

Die resultate toon dat sommige van die analoë baie kragtige inhibeerders van menslike MAO-B is. Die mees potente MAO-B-inhibeerder was 8-(3-bromofenoksiemetiel)kafeïen, met 'n IC_{50}-waarde van 0.148 µM. Sommige van die analoë het MAO-A geïnhibeer met IC_{50}-waardes van 4.58 µM tot 34.0 µM, maar, in vergelyking met die 8-bensieloksiekafeienanaloë, wat nie-selektiewe inhibeerders was, was al die fenoksiemetiel)kafeïenanaloë selektief vir MAO-B. 8-(3-Bromofenoksiemetiel)kafeien was byvoorbeeld 141 meer selektief vir MAO-B as vir MAO-A. Die toetsverbindings was minder potente inhibeerders van MAO-B as die 8-bensieloksiekafeienanaloë. Die IC_{50}-waarde van 8-bensieloksiekafeïen, vir die inhibisie van MAO-B, was byvoorbeeld 1.77 µM, terwyl hierdie waarde vir 8-(fenoksiemetiel)kafeïen slegs 5.78 µM was. Daar is ook vasgestel dat die 8-(fenoksiemetiel)kafeïenanaloë omkeerbaar aan beide MAO-A en -B bind en dat die inhibisie kompeterend is.

Kwalitatiewe ondersoek van die resultate het interessante struktuuraktiwiteitsverwantskappe bloot gelê. Halogeensubstitusie op beide die C-3 en -4 posisies van die fenielring van die 8-(fenoksiemetiel)kafeïenanaloë het 'n dramatiese verhoging van MAO-B-aktiwiteitbewerkstellig. Verder is daar ook gevind dat hoe meer elektronegatief die halogeen, hoe beter die inhibisie. 'n Hansch-tipe QSAV-studie is uitgevoer om hierdie verwantskappe te kwantifiseer. Uit die resultate was dit duidelik dat daar 'n korrelasie was tussen die logaritme van die IC_{50}-waardes van die C-3 gesustitueerde fenoksiemetielanaloë en die Hansch-lipofilisiteit (π) en ook met die Swain-Lupton-konstante (F). 'n R^2-waarde van 0.87 en 'n statistiese F-waarde van 13.6 is vir hierdie korrelasie bereken. Uit hierdie resultate kan afgelei word dat 'n elektrononttrekkende groep op C-3, wat hoogs lipofiel is, die potensie van MAO-B-inhibisie sal verhoog. Hierdie resultate stem ook baie ooreen met dié van die 8-bensieloksiekafeïenanaloë. By laasgenoemde reeks, het die potensie van MAO-B-inhibisie gekorreleer met die Hansch-lipofilisiteit (π) en die Hammett elektoniese konstantes (σ) van die substituente op C-3 van die bensieloksiering. By die 8-bensieloksiekafeïenanaloë, het elektrononttrekkende substituente met 'n hoë lipofilisiteit ook hul vermoë verbeter om MAO-B te inhibeer, net soos by die 8-(fenoksiemetiel)kafeïenanaloë.

CHAPTER 1

Introduction

1.1 Parkinson's disease

Parkinson's disease (PD), first described by James Parkinson in 1817, is a progressive neurodegenerative disorder that affects movement, muscle control and balance as well as numerous other functions. It is normally associated with the elderly and leads to a lowered life quality without being fatal. It is part of a group of conditions known as motor systems disorders (Youdim *et al*., 2006).

The neurodegeneration experienced in PD is caused by a loss of nigrostriatal dopaminergic neurons that differs from the normal loss due to ageing. It is further characterized by the aggregation of misfolded proteins (termed Lewy bodies) in the inflicted areas, increased monoamine oxidase B (MAO-B) activity and decreased aldehyde dehyrogenase activity and glutathione levels. Mitochondrial dysfunction, which leads to the formation of potentially toxic hydrogen peroxide, has also been observed. These factors all lead to further dopamine depletion and increased levels of neurotoxic substances in the brain (Przedbrski, 2005; Dauer *&* Przedborski, 2003).

Fig. 1.1. Schematic representation of neurodegeneration in Parkinson's disease (Dauer *&* Przedborski, 2003).

The pathogenesis may occur by at least 3 interrelated mechanisms (Dauer *&* Przedborski, 2003). The first mechanism (Fig. 1.1.) proposes that misfolded proteins within the nigrostriatal neurons may aggregate and lead to neurotoxicity by deforming the cell, by interfering with intracellular trafficking and by sequestering proteins that are important for the survival of the neuron (Cummings *et al*., 1999; Warrick *et al*., 1999; Cummings *et al*., 2001; Auluck *et al*., 2002). The second mechanism proposes that mitochondrial dysfunction within nigrostriatal neurons may lead to the generation of reactive oxygen species (ROS) which in turn leads to neuronal death. The parkinsonian nigrostriatal neuron appears to be a particularly fertile environment for the formation of ROS since it is reported to contain elevated levels of iron which is required for the conversion of hydrogen peroxide to the highly reactive and toxic hydroxyl radical (Cohen, 2000). The presence of ROS within the nigrostriatal neuron may in turn lead to the misfolding of proteins. The third mechanism proposes that dopamine oxidation by MAO-B within the basal ganglia may lead to the formation of toxic products and neurodegeneration (Fernandez & Chen, 2007). For each mole of dopamine oxidized by MAO-B, one mole of hydrogen peroxide and dopaldehyde are formed. Both these products are potentially toxic if not quickly cleared. The levels of both aldehyde dehydrogenase (ADH), which metabolises dopaldehyde, and glutathione peroxidise, which metabolises hydrogen peroxide, are reported to be reduced in the basal ganglia of the parkinsonian brain (Yacoubain & Standaert, 2009). MAO-B therefore plays an important role in the neurodegenerative processes associated with PD and inhibitors of this enzyme have become important drugs for the treatment of this disease. Since MAO-B inhibitors block dopamine metabolism and reduce the formation of the toxic by-products, they are considered useful as a treatment strategy to slow the progression of the disease (Burke, 2003). This approach is termed neuroprotection. In the next section, a brief overview of MAO-B will be given and it will be shown that MAO-B inhibitors not only may slow the neurodegenerative process of PD but may also provide symptomatic relief, especially when combined with the dopamine precursor, levodopa.

1.2 Monoamine oxidase

The monoamine oxidases (MAOs) are enzymes that catalyze the oxidation of monoamines. The two isoforms, MAO-A and –B, share a 70% sequence identity and their FAD co-factor moieties are responsible for the oxidation of the amines (Youdim *et al*., 2006). Both enzymes are found bound to the outer membrane of mitochondria in most cell types in the body. As mentioned above, MAO-B plays a key role in PD since this is the major enzyme responsible for the catabolism of dopamine in the substantia nigra of the brain (Fernandez & Chen, 2007). As discussed above, MAO-B inhibitors may possess neuroprotective properties in PD, but may also provide symptomatic relieve, especially when combined with levodopa. By blocking the MAO-B catalysed metabolism of dopamine, MAO-B inhibitors may conserve dopamine in the brain and provide symptomatic relief of PD. MAO-B inhibitors also elevates dopamine levels derived from the dopamine precursor, levodopa, and are therefore frequently used in combination with levodopa in PD therapy (Birkmayer *et al.,* 1977). The MAO-B inhibitors that are currently used in the treatment of PD are rasagiline and selegiline. These drugs are irreversible inhibitors of MAO-B. Irreversible inhibitors may be considered less desirable than reversible enzyme inhibitors since, following treatment with irreversible inhibitors, the rate by which the enzyme activity is recovered may be variable and may require several weeks (Riederer *et al*., 2004b). In contrast, following treatment with reversible inhibitors, the enzyme activity is usually recovered when the inhibitor is withdrawn and cleared from the tissues. Based on the important role of MAO-B inhibitors in PD and the potential advantages that reversible inhibitors may have over irreversible MAO-B inhibitors, the design and development of new reversible inhibitors of MAO-B are of importance.

The goal of this research project is therefore to design new reversible inhibitors of monoamine oxidase B, which may potentially be used for the symptomatic treatment of PD and which may also possess neuroprotective properties.

1.3 Rationale of this study

The lead compound for the design of new MAO-B inhibitors in the current study is caffeine. Although caffeine is a weak MAO-B inhibitor, substitution at C8 with a variety of substituents has been shown to enhance the MAO-B inhibition potency of caffeine several orders of a magnitude. For example, substitution with a 3-chlorostyryl substituent at C8 of the caffeine ring yields (E)-8-(3-chlorostyryl)caffeine (CSC) (Fig. 1.4.) which is reported to be a potent inhibitor of MAO-B with an IC_{50} value of 146 nM (Pretorius *et al*., 2008). Similarly, substitution of caffeine with a 3-chlorobenzyloxy substituent at C8 yields 8-(3-chlorobenzyloxy)caffeine

which inhibits MAO-B with an IC_{50} value of 107 nM (Strydom *et al*., 2008). Besides the 3-chlorobenzyloxy substituent, a variety of other C3-substituted benzyloxy substituents enhance the MAO-B inhibition potency of caffeine. For example, 8-(3-bromobenzyloxy)caffeine was shown to inhibit MAO-B with an IC_{50} value of 68 nM (Strydom *et al*., 2008).The benzyloxy substituent therefore appears to be particularly applicable for MAO-B inhibition. In accordance with this notion, safinamide, a reversible MAO-B inhibitor which is currently in phase III clinical trials for the treatment of PD, contains a 3-fluorobenzyloxy side chain which is considered to be important for the inhibition of MAO-B (Strydom *et al.,* 2010).

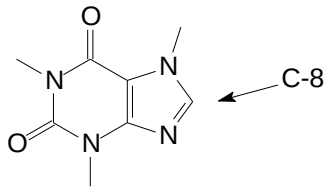

Fig.1.2. The structure of caffeine.

In the current study 8-(phenoxymethyl)caffeine (**1**) and nine 8-(phenoxymethyl)caffeine analogues (**2**-**10**) were synthesized and evaluated as inhibitors of recombinant human MAO-A and –B. The phenoxymethyl substituent is a close structural analogue of the benzyloxy substituent and may therefore possess similar biological properties. This study will determine if C8 substitution of caffeine with a variety of phenoxymethyl substituents also enhances caffeine`s MAO-B inhibition activity to a similar degree than observed with the benzyloxy substituents (Strydom *et al*., 2010). Interestingly, 8-benzyloxycaffeine analogues are also reported to be inhibitors of MAO-A (Strydom *et al*., 2010). The 8-(phenoxymethyl)caffeine analogues examined here only differed in substitution on C3 and C4 of the phenoxymethyl phenyl ring. The substituents that were selected were halogens (Cl, F, Br), the methyl group, the methoxy group and the trifluoromethyl group (Figure 1.3.). These substituents are similar to those selected in the previous study where 8-benzyloxycaffeine analogues were evaluated as MAO inhibitors (Strydom *et al*., 2010). The selection of these substituents for inclusion in this study is based on the fact that the physicochemical properties of the substituents are sufficiently diverse to allow for a Hansch-type quantitative structure-activity relationship (QSAR) study. For example, among the substituents are electron-withdrawing (Cl, F, Br, CF_3) and electron-releasing/donating (CH_3, OCH_3) substituents, substituents which are relatively large (Br, OCH_3), substituents considered to be sterically bulky (Br, CF_3, CH_3) and substituents with a relatively large (CF_3) and low degree (OCH_3) of lipophilicity.

This study therefore (1) explores the possibility that 8-(phenoxymethyl)caffeine analogues may act as MAO-A and –B inhibitors and (2) examines the effect that a variety of substituents on C3 and C4 of the phenoxymethyl phenyl ring will have on the MAO-A and –B inhibition potencies of 8-(phenoxymethyl)caffeine. The MAO-A and –B inhibition potencies of the 8-(phenoxymethyl)caffeine analogues will then be compared to that of the previously studied 8-benzyloxycaffeine analogues. The major potential outcomes of this study may be (1) the identification of new potent reversible 8-(phenoxymethyl)caffeine derived MAO-A and –B inhibitors, (2) the proposal of more promising 8-(phenoxymethyl)caffeine analogues that may be investigated in future studies and (3) the generation of model that correlates the MAO inhibition potencies with the structures of the 8-(phenoxymethyl)caffeine inhibitors.

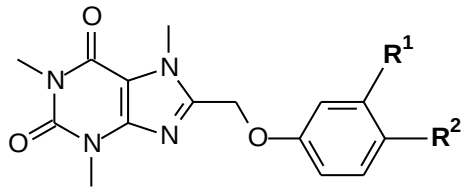

Compd.	R^1	R^2
1	H	H
2	Cl	H
3	Br	H
4	F	H
5	CF_3	H
6	CH_3	H
7	OCH_3	H
8	H	Cl
9	H	Br
10	H	F

Fig. 1.3. The structures of the 8-(phenoxymethyl)caffeine analogues that were examined in the current study.

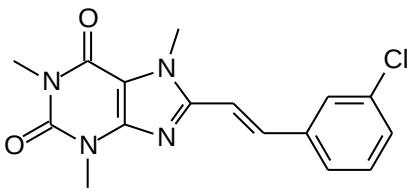

(E)-8-(3-Chlorostyryl)caffeine

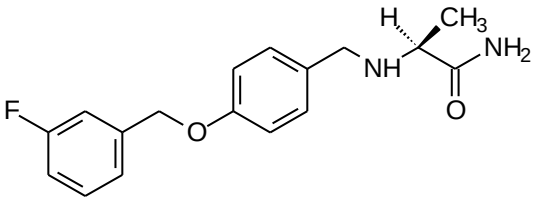

Safinamide

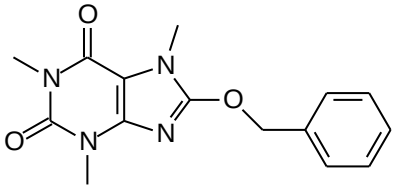

8-Benzyloxycaffeine

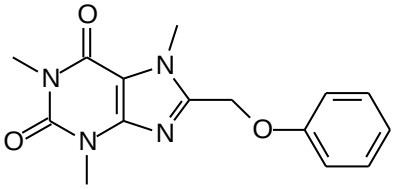

8-(Phenoxymethyl)caffeine

Fig. 1.4 Structures of the compounds discussed in the text.

1.4 Objectives of this study

Based on the discussion above the objectives of this study are summarized below:

- 8-(Phenoxymethyl)caffeine (**1**) and nine 8-(phenoxymethyl)caffeine analogues (**2**-**10**) will be synthesized. For this purpose 1,3-dimethyl-5,6-diaminouracil and the appropriate substituted phenoxyacetic acid will serve as starting materials. In most cases, the required phenoxyacetic acids are not commercially available and will be prepared from the corresponding phenol.

- The 8-(phenoxymethyl)caffeine analogues will be evaluated as inhibitors of MAO-A and –B. For this purpose the recombinant human enzymes, which are commercially available, will be employed. The inhibition potencies will be expressed as the IC_{50} values (concentration of the inhibitor that produces 50% inhibition). A fluorometric assay will be used to measure the enzyme activities. The MAO activity measurements will be based on measuring the amount of H_2O_2 that is produced in the oxidation process. The H_2O_2 reacts with Amplex Red added to the reaction mixtures to form resorufin. The quantity of resorufin in the reactions will subsequently be determined by measuring the fluorescence of the supernatant at an excitation wavelength of 560 nm and an emission wavelength of 590 nm (Zhou & Panchuk-Voloshina, 1997).

- The time-dependency of inhibition of both MAO-A and –B by selected 8-(phenoxymethyl)caffeine analogues will evaluated. This will be done in order to determine if the inhibitors interact reversibly or irreversibly with the MAO isozymes. As stated above, reversible inhibitors are more desirable than irreversible enzyme inhibitors.

- If the inhibition is found to be reversible, a set of Lineweaver-Burke plots will be generated for a selected inhibitor in order to determine if the mode of inhibition is competitive.

- A Hansch-type QSAR study will carried out in order to quantify the effect that different substituents on the phenyl ring of the 8-(phenoxymethyl)caffeine analogues have on MAO-B inhibition activity. For this purpose only the 8-(phenoxymethyl)caffeine analogues bearing C3 substituents will be employed. The results of this study will be compared to those obtained previously for a series of C3 substituted 8-benzyloxycaffeine analogues (Strydom *et al*., 2010).

CHAPTER 2

Literature study

2.1 Parkinson's disease

2.1.1 Background and overview

James Parkinson was the first person to describe all the clinical features of PD in his 1817 monograph "Essay on the Shaking Palsy." About 100 years passed before the pathological feature of PD was discovered to be an abnormally high loss of neurons in the substantia nigia pars compacta. (SNpc) Fortunately the pace of research picked up after Arvid Carlsson in 1958, discovered the presence of dopamine (DA) in the human brain (Dauer & Przedborski , 2003).

PD is normally associated with the elderly and leads to a lowered life quality, without being fatal. As the human brain ages there is a normal loss of neurons, but in PD an increased loss of dopaminergic neurons occurs in the (SNpc) and this leads to low levels of the neurotransmitter, dopamine in the striatum. These low dopamine levels are responsible for the movement disorders associated with the disease. Freezing, tremors, bradykinesia, postural instability, tremor at rest, rigidity and slowness are some of the symptoms of Parkinson's disease (Lees *et al*., 2009).

PD, also called sporadic PD, has no genetic linkage and only in a small number of cases are inherited due to a genetic mutation that causes production of faulty, unwanted protein. Another important neuropathological feature in PD is the occurrence of Lewy bodies (LBs), an intraneuronal inclusion in nigral dopamineric neurons. LBs consist of a number of proteins and are always present in inflicted brain areas. However LBs are not only found in PD, but also in Alzheimer's disease and its role in cell death and the link between incidental LBs and the occurrence of PD are still very controversial (Przedborski, 2004; Dauer *&* Przedborski, 2003).

Increased MAO-B activity and decreased ADH activity and glutathione (GSH) levels have been observed in PD patients, leading to further depletion of dopamine and increases in the levels of neurotoxic substances in the brain (Youdim *et al*., 2006).

2.1.2 Mechanism of PD

The exact cause of PD is still open to discussion, as well as the role of genetics and environmental toxins in the etiology of the disease. In the previous century the theory that PD was caused by environmental toxins was the way of thought of many researchers. This perception was brought on by the discovery of 1-methyl-4-phenyl-1,2,3,6-tetrahydropyridine (MPTP)-induced parkinsonism. After the discovery of genetic mutations associated with PD, it is now commonly accepted that both genetics and environmental toxins play a role in PD (Dauer & Przedborski, 2003; Tanner, 2003; Taylor *et al*., 2005; Dick *et al*., 2007; Healy *et al*., 2008).

Among the possible mechanisms that may be responsible for neuronal death and the resulting dopamine depletion is: neurotoxic aldehyde accumulation and ROS formation (Fig. 2.1.). Although other mechanisms may exist, these appear to be the main culprits in the etiology of PD (Cohen, 2000; Fernandez & Chen, 2007).

Neurotoxic aldehyde accumulation is caused by amine oxidation which forms aldehyde products that may be neurotoxic and have a lesion forming effect on the midbrain dopaminergic neurons (Youdim *et al*., 2006). ADH is always present in the brain and converts aldehydes to harmless by-products. However, in patients with PD, there are low levels of ADH causing an accumulation of the neurotoxic aldehydes (Grunblatt *et al*., 2004). Since MAO is linked to or may be responsible for the production of aldehydes as well as oxygen species, the assumption can be made that PD patients would benefit from drugs that block the function of MAO.

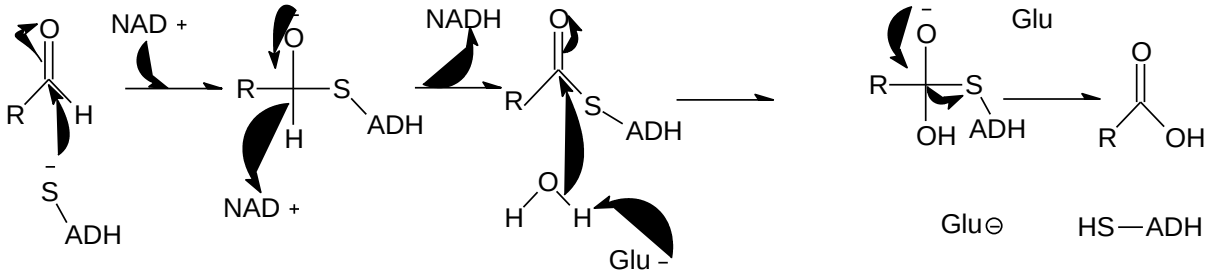

Fig. 2.1. The oxidation of aldehydes by ADH.

The second mechanism that may lead to neuronal degeneration is the formation of ROS. Oxidative stress may occur when ATP production is halted, leading to compromised energy production and neuronal death. In the MPTP model of PD, MAO (in this case the B-isoform) converts MPTP to the active product 1-methyl-4-phenylpyridinium (MPP^+). MPP^+ combines with NADH dehydrogenase, which leads the inactivation of this enzyme. Mitochondrial H^+

transport is blocked and therefore also oxidative phosphorylation. All of the above is responsible for ATP depletion and cell death. The model suggests that the monoamine oxidation process could produce other similar products (to MPP^+), which could also lead to oxidative stress (Singer *et al*., 1988). ATP depletion is not the only result when mitochondrial respiration is blocked. ROS formation also results when mitochondrial electron transport is inhibited. High ROS levels have been linked to several neurodegenerative diseases (Youdim *et al*., 2006). ROS can either react with nitric oxide or form the even more dangerous peroxynitrite or hydroxyl radicals (from the Fenton reaction, discussed later). Both these substances are highly neurotoxic (Dauer & Przedborski, 2003). As the human brain ages, the Fe^{2+} levels in the brain increase as well as H_2O_2 levels. In PD patients, due to lower GSH levels, the conditions become extremely favourable for the formation of hydroxyl radicals via the Fenton reaction.

Fig. 2.2. Schematic representation of the potential mechanisms of neurodegenaration in PD (Betarbet *et al.,* 2002).

2.1.3 PD therapy

To date the only treatment for PD is symptomatic, although many studies have been done on possible prophylactic treatment. Symptomatic medication only treats the effects of the lowered DA levels and has no effect on slowing the rate of neurodegeneration. Therefore, once a patient has been diagnosed with PD, only symptomatic treatment is currently available and this medication will probably be necessary for the remainder of the patient's lifespan. Various studies have been carried out with the aim to slow or stop the progression of PD, but without registered treatment to date (Standaert & Young, 2006).

Treatment or therapy strategies today address the symptomatic effects of PD, as there have not been any definite signs of neuroprotection by any drugs in clinical studies or currently on the market. When selecting a treatment strategy, the long and short term effects must be taken into account. A recent tendency is to start with a well-tolerated drug at the first stages of PD, even in the absence of any impairment, to improve the long term effects. In most instances, therapy begins as monotherapy with a nondopaminergic drug or, in relative young patients, using a dopamine agonist. PD is a progressive disorder and therefore changes and/or adjustments to the therapy are usually necessary over the course of time. Levodopa therapy could be considered in older patients who suffer from increased symptoms. MAO-B inhibitors are considered when signs of motor fluctuations are observed. When there is evidence of levodopa-induced dyskinesias, amantadine may be added (Standaert & Young, 2006).

2.1.3.1 Symptomatic treatment of PD

Levodopa is the most effective drug used to provide symptomatic relief and is the immediate precursor to dopamine. Levodopa crosses the blood-brain barrier and is converted to dopamine and is therefore usually used in combination with drugs such as carbidopa and benserzide to block excess peripheral conversion of levodopa to dopamine. This reduces the adverse effects of high peripheral dopamine levels (Factor, 2008).

Once the blood-brain barrier has been crossed by levodopa, it is converted to dopamine by L-amino acid decarboxylase. The high level of dopamine is stored presynaptic, ready to be released into the synaptic cleft, where it binds to the postsynaptic D_1 and D_2 receptors, providing symptomatic relief. Eventually, every patient diagnosed with PD, will have to include levodopa in their treatment strategies (Factor, 2008).

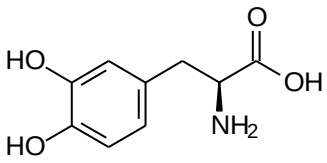

Fig. 2.3. The structure of levodopa.

The purpose of MAO inhibitors is to increase either the levels of dopamine formed from levodopa or the half life of endogenous striatal dopamine. Early non-selective MAO inhibitors were very successful in reducing dopamine metabolism. The biggest disadvantage of MAO inhibitors is that they may cause dangerous hypertensive crises in certain patients which limit their clinical use. After the development of selective MAO inhibitors, however, it was possible to block only the B isoform which is the main isoform responsible for dopamine oxidation. These inhibitors conserve endogenous dopamine and dopamine derived from administered levodopa. MAO-B inhibitors can therefore either be used as monotherapy or in patients that have motor fluctuations (caused by levodopa) as adjunctive therapy. Since MAO-B inhibitors conserve the dopamine supply in the brain and prevent the production of potential neurotoxic species from dopamine oxidation, these drugs may be used to provide both symptomatic relief of PD symptoms and to slow the neurodegenerative process (Chen & Swope, 2007).

Amantadine has shown enhanced dopamine release, reuptake blocking (at high doses) and antimuscarinic effects (mildly) and also blocks NMDA glutamate receptors noncompetitively. All of these effects are beneficial in PD treatment. In PD patients, amantadine is highly beneficial due to its capability to treat motor functions and dyskinesias that have developed from chronic levodopa use. Amantadine can be used both as monotherapy and as add-on therapy for symptomatic control. The neuroprotective effect of amantadine is a result of its capability to block NMDA glutamate receptors, which limits excitotoxic reactions (caused by excessive glutamatergic stimulation) and results in neuroprotection in early PD (Lees, 2005).

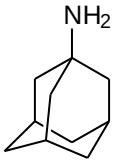

Fig. 2.4. The structure of amantadine.

Anticholinergic drugs block muscarinic receptors, thus lowering the effect of acetylcholine and restoring the equilibrium between the effects of acetylcholine and dopamine in the striatum. Some also show antagonistic activity on the NMDA receptors and therefore a potential neuroprotective action. Benzhexol (trihexyphenidyl), benztropine (benzatropine), procyclidine and orphenadrine are most commonly used by prescribers in the treatment of PD. Mild symptomatic control in PD is reported in their usage either as monotherapy or in combination with other drugs. One of the limiting factors in their usage as PD therapy is the adverse anticholinergic effects, including; inhibition of micturition, lower gastrointestinal tone and impaired neuropsychiatric and cognitive functions. Due to the last two adverse effects, anticholinergic drugs should be used with caution in older patients and patients with impaired cognitive function (Lees, 2005).

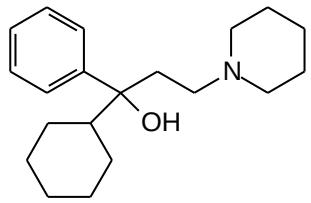

Fig. 2.5. The structure of benzhexol.

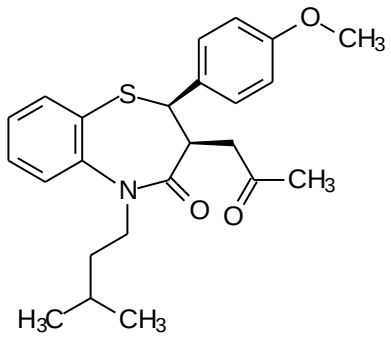

Fig. 2.6. The structure of benztropine.

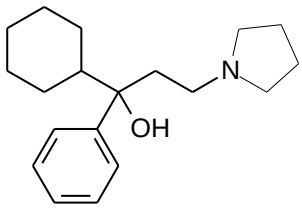

Fig. 2.7. The structure of procyclidine.

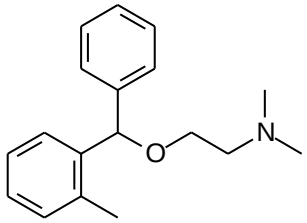

Fig. 2.8. The structure of orphenadrine.

Deprenyl (selegiline) is the most common MAO-B inhibitor used in the treatment of PD. A 5 mg twice daily dose leads to irreversible inhibition of the B isoform of MAO. In a DATATOP (Deprenyl and Tocopherol Antioxidative Therapy of Parkinsonism) study it was shown that selegiline has only a minor beneficial symptomatic effect and causes only a small delay in levodopa therapy, when used as monotherapy. Some of selegiline`s disadvantages include high first-pass metabolism, low bioavailability and the formation of amphetamine metabolites (L-N-desmethylselegiline, L-methamphetamine and L-amphetamine) that may cause psychotoxic effects, postural hypotension and cardiovascular reactions. However, it is suggested that selegiline may have a neuroprotective effect and may delay the occurrence of symptoms that require the initiation of levodopa therapy. In the DATATOP study, this effect was shown to be symptomatic rather than a protective effect (Parkinson Study Group, 2005). Therefore the combination of selegiline and levodopa is not recommended in elderly or advanced disease stages, due to its low efficacy and questionable safety. Zydis (a new selegiline formulation) that has recently been developed has greatly reduced the “on-off” effect of levodopa. Due to sublingual absorption of Zydis-selegiline, the first-pass metabolism is avoided (absorbed pre-gastrically) and a lower percentage of the drug is converted to amphetamine metabolites and therefore the percentage delivered to the brain is higher, indicating that Zydis-selegiline is more effective and safer (Youdim & Bakhle, 2006).

Rasagiline is a very potent irreversible inhibitor of MAO-B. It is also highly selective for the B-isoform. It is well tolerated and has direct neuroprotective and antiapoptotic properties. With rasagiline there are no amphetamine-like adverse effects since it is not metabolised to amphetamine derivatives (Finberg & Youdim, 1985).

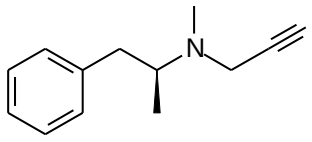

Fig. 2.9. The structure of (R)-deprenyl (selegiline).

Dopamine agonists bind well on both pre- and postsynaptic D_2 receptors. Binding with postsynaptic D_2 receptors results in an antiparkinsonian effect. Some off the advantages of dopamine agonists, compared to levodopa are: they have direct receptor stimulation, they do not make use of carrier-mediated brain absorption and there are no reports of them producing free radicals and toxic metabolites. Today's treatments provide continuous stimulation of dopamine receptors over longer periods. There are two types of dopamine agonists, ergoline (ergot-like structure) and non-ergoline agonists. Bromocriptine, lisuride, pergolide and cabergoline are ergoline agonists currently used and apomorphine, ropinirole, piribedil and pramipexole are non-ergoline agonists in use. At low/normal doses, adverse affects that occur commonly include vomiting, somnolence, nausea, peripheral oedema, dizziness and orthostatic hypotension. In elderly patients, high doses may lead to confusion and psychosis and is therefore not recommended (Fernandez & Chen, 2007; Lees *et al.,* 2009).

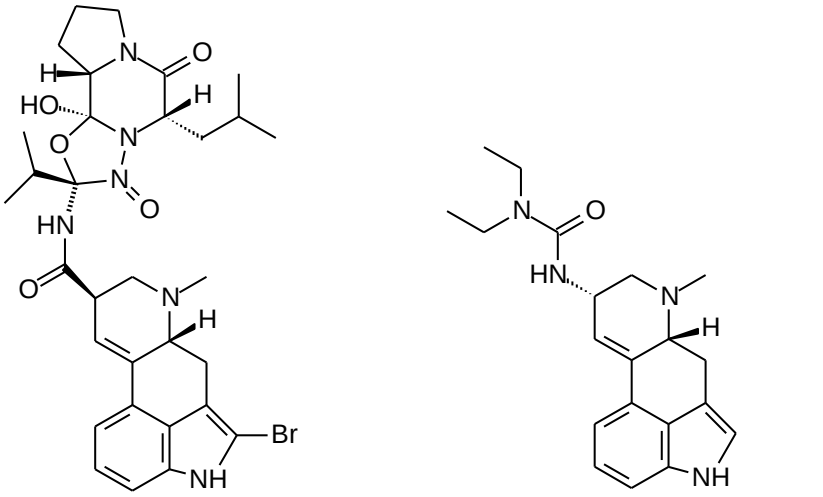

Fig. 2.10. The structures of bromocriptine and lisuride.

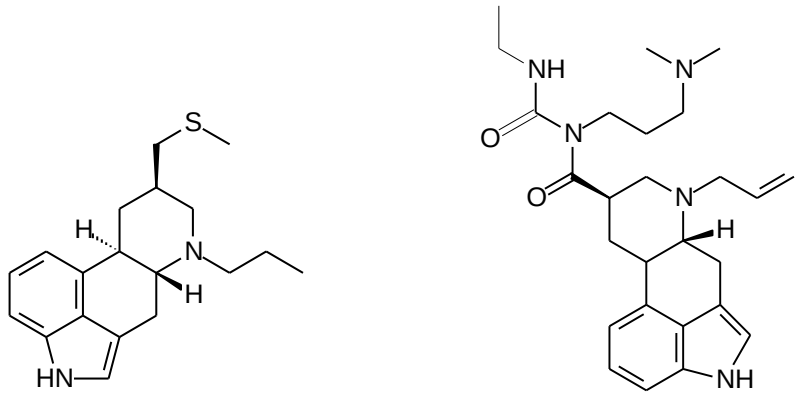

Fig. 2.11. The structures of pergolide and cabergolide.

2.1.3.2 Neuroprotection in PD

As explained in the section above, there is to date no registered prophylactic treatment for PD. However there are numerous studies pursuing this subject and some progress has been made. One of the most promising approaches has been a methodological approach that has recently been incorporated into PD neuroprotection research. “Futility trial” provides one way for economic initial drug exploration. With this approach any unnecessary further investigation of a therapeutic intervention is avoided. If the initial results are such that a statistically significant endpoint of “futility to proceed further” is not reached, further more extensive efficacy investigation is indicated. The “futility trial” design therefore leads to much faster and more efficient clinical trials and considering that PD neuroprotective trials are relatively large, will lead to a faster pace of drug discovery (Le Witt *&* Taylor, 2008).

The latest developments in neuroprotection therapy are: antioxidant strategies, mitochondrial energy enhancement, anti-apoptotic compounds, anti-glutamatergic agents, MAO inhibitors and dopaminergic drugs. These drugs may find application in slowing the progression of neurodegeneration in PD.

Although several compounds have a neuroprotective effect because of their antioxidant properties, only α-tocopherol, has been clinically evaluated. α-Tocopherol quenches oxyradical species present in lipid-soluble membrane areas. From this study it was concluded that lowering oxidative stress could have beneficial effects (Vatassery *et al.,* 1998).

Mitochondrial energy enhancement is another neuroprotective stategy in PD. PD patients experience altered mitochondrial function and lowered activity of the electron transport chain, which causes a decline in energy production and subsequent cell death. Therefore, if intracellular energy is increased, cell death could be prevented and hence a neuroprotective effect may be obtained. Co-enzyme Q_{10} and creatine may be promising in this area (Le Witt *&* Taylor, 2008). Co-enzyme Q_{10} serves both as a co-factor in the electron transport chain (at Complex I) and as a very important antioxidant in lipid-soluble membrane areas. Therefore, co-enzyme Q_{10} can enhance the function of the electron transport chain, which results in higher intra-cellular energy. Co-enzyme Q_{10} can also reduce radical species present in the membrane areas. Augmentation of the brain creatine concentration is also useful for enhancing energy levels. Creatine is converted into phosphocreatine, which is an energy intermediate that transfers phosphoryl groups for ATP synthesis in the mitochondria. Increased creatine leads to increased phosphocreatine, that in turn leads to lowered oxidative stress by stabilization of mitochondrial creatine kinase and hence a potential neuroprotective effect (Yacoubian & Standaert, 2009).

Apoptosis has been implicated as a mechanism of neurodegeneration in PD. The following three compounds may be neuroprotective by acting as anti-apoptotic drugs:

- Pretreatment with minocycline, improves dopaminergic SN neuron survival in MPTP and 6-hydroxydopamine (6-OHDA) rodent models. Minocycline inhibits the activation of microglia that is present in PD patients' brains and also in some experimental neurotoxin models. Minocycline also reduces apoptosis mediating factors such as caspase-I. Although all of these actions of minocycline are promising, preclinical trials have not shown consistent neuroprotective action (Yacoubian & Standaert, 2009).

- TCH 346, is a novel compound, that share many structural similarities with selegiline, but do not have MAO-B inhibition activity. TCH 346 acts as an inhibitor of neuronal apoptosis associated with normal aging, by binding to glyceraldehyde-3-phosphate dehydrogenase, a glycolytic enzyme. Increased P12 and human neuroblast cell survival have been reported with TCH 346 therapy (Kragten *et al.,* 1998). Near complete protection was reported in rhesus monkeys injected with the neurotoxin MPTP and no or minimal motor impairment was reported (Andringa & Cools, 2000).

- CEP-1347 is an inhibitor of mixed lineage kinase-3 which is an important component in the c-Jun-mediated transcription factor terminal kinase signaling pathway. This pathway is responsible for neuron death due to apoptosis and has been linked to neuron death in PD (Le Witt *& Taylor*, 2008; Maroney *et al.,* 1998; Parkinson Study Group, 2004).

Glutamate can act in the brain as an excitotoxin and hence may cause neurodegeneration. Therefore, blocking glutamate neurotransmission in the brain can be a potential approach to slow or halt neurodegeneration. Riluzole, an FDA approved drug, has a limiting blocking effect on pre-synaptic release of glutamate. Because it is a limited effect, there is no CNS toxicity, such as caused by other drugs that totally block glutamate release (Yacoubian *&* Standaert, 2009).

The three MAO inhibitors that have demonstrated the ability to attenuate the neurodegenerative process are selegiline, lazabemide and rasagiline (Le Witt *& Taylor*, 2008). As mentioned before the MAO inhibitors block the oxidation of monoamines and the production of harmful by-products. These harmful products may cause neuronal death and, by blocking the oxidation process, the inhibitors have a neuroprotective effect.

Symptomatic treatment of PD was the main reason for the development of dopaminergic drugs. However in some clinical trials, it was found that these drugs may also have a

neuroprotective effect. Two drugs that exhibited promising effects were the dopamine agonist drugs, pramipexole and ropinirole (Parkinson Study Group, 2000 & 2002). The effects of various toxins have been shown, in several studies, to be blocked by these drugs. Dopaminergic stimulation may also cause recovery of damaged dopaminergic nigrostriatal neurons (Le Witt *& Taylor.* 2008).

2.2 The neurotoxin MPTP

1-Methyl-4-phenyl-1,2,3,6-tetrahydropyridine (MPTP) was accidentally discovered in the early 1980s after young people exhibited symptoms of PD. It was found that these young people were drug users and that they had all used a street drug produced form of 1-methyl-4-phenyl-4-propionoxypiperidine (MPPP). MPPP has similar effects to that of meperidine. The batch of MPPP administered by the drug abusers contained a by-product, MPTP, a powerful neurotoxic agent that induces PD (Dauer & Przedborski, 2003).

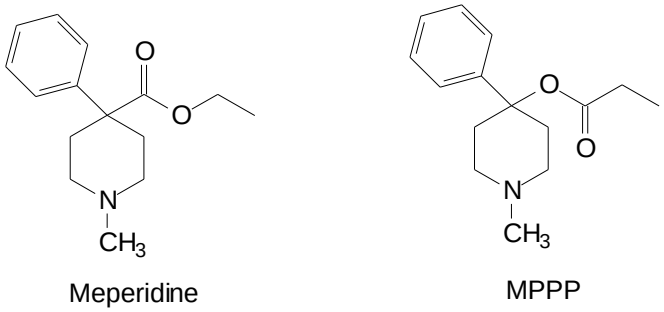

Fig. 2.12. The similarities between meperidine and MPPP.

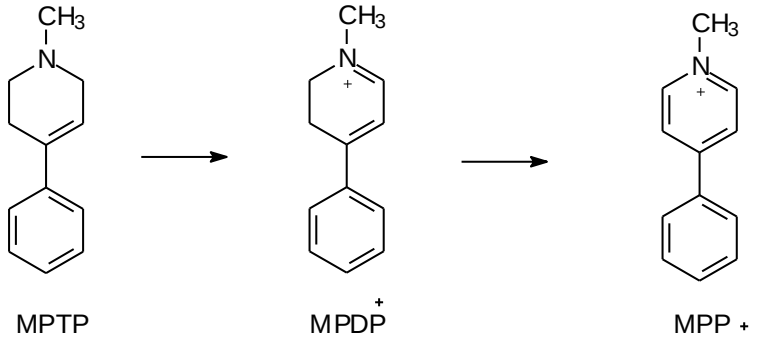

Fig. 2.13. The oxidation of MPTP to MPP^+

The MPTP model is widely used by researchers to induce PD in test animals. MPTP is oxidized to 1-methyl-4-phenyl-2,3-dihydropyridinium ($MPDP^+$) by MAO-B. $MPDP^+$ in turn, is oxidized further to MPP^+, by an unknown mechanism. MPP^+ is the substance responsible for

the neuronal damage due to the fact that it inhibits energy production by the electron transport chain. MPP^+ is a highly polar compound and only enters neurons via the dopamine transport system (DAT) (Ogunrombi *et al.,* 2007).

There are also other mechanisms by which MPTP cause neurodegeneration and PD. For example, MPP^+ may enhance the levels of oxygen radicals, which are destructive to neurons as a result of the inhibition of the electron transport chain (Smeyne *& Jackson-Lewis*, 2004).

Fig. 2.14. The mechanism of the neurotoxic action of MPTP.

MPTP is a very good PD model and the symptoms are closely matched to that of idiopathic PD, with two exceptions. Firstly, in induced PD there is no consistent loss of monoaminergic

nuclei and secondly, although there are signs of LBs, it is not nearly as pronounced as in idiopathic PD (Dauer *&* Przedborski, 2003).

In vitro, MPTP is readily oxidized to its toxic by-product, MPP^+ by MAO-B, a process which is inhibited by MAO inhibitors. However, *in vivo* the situation is different. The formation of MPP^+ is only totally blocked with a combination of both an MAO-A and an MAO-B inhibitor. This is due to the possibility that MAO-A is very rapidly inactivated by MPTP *in vitro,* while *in vivo* this process may require a longer time. Therefore, in order to totally block neurotoxicity both inhibitors have to be used (Singer *et al*., 1988).

2.3 Monoamine oxidase

2.3.1 Background

MAO is an enzyme present in all living cells and bound to the membrane of the mitochondria. There are 2 isoforms, MAO-A and MAO-B. They contain a flavine adenine dinucluetide (FAD) cofactor and require no iron or copper ions for its activity (Youdim *et al*., 2006). MAO acts as a catalyst in the oxidative deamination of various monoamines, including 5-hydroxytryptamine (serotonin), dopamine, histamine, adrenaline and noradrenalin. As already mentioned, the outcome of this oxidative process is the formation of products that may cause neurodegeneration, such as hydrogen peroxide, aldehydes, ammonia and substituted amines (Salach *& Weyler,* 1987).

MAO-B deaminates benzylamine and 2-phenylethylamine (arylalkylamines) and is inhibited by (R)-deprenyl. MAO-B consists of 520 amino acids. MAO-A deaminates 5-hydroxytryptamine (serotonin), is inhibited by clogyline and consists of 527 amino acids. MAO-A and MAO-B are 70% identical at the amino acid sequence level (Youdim *et al*., 2006).

Difficulties have however arisen in studies with MAO-B because inadequate expression systems for the enzyme made it difficult to produce the enzyme in large qualities (Lan *et al*., 1989). Among the sources of the enzyme are human placenta (MAO-A and B), blood platelets (MAO-B), bovine liver (MAO-B), and baboon liver (MAO-B) and recently researchers have been able to express human MAO-B from yeast cells (Weyler *et al.,* 1990). The yeast cells produced enough pure enzymes for an X-ray crystal structure to be determined (Grimsby et al., 1996). Another problem is that MAO is bound to the membrane of the mitochondria, which makes mechanical extraction difficult. Also, removing MAO-A and –B from the membrane may have a significant effect on its activity (Youdim & Bakhle, 2006).

2.3.2 Pharmacology

As already mentioned, the main chemical and pathological characteristics of PD are depleted dopamine and high levels of toxic by-products derived from the oxidation of dopamine by MAO-B and to a lesser extent, by MAO-A. Therefore, MAO plays a relatively large role in the treatment of PD and inhibitors of MAO have a role in the symptomatic and neuroprotective therapy of PD. MAO inhibitors not only increase dopamine levels but also reduce the formation of harmful by-products (Dostert *et al.,* 1989).

2.3.3 Catalytic cycle of MAO-B

The catalytic mechanism of amine oxidation is dependent on two factors namely the FAD cofactor and oxygen. Primary, secondary and certain tertiary amines undergoes α-carbon oxidation to yield the corresponding imines. The imines are subsequently hydrolyzed to aldehydes by water. This process therefore, leads to increased levels of aldehydes which can be toxic. In PD patients there is an abnormal low concentration of aldehyde dehydrogenase (ADH) in the affected brain areas and therefore these patients have a reduced capacity to convert aldehydes to harmless by-products (Edmondson *et al*., 2007).

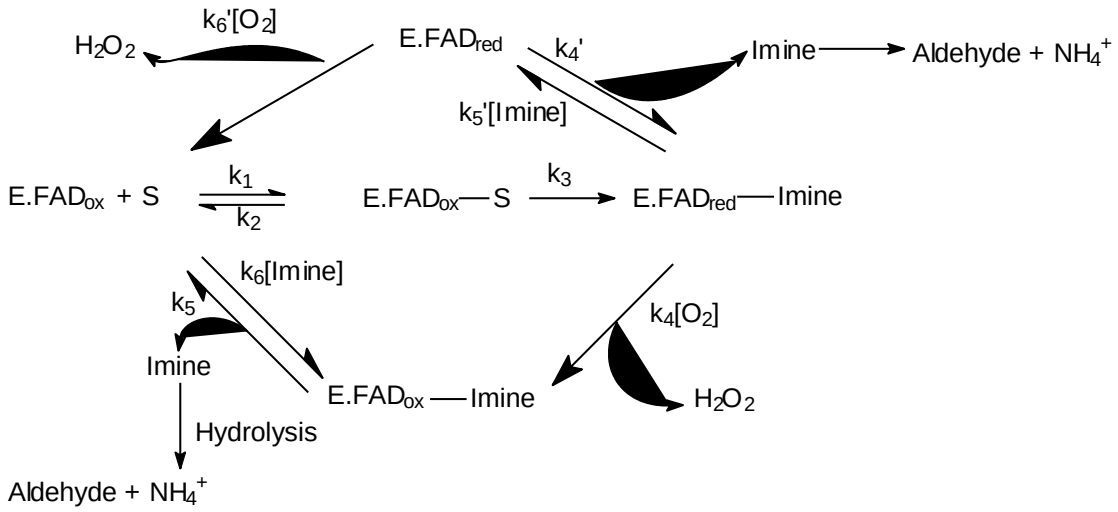

Fig. 2.15. The catalytic pathway followed by MAO-A and MAO-B

Various mechanisms of flavin-dependent amine oxidation have been proposed over the years. The single electron transfer mechanism (aminium cation radical) was first suggested but has however been questioned (Edmondson *et al*., 2004; Binda *et al*., 2002). In the first step of the mechanism, the amine provides a single electron to the flavin (oxidant) to form

the aminium cation radical. This aminium cation radical then has an α-proton acidic enough to allow a basic amino acid residue, present at the active site, to abstract the proton. This results in the formation of the imine product and the reduced flavin. However, recent studies have shown no evidence of flavin radical intermediates during catalysis and in the structure of MAO there are no basic amino acids residues present at the active site (Edmondson *et al*., 2004).

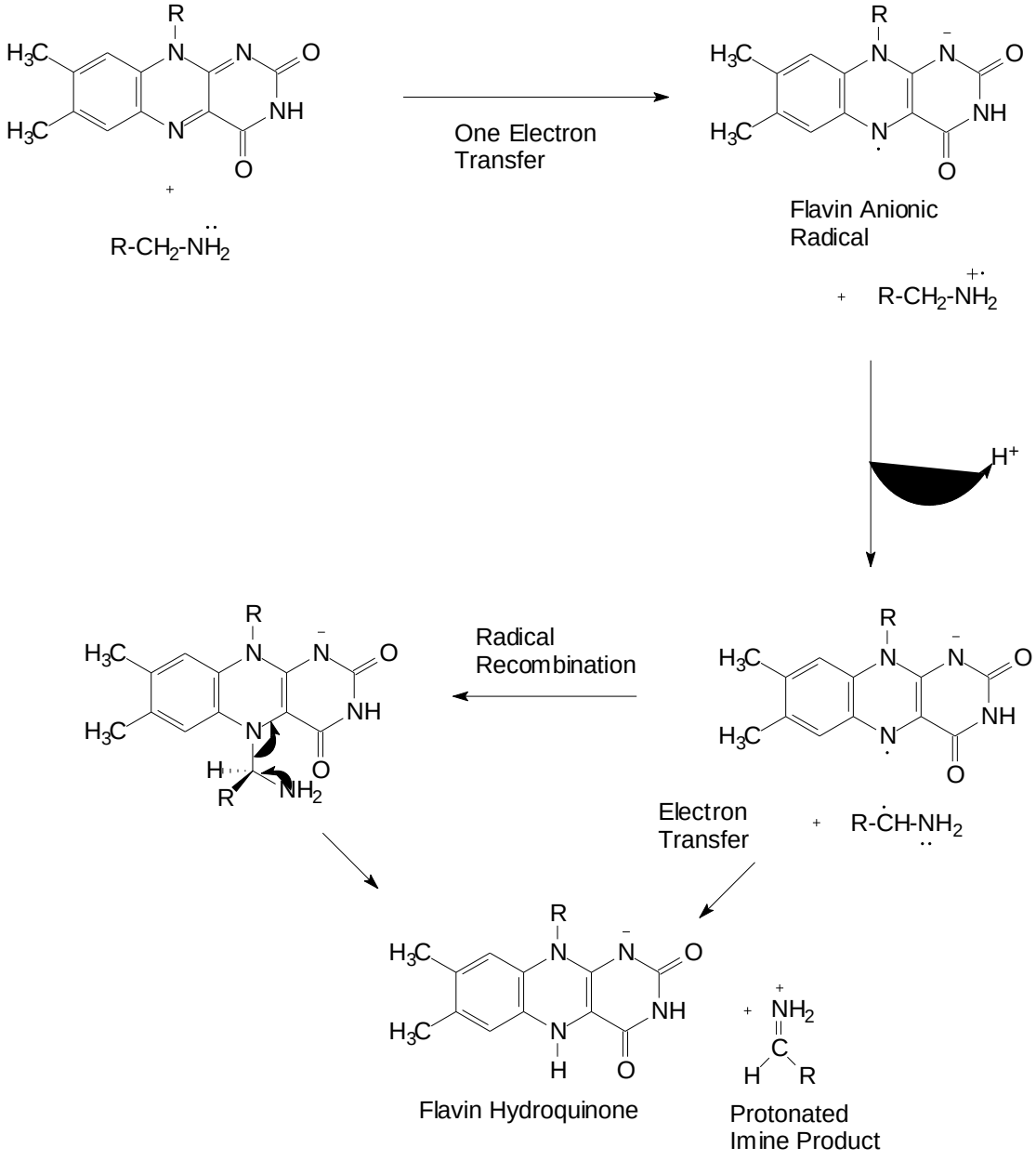

Fig. 2.16. Single electron transfer mechanism for MAO catalysis.

Evidence however, favours another mechanism, the polar nucleophilic mechanism. The flavin, in this mechanism, is attacked at the 4a-position by the deprotonated amine in a nucleophilic manner, which in turn activates the N-5-position. This transforms the N-5-

position into a very strong active site base which could abstract the α-pro-R-H form of the substrate. The pK_a of benzyl protons are approximated by that of reduced flavins. This mechanism appears to be much more likely than the SET mechanism (Edmondson *et al*., 2004).

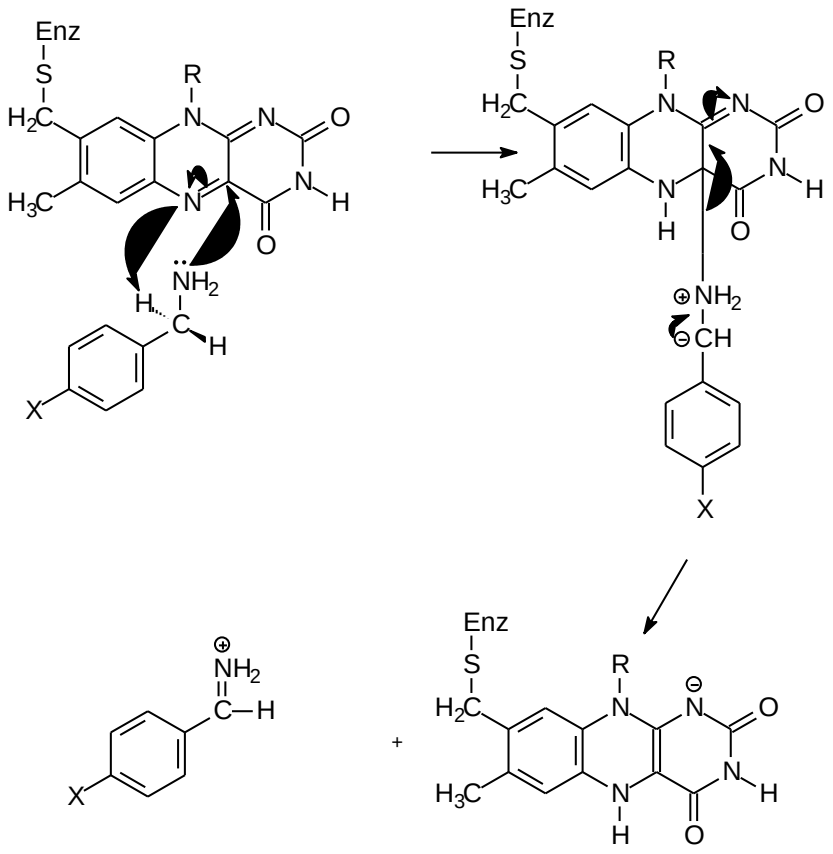

Fig. 2.17. Polar nucleophilic mechanism of MAO-A and MAO-B catalysis.

2.3.4 The three-dimensional structure of MAO

Of the 520 residues of MAO-B, the first 500 has a well-defined three-dimensional structure and a very good electron density in X-ray crystallographic studies. For MAO-A on the other hand, the entire C-terminal domain (501 - 520 residues in MAO-B) can be elucidated from its diffraction pattern. Human MAO-A crystallizes as a monomer, whereas MAO-B crystallizes as a dimer. Rat MAO-A also crystallizes as a dimer. This may be due to a difference of the residue 151 in human and rat MAO-A. This residue is at the dimer interface position in rat MAO-A and human MAO-B. (Son *et al*., 2008; Binda *et al.*, 2007a)

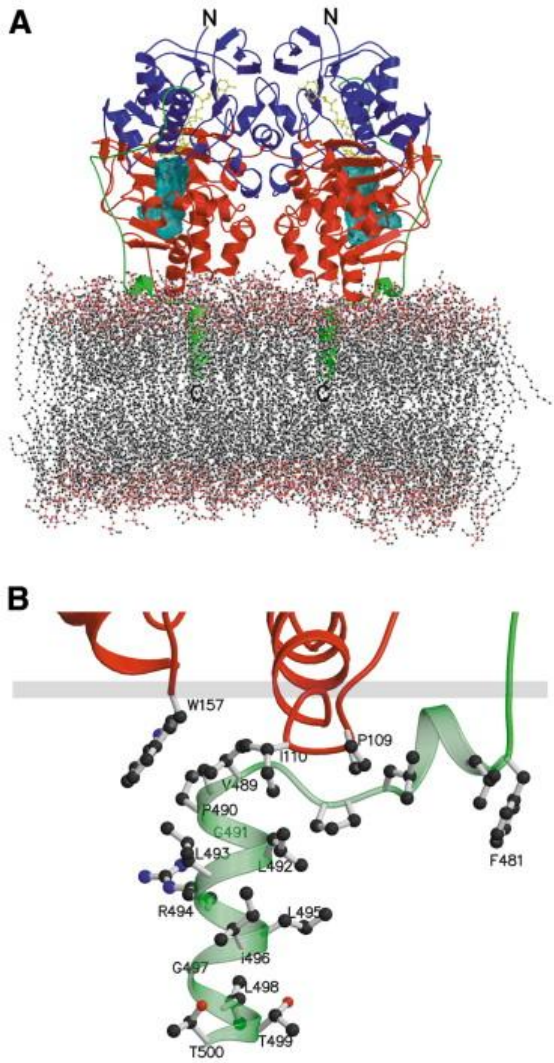

Fig. 2.18. The three dimensional structure of the MAO-B dimer. A: Structure of MAO B dimer bound to the phospholipid bilayer. B: The C-terminal transmembrane helix and the neighbouring apolar sites involved in membrane binding (Binda *et al.*, 2003).

Both MAO-A and MAO-B are bound to the outer membrane of the mitochondria. The C-terminals α-helices anchor the enzyme to the mitochondria. The substrate cavity entry sites of both MAO-A and –B are near the intersection of the mitochondrial membrane and the enzyme. MAO-B has two cavities, the entrance cavity and the substrate cavity and the boundary between them is formed by four residues namely Tyr 326, Ile 199, Leu 171 and Phe 168. The entrance of the cavity is partially covered by a loop of residues (99 - 112) and this must be negotiated by the substrate before it can enter into the active site. The cavity of MAO-B is hydrophobic and flat, and has a 490 Å volume. The redox-active isoalloxazine ring of the covalently bound FAD coenzyme is located at the back of the substrate cavity (Hubalek *et al.,* 2005).

Fig. 2.19. Stereo view of the active site cavities of rat MAO-A, human MAO-B, and human MAO-A. Residues of rat MAO-A are in orange, human MAO-A is shown in yellow, and human MAO-B in cyan (Son *et al.,* 2008).

Human MAO-A on the other hand, has only a single cavity with a slightly bigger volume (550 Å) than MAO-B. Rat MAO-A is smaller with a volume of 450 Å. The difference between human MAO-A and rat MAO-A are conformational differences in the cavity-shaping loop (residues 210 - 216). These differences are responsible for the smaller cavity volume of rat MAO-A (Edmondson *et al.,* 2004).

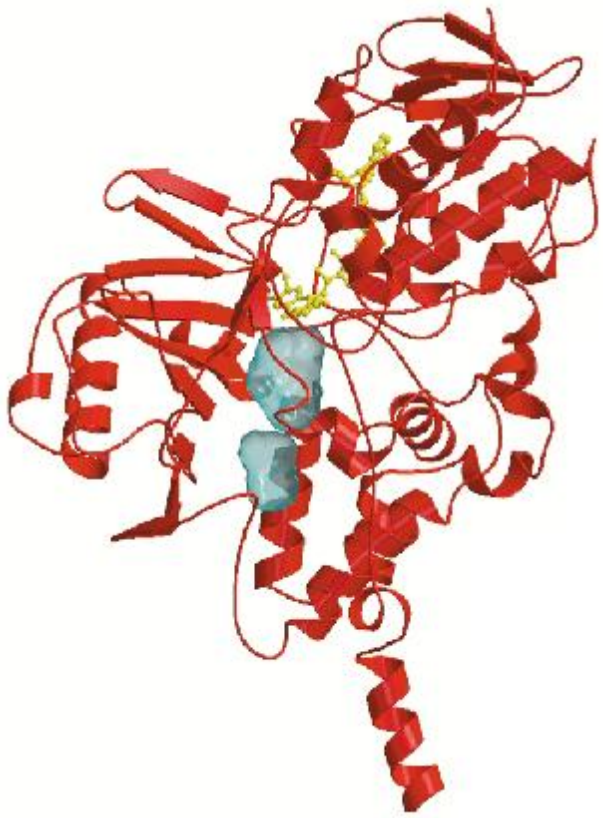

Fig. 2.20. Three-dimensional structure of human MAO B. The FAD-cofactor is in ball-and-stick representation coloured in yellow. The two cavities, entrance and substrate are also shown (Hubalek *et al.,* 2005).

In studies where inhibitors were covalently bound to the flavin moiety (N5 position) it was found that inhibitors position between Tyr 398 and Tyr 435 (Binda et al., 2007). These two amino acid residues are found to be almost perpendicular to the flavin ring, with a very small space (7.8 Á) between them. The neighbouring Cys 397 is linked to the 8α-position of the flavin ring via a covalent thioether linkage and this linkage is in a cis conformation (low energy). This linkage allows the phenolic side chain of Tyr 398 to form an aromatic sandwich with Tyr 435 and the FAD cofactor. This structure is present in all sources of MAO-B and MAO-A. The structure also has an important function in that any inhibitor or substrate must first be able to pass through it before being able to interact with the flavin ring (Hubalek *et al.,* 2005).

2.3.5 Measurement of *in vitro* catalytic activity of MAO

In vitro activity of both MAO-A and -B can be measured in a number of ways. Spectrophotometric measurement is however the most used method (Inoue *et al*., 1999). Other methods include: radiometric, ammonia, polarographic, fluorometric and luminometric detection. A frequently used method is the spectrophotometric method using benzylamine as substrate. Benzylamine is an MAO-B selective substrate and is oxidized to benzaldehyde which is subsequently measured spectophotometrically at a wavelength of 250 nm (Edmonson *et al*., 2007).

Another method is the measurement of the amount of ammonia produced throughout the oxidation process. One problem with this method is that not all amines form ammonia after being oxidized by MAO (Holt *et al*., 1997).

Luminometric detection was developed by O'Brien *et al.* (1978). This method is a very accurate and specific. The extent to which H_2O_2 catalyses the transformation of luminol into light is measured. H_2O_2 is formed in the oxidation process of MAO and the amount of light correlates directly to the amount of substrate oxidized by MAO. However, the substrate should not be oxidized by H_2O_2 more readily than luminol.

The polarographic method lacks specificity and sensitivity by MAO, but is very accurate and reproducible. With this method the rate of oxygen consumption is measured (Meyerson *et al*., 1978).

The radiometric method is widely used due to the availability of substrates that is radiolabelled and its high level of sensitivity and specificity. The formation of radiolabelled aldehydes is measured by this method (Nicotra *& Pervez*, 1999).

The fluorometric method measures the amount of a fluorescent product formed. This method is only possible when substrates are used that are oxidized into fluorescent products by MAO. The extent to which oxidation has taken place can then be measured via a fluorecence spectrophotometer. The use of kynuramine as substrate is an example of this method and will be used in this study. Kynuramine is non-fluorescent until undergoing MAO catalysed oxidation to yield 4-hydroxyquinoline, a fluorescent product (Zhou *et al.,* 1996). In a variation of this method, the amount of H_2O_2 that is produced by MAO can be measured by reacting the H_2O_2 with Amplex Red in the presence of peroxidise. This reaction produces resorufin which can be measured at an excitation wavelength of 560 nm and an emission wavelength of 590 nm (Zhou & Panchuk-Voloshina, 1997). This method will also be employed in this study.

2.3.6 Known inhibitors of MAO-B

Early MAO inhibitors were used as antidepressants. However, there was little success due to the so called “cheese effect”. The combination of MAO inhibitors with products containing tyramine can cause a very dangerous hypertensive crisis. Normally tyramine is metabolized in the gut by MAO-A. Non-selective MAO inhibition blocks this process and enhanced the amounts of tyramine reaching the systemic circulation. Tyramine causes the release of amines such as adrenaline in the brain and thus may lead to a hypertensive crisis (Youdim *et al*., 1988; Bakhle, 1990).

MAO inhibitors may be classified into two categories, irreversible and reversible inhibitors. Irreversible inhibitors bind to MAO in a reversible manner and are subsequently oxidized. This oxidized product forms covalently bonds to the FAD cofactor inside the active site of the enzyme. This stops any further amine metabolism and normal enzyme activity is only restored after an extended time period (Riederer *et al*., 2004b). Reversible inhibitors also bind to MAO in a reversible manner. However they are not metabolized by MAO. They bind to the active site for only a short period of time. Reversible inhibitors are more desirable because the enzyme activity can be regained after the inhibitor treatment (Youdim & Bakhle, 2006).

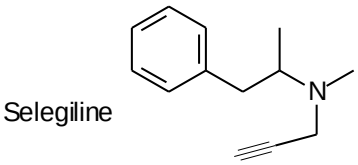

Selegiline

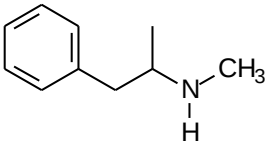

Methamphetamine

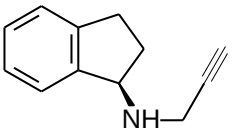

Rasagiline

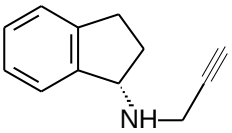

TVP-1022

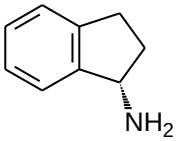

Aminoindan

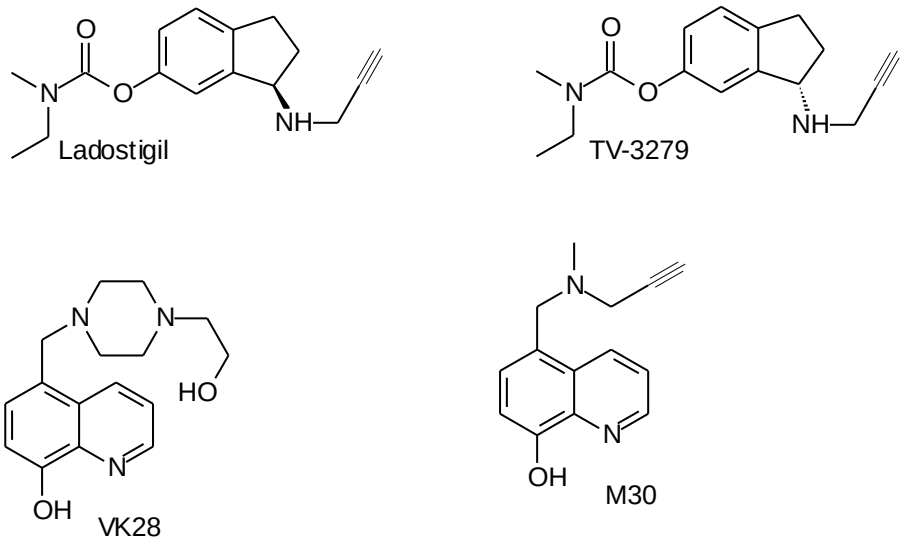

Fig. 2.21. The structures of selected MAO inhibitors.

The known inhibitors of MAO in use today are primarily used for PD but some can also be used for severe depression and illnesses like phobias, anxiety, panic and/or dysphoria and possibly also in chronic dysthymic conditions (Standaert & Young, 2006).

Fig.2.22. MAO inhibitors used in depression.

2.3.7 Genetic aspects of MAO

The role of genetics in brain diseases such as PD has become more and more recognized over the years. After the first cloning of both MAO-A and B and determination of their structures, it was clear that they were derived from a common ancestral gene. They consist of 527 (MAO-A) and 520 (MAO-B) amino acids, respectively, and also have 70% amino acid sequence identity. Using MAO's cDNA it has been found that the genes are located on the X-chromosome (Xp 11.23). The genes consist of 15 exons with identical intron-exon orientation Exon 12 codes for the binding region of FAD, and have 93.9% similarity for the two MAOs (Lees *et al*., 2009).

Fig. 2.23. Structural map of the MAO-A and -B genes showing the location of the exons (Grimsby *et al.,* 1990).

MAO knock-out mice has been engineered where these mice exhibit no expression of MAO and high levels of serotonin, norepinephrine and dopamine as well as high aggression levels, a characteristic also found in human male subjects with low MAO-A levels. On the other hand, MAO-B knock-out mice have little or no behavioural changes and only their phenylethylamine levels are elevated. Another interesting finding is that MAO-B knock-out mice are resistant to MPTP, the parkinsongenic neurotoxin. Both MAO-A and MAO-B knock-out mice display increased levels of stress. These mice are extensively used in studies of the role of monoamines in psychoses and neurodegenerative and stress disorders (Nagatsu, 2004; Shih *et al*., 1999; Lees *et al*., 2009).

2.4 Enzyme kinetics

2.4.1 Introduction

Kinetics plays a very important role in determining the affinity of an inhibitor for an enzyme. The affinity of an inhibitor for an enzyme is a measure of the degree to which an inhibitor inhibits an enzyme. Inhibitor potency is usually expressed as the K_i, the inhibitor constant. A lower K_i value results in a more effective inhibitor. The equation used for a substrate combining with an enzyme is given as:

Where S is the substrate and E the enzyme and V_i the initial rate of the reaction. There are some cases where, in the presence of excess substrate, V_i will be directly proportionate to the enzyme concentration and therefore (V_i α [E]). This leads to V_{max}, a stage where the enzyme is saturated and a further increase of substrate will have no effect on V_i and therefore the maximum rate, V_{max} is reached (Fig. 2.25.) (Dowd & Riggs, 1964).

Fig 2.24. A graph showing V_{max} and K_m.

2.4.2 The Michaelis-Menten equation

The equation describes the relationship between V_i and [S], the substrate concentration:

V_{max} is the limiting velocity as substrate concentrations get very large. V_{max} (and V) are expressed in units of product formed per time. K_m, the Michaelis constant, is the concentration of substrate that leads to half-maximal velocity (Fig. 2.25). To show this, [S] may be set equal to K_m in the equation above. Canceling terms gives $V = V_{max}/2$ (Meyer-Almes & Auer. 2000).

The velocity of an inhibitor can be evaluated under three different forms of the Michaelis-Menten equation. Firstly where [S] is much lower than K_m, then K_m+ [S] can be replaced by K_m:

Secondly where [S] is much higher than K_m, then K_m + [S] can be replaced by [S]:

And thirdly where K_m is equal to [S], and V_i can be set equal to V_{max} / 2

2.4.3 The Lineweaver-Burke plot

A convenient way to analyze enzyme kinetic data is to fit the data directly to the Michaelis-Menten equation using nonlinear regression. Before nonlinear regression was available, investigators had to transform curved data into straight line which could be analyzed by linear regression.

One way to do this is with a Lineweaver-Burk plot. This approach is based on the observation that the inverse of the Michaelis-Menten equation is a linear equation (Dowd & Riggs, 1964).

A Lineweaver-Burke plot can be created from this equation (Fig. 2.26.). The x-intercept represents the value of $-1/K_m$.

$1/V_i$ K_m/V_{max} (slope)

V_{max}(y-intercept)

$-1/K_m$ 0 1/[S]

Fig 2.25. Determination of K_m via a Lineweaver-Burke plot.

Competitive and non-competitive inhibition of enzymes can also be determined by evaluating Lineweaver-Burke plots. In competitive inhibition, V_{max} values stay consistent and the K_m values differentiate and in non-competitive inhibition the V_{max} values differentiate and the K_m values stay the same (Rodwell, 1993).

Competitive inhibition shows two straight lines, one where an inhibitor is present and the other without, that has the same y-intercept (Fig. 2.27.). For non-competitive inhibition, under the same conditions, two straight lines are also observed, but with different y-intercepts and the same x-intercept (Fig. 2.28.) (Dixon, 1952).

Fig. 2.26. Lineweaver-Burke plots showing competitive inhibition.

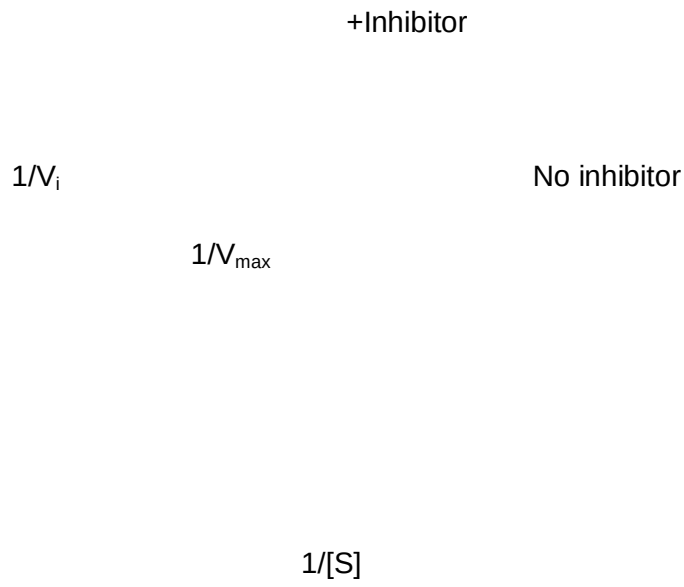

Fig. 2.27. Lineweaver-Burke plots showing non-competitive inhibition.

Because competitive inhibition has no effect on V_{max}, but increases the K_m value the K_i value can be calculated, after calculating the K_m value, using the following equation (Dixon, 1952):

An alternative way of determining the K_i value was described by Dixon in 1952 where $1/V_i$ is plotted against the inhibitor concentration [I], using a fixed substrate concentration. This process is repeated using a second, fixed substrate concentration. The two resulting lines for the two substrate concentrations are plotted and the x-coordinate of the interception represents the K_i value (Fig. 2.29. & 2.30.)

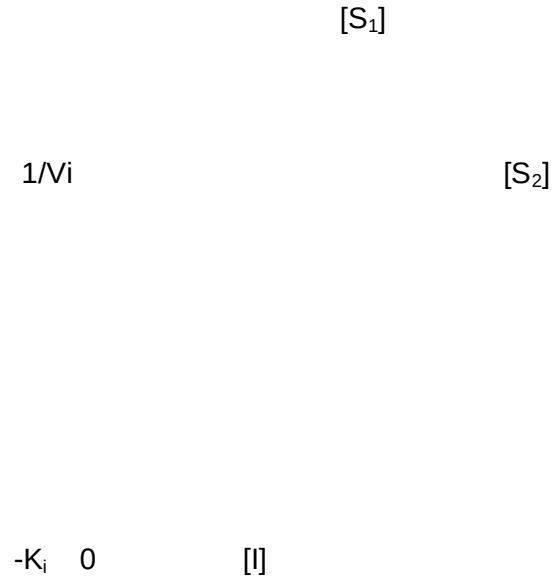

Fig 2.28. Determination of the K_i value of a competitive inhibitor according the the method by Dixon.

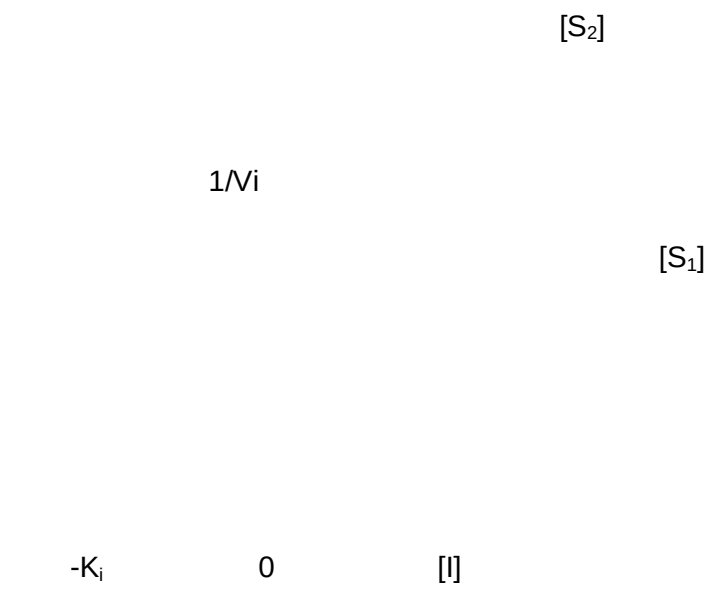

Fig 2.29. Determination of the K_i value of a non-competitive inhibitor according to the method by Dixon.

2.5 Other amine oxidases

Traditionally, amine oxidases (AOs) have been divided into two groups, based on the type of cofactor attached. The first group is the FAD-containing enzymes, MAO-A and –B, and polyamine oxidases which are intracellular enzymes. Diamine oxidases, lysyl oxidase, plasma membrane and soluble MAOs are the second class. They contain a cofactor possessing one or more carbonyl groups, which has been shown to be topa-quinone (TPQ) (Klinman & Mu, 1994). Collectively they are known as semicarbazide sensitive amine oxidases (SSAOs) due to their characteristic sensitivity to inhibition by a carbonyl-reactive compound, semicarbazide (Jalkanen *&* Salmi*,* 2001).

Fig. 2.30. A diagram illustrating the different types of amine oxidases (Jalkanen *&* Salmi*,* 2001).

The SSAOs, also called copper containing amine oxidases, differ from MAO in that their function is blocked by semicabazide (Jalkanen *&* Salmi*,* 2001). There are soluble and membrane bound forms of the enzyme in humans with the highest levels concentrated in the lung, cartilage, cardiovascular smooth muscle cells and adipose tissue. There is however little SSAO enzyme found in the microvessels of the brain and none in the nerves and glial cells (Castillo *et al.,* 1999). In the microvessels, they function as part of the protective effect

of the blood-brain barrier. MAO functions only as an intracellular enzyme and hence SSAO fills the extracellular gap that is left by MAO. In the extracellular space, SSAO can be found in blood and protects the body from harmful exogenous amines (O'Sullivan *et al*., 2004).

Copper-containing semicarbazide-sensitive amine oxidases oxidatively deaminate primary amines, via transient covalent enzyme–substrate intermediates. This reaction results in the production of aldehydes, hydrogen peroxide and ammonium which are all biologically active substances. The physiological functions of these enzymes are as yet unknown, although it has been suggested that they are involved in the metabolism of biogenic amines. A recent, new role has been proposed for these enzymes in the regulation of glucose uptake and in leukocyte–endothelial cell interactions. The functions of ectoenzymes in signalling and cell–cell adhesion suggest a new mode of molecular control of these complex processes (Jalkanen *& Salmi,* 2001).

Currently there is a good understanding of the kinetics of the enzymes' catalytic reaction. Molecular identification over the last decade of some of the SSAO subtypes by means of molecular cloning, has facilitated a better understanding of the function in humans. One of the unanswered questions is the nature of physiological SSAO substrates. Another interesting finding is that SSAO functions may be cell-type specific and except for the obvious oxidation of amines they may have other roles in the human body. Two possibilities are that SSAO may be involved in glucose metabolism and in leukocyte trafficking (Jalkanen *& Salmi*, 2001).

2.6 New developments in PD treatment

2.6.1 Adenosine A_{2A} antagonists

Non-dopaminergic therapy for PD is potentially an important new treatment strategy. Recently, adenosine A_{2A} receptor antagonists have emerged as candidates for the non-dopaminergic treatment of PD. (Pinna *et al*, 2005)

(E)-8-(3-Chlorostyryl)caffeine (CSC), is a selective antagonist of A_{2A} adenosine receptors and has been extensively employed as a referent A_{2A} antagonist. Apart from its A_{2A} antagonism, it has recently been discovered that it also has an inhibitory effect on MAO-B with an IC_{50} value of 146 nM (Pretorius *et al*., 2008). Several analogues of CSC have been synthesized to determine the structural properties required for MAO-B inhibition. A_{2A} antagonists may be used as symptomatic treatment in patients diagnosed with PD. The compound, KW-6002 (Fig. 2.33) was the first A_{2A} antagonist to undergo clinical trials for the

treatment of PD. A_{2A} agonists may not only relieve PD symptoms but may also be neuroprotective (Vlok *et al.,* 2006).

CSC, as previously mentioned, is both an MAO-B inhibitor and an A_{2A} antagonist. Since both these effects can be used in the symptomatic and neuroprotective treatment of PD, such a dual action drug may improve the treatment of PD.

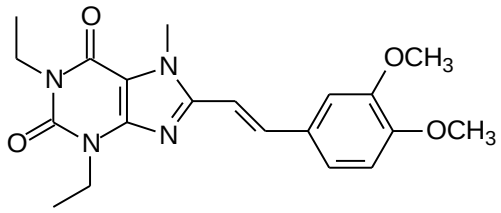

Fig. 2.31. The structure of KW-6002.

2.6.2 Antioxidants

One of the major causes of damage to dopaminergic neurons is oxidative stress. When the body and brain uses oxygen in its metabolic systems the process produces small molecules known as ROS. When they accumulate in the brain they cause oxidative stress, cell death and eventually neurodegeneration. Dopaminergic neurons are particularly sensitive to oxidative stress because the metabolism of dopamine generates very high levels of ROS. Antioxidants lower ROS levels and therefore stop the damage they cause (Yacoubian & Standaert, 2009).

2.6.2.1 Vitamins

Vitamins C and E are natural antioxidants. They are mainly responsible for lowering ROS levels. There is therefore significant interest in developing vitamin based neuroprotective therapies for PD. Some studies have found that high doses of vitamin C and E could delay the need for symptomatic medication by 2.5 years in early PD. A large-scale clinical trial of Vitamin E, however, failed to find any significant protective effect in PD (LeWitt & Taylor, 2008).

2.6.2.2 Coenzyme Q_{10}

One of the main areas in a cell that produces ROS as well as systems to scavenge ROS is the mitochondrial complex. CoQ_{10}, or ubiquinone, is a molecule that participates in the mitochondrial metabolic process and is therefore crucial to the fate of ROS in the body and brain. Some studies have shown that doses of 1200 mg/day of CoQ_{10} could slow down the progression of PD. Coenzyme Q_{10} works by improving the function of mitochondria. Coenzyme Q_{10} levels in the mitochondria of PD patients are reduced and mitochondrial function in these patients is impaired (Yacoubian & Standaert, 2009).

2.6.3 Anti inflammatory drugs

The role of inflammation and the inflammatory process has been recognized as a causative factor in PD. Some of the processes of inflammation in PD include activation of microglia, increased cytokine production and increased complement protein levels. Therefore, anti-inflammatory agents, such as non-steroidal anti-inflammatory drugs (NSAIDs) and minocycline, have been pursued as potential disease-modifying treatments for PD. Several studies have shown that certain NSAIDs, such as aspirin, have neuroprotective qualities. A recent study showed that the use of NSAIDs lowers the risk of PD by up to 45%, and in a following study it was noted that only ibuprofen had this neuroprotective effect (Chen & Swope, 2007).

A second generation tetracycline, minocycline, long used as an antimicrobial agent, also has anti-inflammatory effects. Minocycline blocks microglial activation and may also have anti-apoptotic activity in cultures. In both the MPTP and 6-OHDA animal models, minocycline protects against dopaminergic cell loss. A recent futility study showed that minocycline was well tolerated (The NINDS NET-PD Investigators, 2006)

Statins have been used as an alternative approach to targeting neuroinflammation. As well as lowering cholesterol, these drugs have anti-inflammatory effects, including reduction of TNFα, nitric oxide, and superoxide production by microglia and may also act as free radicals scavengers. Reduced dopamine loss in MPTP animal models has been reported after the use of simvastatin (Shelley, 2005).

Simvastatin prevents MPTP-induced striatal dopamine depletion and protein tyrosine nitration in mice (Shelley, 2005).Recent epidemiological studies showed that the use of simvastatin is associated with reduced PD incidence (Wolozin *et al.,* 2007; Wahner *et al*., 2008).

The general strategy of targeting neuroinflammation and the mechanisms thereof seems very promising, although there is still some controversy about its effectiveness (Yacoubian & Standaert, 2009).

CHAPTER 3

Synthesis of 8-(phenoxymethyl)caffeine analogues

3.1 Introduction

As mentioned in the introduction chapter the current study aims to synthesize 8-(phenoxymethyl)caffeine (**1**) and nine 8-(phenoxymethyl)caffeine analogues (**2**-**10**) and evaluate them as inhibitors of MAO-B. Although caffeine is a weak MAO-B inhibitor, substitutions at C8 with a variety of substituents have been shown to enhance the MAO-B inhibition potency of caffeine by several orders of a magnitude. For example, the (E)-8-(3-chlorostyryl) substituent of CSC is an illustration of a substituent that enhances the MAO-B inhibition potency of caffeine to a large extent. Also, it has been found that substitution of caffeine at C-8 with a benzyloxy side-chain also dramatically enhances the MAO-B inhibition potency of caffeine. In this study caffeine will be substituted with a phenoxymethyl functional group at C-8 instead of the benzyloxy moiety. The aim of this study is therefore to compare the MAO-B inhibition potencies of the 8-(phenoxymethyl)caffeine analogues with the previously studied 8-benzyloxycaffeine analogues. Since 8-benzyloxycaffeines are also reported to be MAO-A inhibitors, the 8-(phenoxymethyl)caffeine analogues that will be synthesized here will also be evaluated as human MAO-A inhibitors. Fig. 3.1 illustrates the 8-(phenoxymethyl)caffeine analogues that will be synthesized in this study.

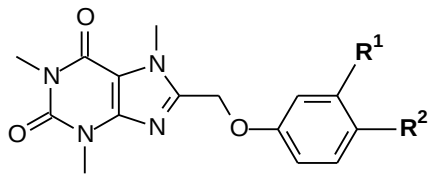

Compound	R^1	R^2
1	H	H
2	Cl	H
3	Br	H
4	F	H
5	CF_3	H
6	CH_3	H
7	OCH_3	H
8	H	Cl
9	H	Br
10	H	F

Fig. 3.1. The chemical structures of the 8-(phenoxymethyl)caffeine analogues that will be synthesized in this study.

Since one of the aims of this study is to compare the MAO-A and –B inhibition potencies of 8-benzyloxycaffeines with those of 8-(phenoxymethyl)caffeine analogues, similar substituents on the phenoxymethyl phenyl ring were selected as those that were previously employed for the series of 8-benzyloxycaffeines (Strydom *et al*., 2010). The 8-benzyloxycaffeines studied before were substituted at C3 of the benzyloxy ring. Similarly, seven of the 8-(phenoxymethyl)caffeine analogues contained substituents on C3 of the phenyl ring. The substituents that were selected included halogens (Cl, F and Br), the methyl group, the methoxy group and the trifluoromethyl group (Fig. 3.1). The halogen derivatives were incorporated into the study due to their strong electron withdrawing capabilities. On the other hand, the metoxy and methyl substituents were employed since they are electron donating/releasing. This series therefore includes substituents which are relatively large (Br, OCH_3), substituents considered to be sterically bulky (Br, CF_3, CH_3) and substituents with a relatively large (CF_3) and low degree (OCH_3) of lipophilicity. As mentioned in the introduction chapter, the selection of these substituents is based on the fact that the physicochemical properties of the substituents are sufficiently diverse to allow for a Hansch-type quantitative structure-activity relationship (QSAR) study.

3.2 General synthetic approaches for the synthesis of 8-(phenoxymethyl)caffeine analogues (1-10)

A general synthetic route used for the preparation of C8 substituted caffeine analogues makes use of 1,3-dimethyl-5,6-diaminouracil as starting compound (Fig. 3.2.) (Shimada *et al*., 1992; Muller *et al*., 1997a; Suzuki *et al*., 1993). The C8 substituted caffeine analogues may be prepared in high yield, according to the procedure previously reported for the preparation of (*E*)-8-styrylcaffeinyl analogues (Suzuki *et al*., 1993). Acylation of 1,3-dimethyl-5,6-diaminouracil (**A**) with the appropriate substituted phenoxyacetic acid (**B**) (prepared from the corresponding phenol analogue) is carried out in the presence of a carbodiimide activating reagent, N-(3-dimethylaminopropyl)-N′-ethylcarbodiimide hydrochloride (EDAC). The intermediary amide so prepared is then treated with sodium hydroxide which results in ring closure to yield the corresponding 1,3-dimethyl-8-phenoxymethyl-7H-xanthinyl analogues (**C**) (Shimada *et al.,* 1992). Without further purification, compound **C** is selectively 7N-methylated in the presence of an excess of iodomethane and potassium carbonate to yield the target compounds (**D**) (Suzuki *et al.,* 1993). Following crystallization from a suitable solvent, analytically pure samples of the target compounds are obtained.

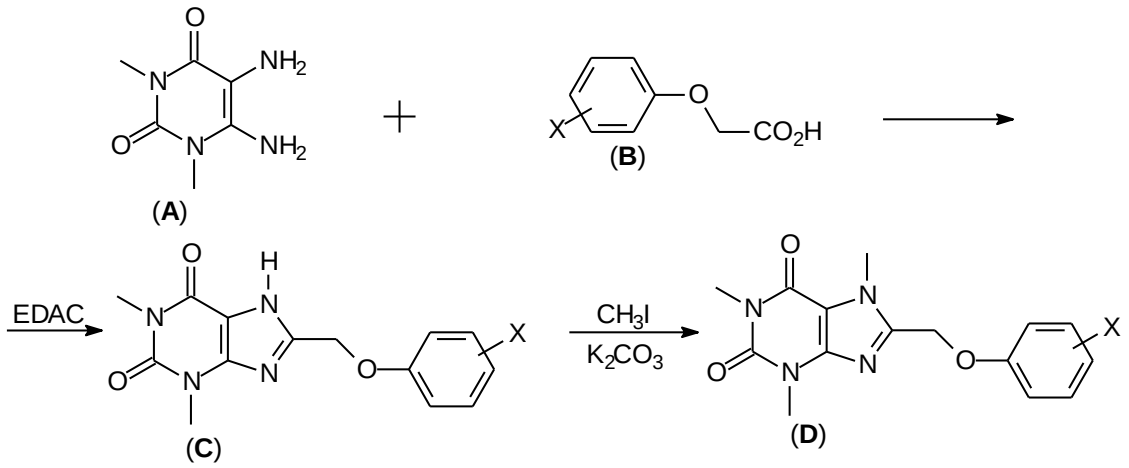

Fig. 3.2. Reaction scheme for the synthesis of 8-(phenoxymethyl)caffeine analogues.

3.3 General synthetic approaches for the synthesis of 1,3-dimethyl-5,6-diaminouracil

1,3-Dimethyl-5,6-diaminouracil can be prepared from a general procedure, described by Traube (1900), where a symmetric urea (**A**) is condensed with cyanoacetic acid (**B**) in the presence of acetic anhydride to produce a cyanoacetylurea (**C**) (Fig. 3.3.). Ring closure is brought forth by treating (**C**) with sodium hydroxide (Papesch & Schroeder, 1951) and yields 1,3-dimethyl-6-aminouracil (**D**). After treating (**D**) with sodium nitrite in the presence of an acid the corresponding nitroso derivative (**E**) is obtained. (**E**) is then reduced to the desired 1,3-dimethyl-5,6-diaminouracil (**F**) with ammonia water and sodium hydrosulfite (Speer & Raymond, 1953).

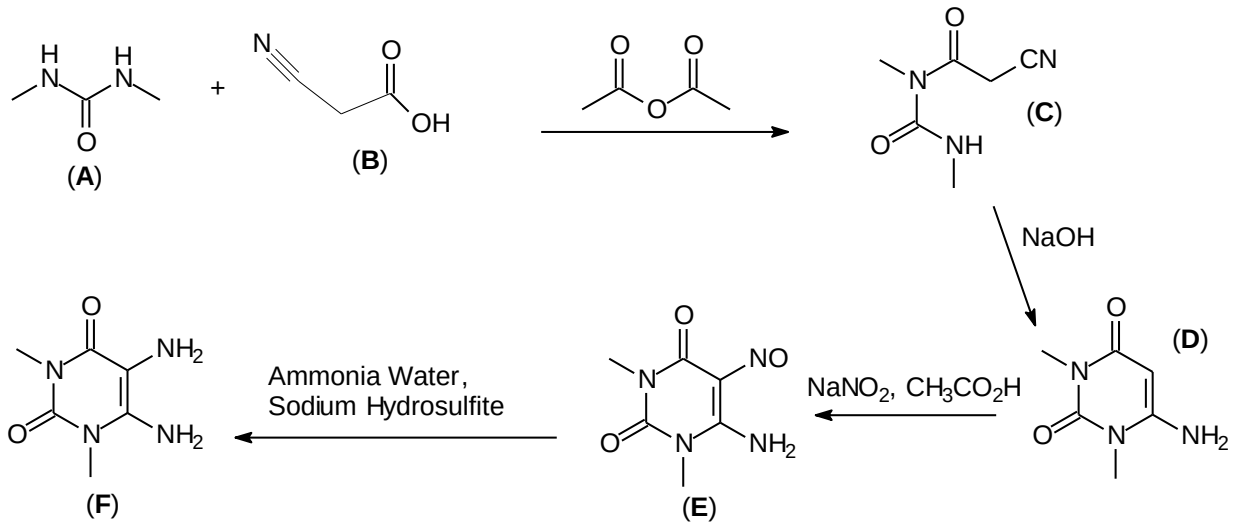

Fig. 3.3. Formation of 1,3-dimethyl-5,6-diaminouracil.

3.4 General synthetic approaches for the synthesis of phenoxyacetic acids.

Since only 6 of the required phenoxyacetic acids were commercially available a general synthetic route was used for the preparation of the other acids required (Zhao *et al.,* 2005; Koelsch, 1931; Hayes & Branch, 1943). The appropriate phenol (**A**) (Fig. 3.4.) is added to a solution of sodium hydroxide in water and then chloroacetic acid is added. The reaction is heated, water is added and the mixture is acidified with concentrated hydrochloric acid. The product (**B**) is then extracted to an organic solvent such as diethylether.

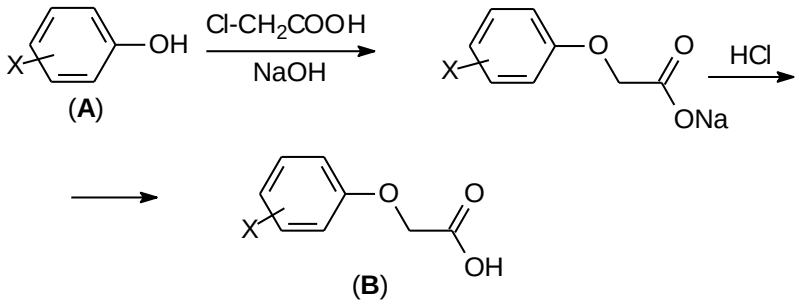

Fig. 3.4. Reaction scheme for the formation of the phenoxyacetic acids that were required for the synthesis of selected 8-(phenoxymethyl)caffeines.

3.5 Materials and Instrumentation

Unless otherwise noted, all starting materials were obtained from Sigma-Aldrich and were used without purification. Proton (^{1}H) and carbon (^{13}C) NMR spectra were recorded on a Bruker Avance III 600 spectrometer at frequencies of 600 MHz and 150 MHz, respectively. All NMR measurements were conducted in $CDCl_3$ and the chemical shifts are reported in parts per million (δ) downfield from the signal of tetramethylsilane added to the deuterated solvent. Spin multiplicities are given as s (singlet), brs (broad singlet), d (doublet), dd (doublet of doublets), t (triplet) or m (multiplet). Direct insertion electron impact ionization (EIMS) and high resolution mass spectra (HRMS) were obtained on a DFS high resolution magnetic sector mass spectrometer (Thermo Electron Corporation) in electron ionization (EI) mode. Melting points (mp) were determined on a Stuart SMP10 melting point apparatus and are uncorrected. Thin layer chromatography (TLC) was carried out, using silica gel 60 (Merck) with UV_{254} fluorescent indicator. To determine the purities of the synthesized compounds, HPLC analyses were conducted with an Agilent 1100 HPLC system equipped with a quaternary pump and an Agilent 1100 series diode array detector (see Supplementary Material). HPLC grade acetonitrile (Merck) and Milli-Q water (Millipore) was used for the chromatography.

3.6 General synthetic procedure

3.6.1 The synthesis of the required phenoxyacetic acids

An appropriately substituted phenol (50 mmol) was added to a solution of sodium hydroxide (187.5 mmol) in 15 ml of water and an orange solution formed. Then chloroacetic acid (85 mmol) was added slowly at 40 °C. The mixture was heated to 85 °C and stirring was continued for 2 h. 100 ml of water was added after the mixture was cooled to room temperature. The solution was filtered and acidified with concentrated hydrochloric acid to pH 1–2. The brown oil fraction was extracted twice to diethylether (50 ml). The ether fraction was further extracted twice with 5% sodium bicarbonate solution (37.5 ml). The sodium bicarbonate solution was acidified to pH 1–2 with concentrated hydrochloric acid and yielded a solid product. The solid product was collected by filtration and dried to obtain the required compounds.

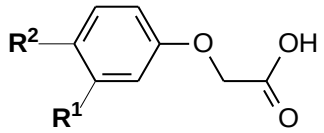

Compound	R^1	R^2
1	H	H
2	Cl	H
3	Br	H
4	F	H
5	CF_3	H
6	CH_3	H
7	OCH_3	H
8	H	Cl
9	H	Br
10	H	F

Fig. 3.5. The chemical structures of the phenoxyacetic acids used in this study.

3.6.2 The synthesis of 1,3-dimethyl-5-nitroso-6-aminouracil

The N,N'-dimethylurea (50 mmol) and the cyanoacetic acid (50 mmol) was placed in a roundbottom flask and acetic anhydride (6.25 ml) was added. With a $CaCl_2$ trap attached, the reaction was heated (60 °C) for 3 hours to yield a colourless to light yellow solution. The reaction was cooled on ice and 10% sodium hydroxide (60 ml) was added to yield a white suspension. The pH tested 11 and the reaction was stirred for a further 30 minutes at room temperature. A solution of sodium nitrate (60 mmol) was added followed by 8 ml of glacial acetic acid. The reaction turned pink. At this stage, the pH tested 5. A further 7 ml glacial acetic acid was added over a period of 1 hour. Stirring was continued for an additional hour and the purple product was collected via filtration and washed with 20 ml diethylether.

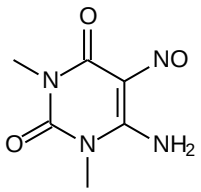

Fig. 3.6. Chemical structure of 1,3-dimethyl-5-nitroso-6-aminouracil.

3.6.3 The synthesis of 1,3-dimethyl-5,6-diaminouracil

1,3-Dimethyl-5-nitroso-6-aminouracil (20 mmol) was powdered and 20 ml ammonia water (32%) was added to yield an orange suspension. The suspension was heated to 40 °C and freshly prepared sodium hydrosulfite (11 g in 50 ml water) was added over a period of 15 minutes. The suspension firstly changed into a red solution which later became green. Approximately 47 ml sodium hydrosulfite was added. The reaction was cooled on ice for a period of 4 hours. The light yellow crystals were collected via filtration and were washed with 20 ml water. The product was left to dry overnight in a fume cupboard.

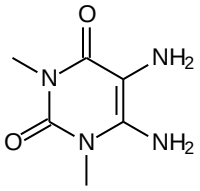

Fig. 3.7. Chemical structure of 1,3-dimethyl-5,6-diaminouracil.

3.6.4 The synthesis of the 1,3-dimethyl-8-substituted-xanthinyl analogues

1,3-Dimethyl-5,6-diaminouracil (4 mmol) and N-(3-dimethylaminopropyl)-N′-ethylcarbodiimide hydrochloride (EDAC; 5.36 mmol) were dissolved in 41.2 mL dioxane/H_2O (1:1) and the appropriate phenoxyacetic acid (4 mmol) was added. A thick suspension was obtained and the pH was adjusted to 5-6 with 20 drops of 4 M aqueous hydrochloric acid. The colour changed from white to light orange. Stirring was continued for an additional 2 h at room temperature. The reaction mixture changed into a thick, pink suspension, which was then neutralized with 65 drops of 1 M aqueous sodium hydroxide upon which the colour turned to light green. The precipitate that formed had a white colour and was collected by filtration. While still wet, the precipitate was suspended in 20 ml dioxane. Upon addition of 20 ml 1 M sodium hydroxide, the precipitate dissolved to yield a dark yellow solution. The reaction was heated (100-110 °C) under reflux for 2 h, cooled to 0 °C and then acidified to a pH of 4 with 4 M aqueous hydrochloric acid (12-13 ml). The resulting precipitate, that is the corresponding 1,3-dimethyl-8-substituted-7H-xanthinyl analogue, was collected by filtration, washed with 50 ml water and oven dried at 50 °C.

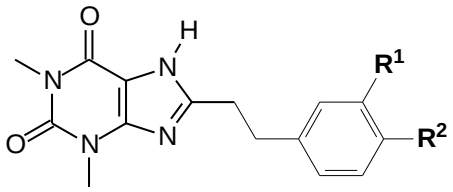

Compound	R^1	R^2
1	H	H
2	Cl	H
3	Br	H
4	F	H
5	CF_3	H
6	CH_3	H
7	OCH_3	H
8	H	Cl
9	H	Br
10	H	F

Fig. 3.8. Chemical structure of the 1,3-dimethyl-8-substituted-xanthinyl analogues.

3.6.5 The synthesis of C-8 substituted caffeine analogues

The 1,3-dimethyl-8-substituted-xanthinyl analogue (2 mmol) was dissolved in a minimum amount of DMF (approximately 20 ml) at 90 °C and a yellow solution formed. Potassium carbonate (5 mmol) was added, but does not dissolve. Iodomethane (4 mmol) was added and the colour of the reaction became lighter. The reaction was then heated at 90 °C for 60 minutes. When TLC indicated completion of the reaction, the insoluble materials were removed by filtration. Water (350 ml) was added to the filtrate to precipitate the product which was cooled on ice for 3 hours. The precipitate was collected via filtration and dried overnight at room temperature.

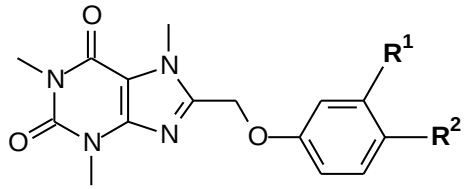

Compound	R^1	R^2
1	H	H
2	Cl	H
3	Br	H
4	F	H
5	CF_3	H
6	CH_3	H
7	OCH_3	H
8	H	Cl
9	H	Br
10	H	F

Fig. 3.9. Chemical structures of the target 8-(phenoxymethyl)caffeine analogues.

3.7 Recrystallization

The product was dissolved in 50 ml ethylacetate and 70 ml methanol was added while boiling. The clear solution so obtained was allowed to recrystallize at room temperature for a minimum of 12 hours. The crystals were washed with 20 ml ethylacetate and analytically pure samples of the target compounds were obtained.

3.8 Physical characterization

The structures of the 8-(phenoxymethyl)caffeine analogues were verified by ^{1}H-NMR and ^{13}C-NMR, as well as by nominal and high resolution mass spectrometry. The purities of the target compounds were verified by HPLC analysis. For the purpose of the HPLC analysis, strong eluting condition (up to 85% acetonitrile) were employed and the eluent was monitored at 210 nm, a wavelength where most organic compounds absorb UV light. It is therefore likely that impurities, if present, will elute and be detected under these conditions. The HPLC conditions and chromatograms obtained is given in the addendum.

3.9 Results

3.9.1 Phenoxyacetic acids

Six phenoxyacetic acids were synthesized in this study and are shown in fig. 3.10. All the phenoxyacetic acids have been synthesized previously and the melting points obtained in this study correspond to those reported. As mentioned above, the phenoxyacetic acids synthesised here are not commercially available and are required to prepare selected 8-(phenoxymethyl)caffeine analogues.

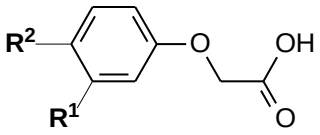

Compound	R^1	R^2	Melting point obtained	Melting point from literature
1	H	H	Commercially available	-
2	Cl	H	108-109°C	108-110°C (Hayes & Branch, 1943)
3	Br	H	107-108°C	107-108.8°C (Hayes & Branch, 1943)
4	F	H	114-115°C	111-112°C (Hayes & Branch, 1943)
5	CF_3	H	92-93°C	93.5-94.5°C (Newman *et al.*, 1947)
6	CH_3	H	101-105°C	102-103.5°C (Hayes & Branch, 1943)
7	OCH_3	H	117-118°C	111-118°C (Hayes & Branch, 1943)
8	H	Cl	Commercially available	-
9	H	Br	Commercially available	-
10	H	F	Commercially available	-

Fig. 3.10. Chemical structures of phenoxyacetic acids used in this study.

3.9.2 The physical data for the 8-(phenoxymethyl)caffeine analogues

8-Phenoxymethylcaffeine (1)

The title compound was prepared from phenoxyacetic acid in a yield of 73%: mp 197–199 °C (methanol/ethyl acetate 7:5). **^{1}H NMR** (Bruker Avance III 600, $CDCl_3$) δ 3.37 (s, 3H), 3.56 (s, 3H), 4.03 (s, 3H), 5.17 (s, 2H), 6.99 (m, 3H), 7.29 (t, 2H, J = 7.53 Hz). **^{13}C NMR** (Bruker Avance III 600, $CDCl_3$) δ 27.9, 29.7, 32.4, 62.0, 108.7, 114.6, 122.0, 129.7, 147.4, 147.9, 151.6, 155.4, 157.5. **Mass spectrometry**: EIMS 300; EI-HRMS *m*/*z*: calcd for **$C_{15}H_{16}N_4O_3$**, 300.1222, found 300.1218. **Purity** (HPLC): 99.8%. **$C_{15}H_{16}N_4O_3$**

8-(3-Chlorophenoxymethyl)caffeine (2)

The title compound was prepared from 3-chlorophenoxyacetic acid in a yield of 83%: mp 201-203 °C (methanol/ethyl acetate 7:5). **^{1}H NMR** (Bruker Avance III 600, $CDCl_3$) δ 3.38 (s, 3H), 3.56 (s, 3H), 4.02 (s, 3H), 5.15 (s, 2H), 6.86 (d, 1H), 6.97 (d, 1H), 7.01 (s, 1H), 7.19 (t, 1H, J = 7.53 Hz). **^{13}C NMR** (Bruker Avance III 600, $CDCl_3$) δ 27.9, 29.7, 32.4, 62.1, 108.8, 113.0, 115.4, 122.3, 130.5, 135.1, 147.2, 147.4, 151.5, 155.4, 158.2. **Mass spectrometry**: EIMS 368; EI-HRMS *m*/*z*: calcd for $C_{15}H_{16}O_3N_4$, 334.0833, found 334.0843. **Purity** (HPLC): 95.5%. **$C_{15}H_{15}ClN_4O_3$**

8-(3-Bromophenoxymethyl)caffeine (3)

The title compound was prepared from 3-bromophenoxyacetic acid in a yield of 78%: mp 200-204 °C (methanol/ethyl acetate 7:5). **^{1}H NMR** (Bruker Avance III 600, $CDCl_3$) δ 3.37 (s, 3H), 3.56 (s, 3H), 4.02 (s, 3H), 5.15 (s, 2H), 6.92 (d, 1H, J = 7.5 Hz), 7.13 (m, 3H). **^{13}C NMR** (Bruker Avance III 600, $CDCl_3$) δ 27.9, 29.7, 32.4, 62.1, 108.8, 113.5, 118.2, 122.9, 125.2, 130.8, 147.2, 147.4, 151.5, 155.4, 158.2. **Mass spectrometry**: EIMS 378; EI-HRMS *m*/*z*: calcd for **$C_{15}H_{15}BrN_4O_3$**, 378.0328, found 378.0301. **Purity** (HPLC): 99.8%. **$C_{15}H_{15}BrN_4O_3$**

8-(3-Fluorophenoxymethyl)caffeine (4)

The title compound was prepared from 3-fluorophenoxyacetic acid in a yield of 67%: mp 198-201 °C (methanol/ethyl acetate 7:5). **^{1}H NMR** (Bruker Avance III 600, $CDCl_3$) δ 3.38 (s, 3H), 3.56 (s, 3H), 4.03 (s, 3H), 5.16 (s, 2H), 6.69 (m, 2H), 6.76 (dd, 1H, J = 2.3, 8.3 Hz), 7.23 (m, 1H). **^{13}C NMR** (Bruker Avance III 600, $CDCl_3$) δ 27.9, 29.7, 32.4, 62.1, 108.8, 113.5, 118.2, 122.9, 125.2, 130.8, 147.2, 147.4, 151.5, 155.4, 158.2. **Mass spectrometry**: EIMS 318; EI-HRMS *m*/*z*: calcd for **$C_{15}H_{15}FN_4O_3$**, 318.1128, found 318.1131. **Purity** (HPLC): 99.5%. **$C_{15}H_{15}FN_4O_3$**

8-(3-Trifluoromethylphenoxymethyl)caffeine (5)

The title compound was prepared from 3-trifluorophenoxyacetic acid in a yield of 52%: mp 172-174 °C (methanol/ethyl acetate 7:5). **^{1}H NMR** (Bruker Avance III 600, $CDCl_3$) δ 3.38 (s, 3H), 3.56 (s, 3H), 4.04 (s, 3H), 5.22 (s, 2H), 7.17 (d, 1H, J = 7.5 Hz), 7.24 (m, 2H), 7.39 (t, 1H, J = 8.3 Hz). **^{13}C NMR** (Bruker Avance III 600, $CDCl_3$) δ 27.9, 29.7, 32.4, 62.2, 108.8, 111.3 (q), 118.2, 118.7 (q), 122.8, 124.6, 130.6, 132.2 (q), 147.0, 147.3, 151.6, 155.4, 157.7. **Mass spectrometry**: EIMS 368; EI-HRMS *m*/*z*: calcd for **$C_{16}H_{15}F_3N_4O_3$**, 368.1096, found 368.1081. **Purity** (HPLC): 99.8%. **$C_{16}H_{15}F_3N_4O_3$**

8-(3-Methylphenoxymethyl)caffeine (6)

The title compound was prepared from 3-methylphenoxyacetic acid in a yield of 72%: mp 195-196 °C (methanol/ethyl acetate 7:5). **^{1}H NMR** (Bruker Avance III 600, $CDCl_3$) δ 2.30 (s, 3H), 3.37 (s, 3H), 3.55 (s, 3H), 4.02 (s, 3H), 5.14 (s, 2H), 6.77 (m, 3H), 7.14 (t, 1H, J = 8.3 Hz). **^{13}C NMR** (Bruker Avance III 600, $CDCl_3$) δ 21.4, 27.9, 29.7, 32.4, 62.0, 108.7, 111.3, 115.5, 122.8, 129.4, 139.8, 147.3, 148.0, 151.5, 155.4, 157.5. **Mass spectrometry**: EIMS 314; EI-HRMS *m*/*z*: calcd for **$C_{16}H_{18}N_4O_3$**, 314.1379, found 314.1386. **Purity** (HPLC): 99.0%. **$C_{16}H_{18}N_4O_3$**

8-(3-Methoxyphenoxymethyl)caffeine (7)

The title compound was prepared from 3-methoxyphenoxyacetic acid in a yield of 37%: mp 165-167 °C (methanol/ethyl acetate 7:5). **^{1}H NMR** (Bruker Avance III 600, $CDCl_3$) δ 3.36 (s, 3H), 3.54 (s, 3H), 3.75 (s, 3H), 4.03 (s, 3H), 5.17 (s, 2H), 6.53 (m, 3H), 7.16 (t, 1H, J = 8.7 Hz). **^{13}C NMR** (Bruker Avance III 600, $CDCl_3$) δ 27.9, 29.7, 32.4, 55.3, 62.0, 101.2, 106.7, 107.5, 108.7, 130.1, 147.3, 147.8, 151.5, 155.4, 158.7, 160.9. **Mass spectrometry**: EIMS 330; EI-HRMS *m*/*z*: calcd for **$C_{16}H_{18}N_4O_4$**, 330.1328, found 330.1320. **Purity** (HPLC): 98.9%. **$C_{16}H_{18}N_4O_4$**

8-(4-Chlorophenoxymethyl)caffeine (8)

The title compound was prepared from 4-chlorophenoxyacetic acid in a yield of 52%: mp 181-183 °C (methanol/ethyl acetate 7:5). **^{1}H NMR** (Bruker Avance III 600, $CDCl_3$) δ 3.36 (s, 3H), 3.54 (s, 3H), 4.01 (s, 3H), 5.13 (s, 2H), 6.90 (d, 2H, J = 8.7 Hz), 7.21 (d, 2H, J = 8.7 Hz). **^{13}C NMR** (Bruker Avance III 600, $CDCl_3$) δ 27.9, 29.7, 32.4, 62.2, 108.7, 116.0, 127.0, , 129.6, 147.3, 147.4, 151.5, , 155.4, 156.0. **Mass spectrometry**: EIMS 334; EI-HRMS *m*/*z*: calcd for **$C_{15}H_{15}ClN_4O_3$**, 334.0833, found 334.0838. **Purity** (HPLC): 99.8%. **$C_{15}H_{15}ClN_4O_3$**

8-(4-Bromophenoxymethyl)caffeine (9)

The title compound was prepared from 4-bromophenoxyacetic acid in a yield of 80%: mp 195-197°C (methanol/ethyl acetate 7:5). **^{1}H NMR** (Bruker Avance III 600, $CDCl_3$) δ 3.35 (s, 3H), 3.53 (s, 3H), 4.00 (s, 3H), 5.12 (s, 2H), 6.91 (d, 2H, J = 8.7 Hz), 7.35 (d, 2H, J = 9.0 Hz). **^{13}C NMR** (Bruker Avance III 600, $CDCl_3$) δ 27.9, 29.7, 32.4, 32.5, 62.1, 108.7, 114.3, 116.4, 132.5, 147.2, 147.3, 151.5, 155.3, 155.4, 156.5. **Mass spectrometry**: EIMS 378; EI-HRMS *m*/*z*: calcd for **$C_{15}H_{15}BrN_4O_3$**, 378.0328, found 378.0317. **Purity** (HPLC): 99.4%. **$C_{15}H_{15}BrN_4O_3$**

8-(4-Fluorophenoxymethyl)caffeine (10)

The title compound was prepared from 4-fluorophenoxyacetic acid in a yield of 79%: mp 212-213°C (methanol/ethyl acetate 7:5). **^{1}H NMR** (Bruker Avance III 600, $CDCl_3$) δ 3.37 (s, 3H), 3.55 (s, 3H), 4.02 (s, 3H), 5.13 (s, 2H), 6.94 (m, 4H). **^{13}C NMR** (Bruker Avance III 600, $CDCl_3$) δ 27.9, 29.7, 32.4, 62.6, 108.7, 115.8, 115.9, 116.2, 147.3, 147.6, 151.5, 153.6, 155.4, 157.1, 158.7. **Mass spectrometry**: EIMS 318; EI-HRMS *m*/*z*: calcd for **$C_{15}H_{15}FN_4O_3$**, 318.1128, found 318.1114. **Purity** (HPLC): 99.4%. **$C_{15}H_{15}FN_4O_3$**

In Table 3.1 the structures of the target 8-(phenoxymethyl)caffeine analogues are given and correlated with the ^{1}H NMR data. All of the appropriate signals were observed for each compound **1**-**10**. These include the 3 singlets for the caffeine methyl groups, the singlet for the CH_2 and the signals for the aromatic protons. The singlet's of the methyl and methoxy groups (substituted on the phenyl ring) of compounds **6** and **7** were also observed. The appropriate integration values and chemical shifts were also observed for all signals. In addition, the ^{13}C NMR data (not tabulated) also corresponded to each of the target structures in terms of the number of ^{13}C signals and their expected chemical shifts.

Table 3.1. Correlation of the ^{1}H NMR data with the structures of the 8-(phenoxymethyl)caffeine analogues

Product name	**Structure**	**^{1}H NMR signal assignment**
1 **$C_{15}H_{16}N_4O_3$**	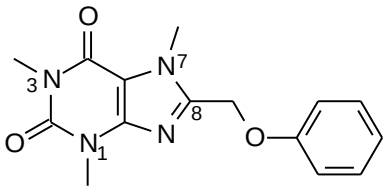	**a**. Methyl groups at N-1, N-3 and N-7 – singlets at 3.37 (3H), 3.56 (3H) and 4.03 (3H) ppm. **b**. CH_2– singlet at 5.17 (2H) ppm **c.** Aromatic protons – signals at 6.99 (3H), 7.29 (2H) ppm
2 **$C_{15}H_{15}ClN_4O_3$**	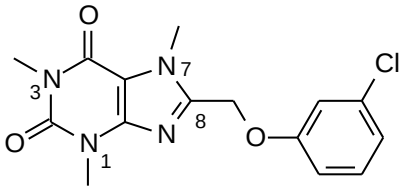	**a**. Methyl groups at N-1, N-3 and N-7 – singlets at 3.37 (3H), 3.56 (3H) and 4.02 (3H) ppm. **b**. CH_2– singlet at 5.15 (2H) ppm **c.** Aromatic protons – signals at 6.86 (1H), 6.97 (1H), 7.01 (1H), 7.19 (1H) ppm
3 **$C_{15}H_{15}BrN_4O_3$**	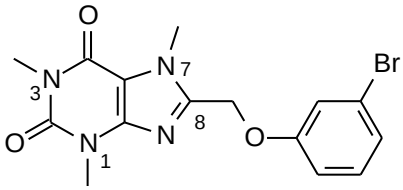	**a**. Methyl groups at N-1, N-3 and N-7 – singlets at 3.37 (3H), 3.56 (3H) and 4.02 (3H) ppm. **b**. CH_2– singlet at 5.15 (2H) ppm **c.** Aromatic protons – signals at 6.92 (1H), 7.13 (3H) ppm

4 **$C_{15}H_{15}FN_4O_3$**	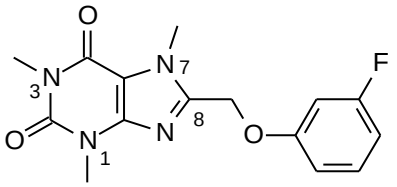	**a**. Methyl groups at N-1, N-3 and N-7 – singlets at 3.38 (3H), 3.56 (3H) and 4.03 (3H) ppm. **b**. CH_2– singlet at 5.16 (2H) ppm **c.** Aromatic protons – signals at 6.69 (2H), 6.77 (1H), 7.23 (1H) ppm
5 **$C_{16}H_{15}F_3N_4O_3$**	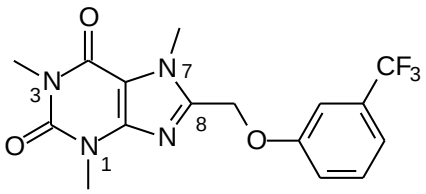	**a**. Methyl groups at N-1, N-3 and N-7 – singlets at 3.38 (3H), 3.56 (3H) and 4.04 (3H) ppm. **b**. CH_2– singlet at 5.22 (2H) ppm **c.** Aromatic protons – signals at 7.17 (1H), 7.24 (2H), 7.29 (1H) ppm
6 **$C_{16}H_{18}N_4O_3$**	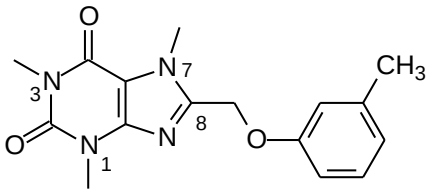	**a**. Methyl group on the phenyl ring – singlet at 2.30 (3H) ppm. **b**. Methyl groups at N-1, N-3 and N-7 – singlets at 3.37 (3H), 3.55 (3H) and 4.02 (3H) ppm. **c**. CH_2– singlet at 5.14 (2H) ppm **d.** Aromatic protons – signals at 6.77 (3H), 7.14 (H) ppm
7 **$C_{16}H_{18}N_4O_4$**	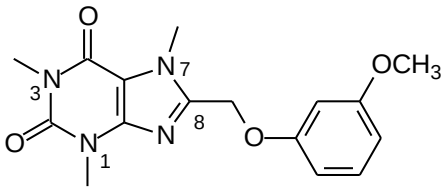	**a**. Methoxy methyl group on the phenyl ring – singlet at 3.75 (3H) ppm. **b**. Methyl groups at N-1, N-3 and N-7 – singlets at 3.36 (3H), 3.54 (3H), and 4.03 (3H) ppm. **c**. CH_2– singlet at 5.13 (2H) ppm **d**. Aromatic protons – signals at 6.53 (3H), 7.16 (1H) ppm

8 **$C_{15}H_{15}ClN_4O_3$**	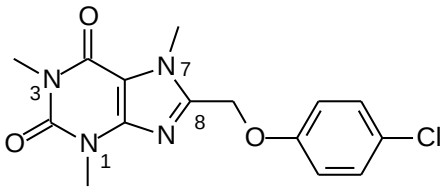	**a**. Methyl groups at N-1, N-3 and N-7 – singlets at 3.36 (3H), 3.54 (3H) and 4.01 (3H) ppm. **b**. CH_2– singlet at 5.13 (2H) ppm **c.** Aromatic protons – signals at 6.90 (2H), 7.21 (2H) ppm
9 **$C_{15}H_{15}BrN_4O_3$**	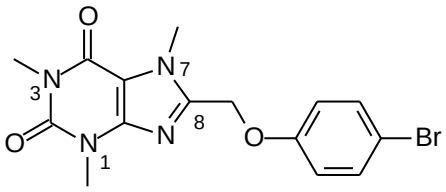	**a**. Methyl groups at N-1, N-3 and N-7 – singlets at 3.35 (3H), 3.53 (3H) and 4.00 (3H) ppm. **b**. CH_2– singlet at 5.12 (2H) ppm **c.** Aromatic protons – signals at 6.91 (2H), 7.35 (2H) ppm
10 **$C_{15}H_{15}FN_4O_3$**	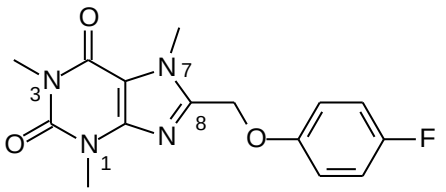	**a**. Methyl groups at N-1, N-3 and N-7 – singlets at 3.367 (3H), 3.55 (3H) and 4.02 (3H) ppm. **b**. CH_2– singlet at 5.13 (2H) ppm **c**. Aromatic protons – signal at 6.94 (4H) ppm

As shown in table 3.2 the high resolution masses that were obtained for each of the 8-(phenoxymethyl)caffeine analogues very closely corresponded to the calculated values. This is further confirmation of the structures of these compounds.

Table 3.2. Correlation of the calculated exact masses with the experimentally obtained masses of the 8-(phenoxymethyl)caffeine analogues

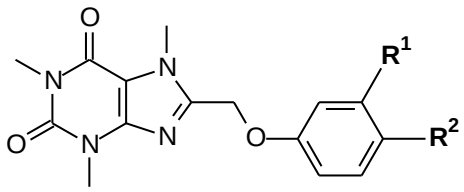

				Mass Spectrometry		
Compound	**R^1**	**R^2**	**Formula**	**Calcd.**	**Found**	**ppm**
1	H	H	**$C_{15}H_{16}N_4O_3$**	300.1222	300.1218	-1.33
2	Cl	H	**$C_{15}H_{15}ClN_4O_3$**	334.0833,	334.0843	2.99
3	Br	H	**$C_{15}H_{15}BrN_4O_3$**	378.0328,	378.0301	-7.14
4	F	H	**$C_{15}H_{15}FN_4O_3$**	318.1128,	318.1131	0.943
5	CF_3	H	**$C_{16}H_{15}F_3N_4O_3$**	368.1096,	368.1096	0
6	CH_3	H	**$C_{16}H_{18}N_4O_3$**	314.1379,	314.1386	2.23
7	OCH_3	H	**$C_{16}H_{18}N_4O_4$**	330.1328,	330.1320	-2.42
8	H	Cl	**$C_{15}H_{15}ClN_4O_3$**	334.0833,	334.0838	1.50
9	H	Br	**$C_{15}H_{15}BrN_4O_3$**	378.0328,	378.0317	-2.91
10	H	F	**$C_{15}H_{15}FN_4O_3$**	318.1128,	318.1114	-4.40

ppm = [(found – calcd.)/calcd]. x 1000000. In general a ppm difference smaller than 5 is considered to be good agreement.

3.10 Conclusion

This chapter describes the successful synthesis of the target 8-(phenoxymethyl)caffeine analogues **(1-10)**. All structures were confirmed by NMR and MS and the purities by HPLC analysis. Both the ^{1}H NMR and ^{13}C NMR spectra corresponded with the proposed structures and the expected exact masses were also recorded for each compound. In addition, HPLC analysis revealed a single peak for each compound analysed.

CHAPTER 4

Enzymology

4.1 Introduction

In this chapter the 8-(phenoxymethyl)caffeine analogues (**1**-**10**) that were synthesized in the previous chapter, were investigated as inhibitors of MAO-A and –B and compared to the 8-benzyloxycaffeine analogues examined previously (Strydom *et al*., 2010). Compounds acting as inhibitors may be considered as potential lead compounds for the development of drugs for the treatment of PD. These studies should establish if the goal of this study was achieved, namely the design of new potent, reversible and competitive inhibitors of the monoamine oxidases. As outlined in the Introduction, the objectives of this chapter were as follows:

- The 8-(phenoxymethyl)caffeine analogues (**1**-**10**) that were synthesized in the previous chapter, will be evaluated as inhibitors of MAO-A and –B. The inhibition potencies will be expressed as the IC_{50} values for the inhibition of the MAO`s. For this purpose, the recombinant human enzymes (which are commercially available) will be employed. A fluorometric assay will be used to measure the enzyme activities. The MAO activity measurements will be based on measuring the amount of H_2O_2 that is produced in the oxidation process. The H_2O_2 reacts with Amplex Red in the presence of peroxidise form resorufin. The quantity of resorufin in the reactions is proportional to the amount of H_2O_2 produced by the enzyme and will subsequently be determined by measuring the fluorescence of the supernatant at an excitation wavelength of 560 nm and an emission wavelength of 590 nm (Zhou & Panchuk-Voloshina, 1997).

- In order to determine if the inhibitors interact reversibly or irreversibly with MAO-A and –B, the time-dependency of inhibition of both human MAO-A and –B by selected 8-(phenoxymethyl)caffeine analogues will be evaluated.

- If the inhibition is found to be reversible, a set of Lineweaver-Burke plots will be generated for a selected inhibitor in order to determine if the mode of inhibition is competitive.

- A Hansch-type QSAR study will be carried out in order to quantify the effect that different substituents on the phenyl ring of the 8-(phenoxymethyl)caffeine analogues have on MAO-B inhibition activity. For this purpose only the 8-(phenoxymethyl)caffeine analogues bearing C3 substituents will be employed. The

results of this study will be compared to those obtained previously for a series of C3 substituted 8-benzyloxycaffeine analogues (Strydom *et al*., 2010).

4.2 Chemicals and instrumentation

For fluorescence spectrophotometry, a Varian Cary Eclipse fluorescence spectrophotometer was employed. Microsomes from insect cells containing recombinant human MAO-A and –B (5 mg/ml) and kynuramine.2HBr were obtained from Sigma-Aldrich. The Amplex Red (10-acetyl-3,7-dihydroxyphenoxazine) reagent, horseradish peroxidise and H_2O_2 (3%) were also from Sigma-Aldrich.

4.3 Biological evaluation to determine the IC_{50} values

4.3.1 Introduction

For these studies a fluorometric method was used to determine the activities of MAO-A and –B (Zhou & Panchuk-Voloshina, 1997). This protocol measures the amount of H_2O_2 produced by the MAO catalysed oxidation process. In this method, H_2O_2 is reacted in a horseradish peroxidise-coupled reaction with the Amplex Red reagent (10-acetyl-3,7-dihydroxyphenoxazine). Amplex Red is a very sensitive probe for H_2O_2 and when reacted in the presence of peroxidase, forms a stable product. When Amplex red and H_2O_2 react with each other the fluorescent dye, resorufin, is formed. The amount of resorufin formed can be measured with fluorescence spectrofluorometry and is directly proportional to the amount of H_2O_2 produced by MAO. Resorufin has an absorption maximum of 571 nm and a fluorescence emission maximum of 585 nm. At these long wavelengths there is little or no interference from other components typically found in biological samples or in the enzymatic reactions carried out here.

4.3.2 Method

Recombinant human MAO-A and -B (5 mg/mL) were obtained from Sigma–Aldrich, pre-aliquoted and stored at −70 °C. Potassium phosphate buffer (100 mM, pH 7.4, made isotonic with KCl) was used for all the enzymatic reactions. The reactions contained MAO-A and –B (0.0075 mg/mL), various concentrations of the test inhibitor (0–100 µL), kynuramine, horseradish peroxidase (HRP) and Amplex Red. The HRP/Amplex Red working solution contained HRP (5 units/mL) and Amplex Red (1 mM) in potassium phosphate buffer. The final concentrations of kynuramine in the reactions were 30 µM and 45 µM where MAO-B and -A, respectively, served as substrates. The final volume of the reactions was 500 µL and was made up of 50 µL kynuramine (substrate), 20 µL test inhibitor, 280 µL potassium

phosphate (buffer), 100 µL HRP/Amplex Red working solution and 50 µL enzyme (0.075 mg/ml). Stock solutions of the test inhibitors were prepared in DMSO and added to the reactions to yield a final concentration of 4% (v/v) DMSO. The reactions were incubated for 20 min at 37 °C and terminated with the addition of 10 µL derenyl (5 mM) for MAO-B and 10 µL clorgyline (5 mM) for MAO-A. Distilled water (1400 µL) was added to each reaction before it was centrifuged for 10 min at 16,000*g*. The different concentrations of the MAO generated resorufin, in the reactions were determined by measuring the fluorescence of the supernatant at an excitation wavelength of 560 nm and an emission wavelength of 590 nm (Zhou & Panchuk-Voloshina, 1997). Quantitative estimations of resorufin were made by means of a linear calibration curve consisting of H_2O_2 at concentrations ranging from 0.05 to 0.65 µM. Each calibration standard was prepared to a final volume of 500 µL in potassium phosphate buffer (100 mM, pH 7.4) and contained 4% DMSO. To each standard was added 10 µL derenyl (5 mM) for MAO-B and 10 µL clorgyline (5 mM) for MAO-A and 1400 µL distilled water. The IC_{50} values were determined by plotting the initial rate of oxidation versus the logarithm of the inhibitor concentration to obtain a sigmoidal dose–response curve.

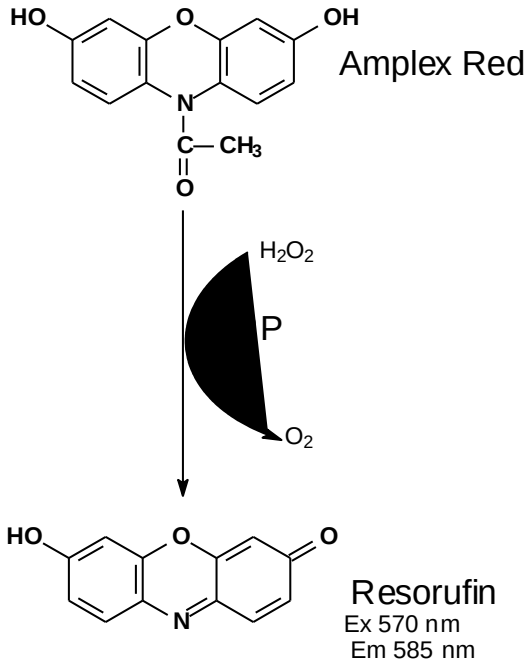

Fig. 4.1. Reaction scheme for the formation of resorufin, the fluorescent product from Amplex Red.

4.3.3 Results – Sigmoidal curves obtained for the IC_{50} determinations

The IC_{50} of a product represents the concentration of a drug that is needed for 50% inhibition *in vitro*. The logarithms of die different concentrations of the inhibitor are plotted graphically against the rate of the MAO catalyzed oxidation of kynuramine and the concentration of the inhibitor which reduces the rate to half of the maximal value is the IC_{50}. As an example, the sigmoidal curve for the determination of the IC_{50} value towards human MAO-B of the most potent compound (**4**) is given in Fig. 4.2.

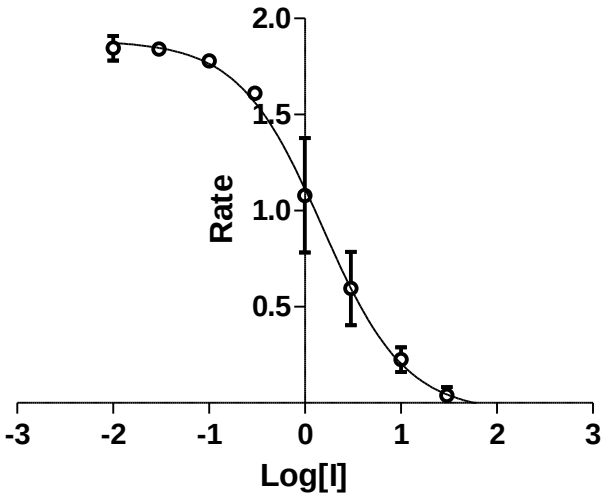

Fig. 4.2. The sigmoidal dose-response curve of the initial rates of oxidation of kynuramine by recombinant human MAO-B vs. the logarithm of concentration of inhibitor (**4**) (expressed in µM). The determinations were carried out in duplicate and the values are expressed as the mean ± SD. The concentration of kynuramine used was 30 µM and the rate data are expressed as nmoles 4-hydroxyquinoline formed/min/mg protein.

4.3.4 Results – Table with IC_{50} values

Presented in Table 1 is the IC_{50} values that were measured for both the inhibition of recombinant human MAO-A and –B by the 8-(phenoxymethyl)caffeine analogues (**1**-**10**). Lower IC_{50} values indicate that an inhibitor has a higher binding affinity for the enzyme and is therefore a more potent inhibitor. Also given are the selectivity indexes of each inhibitor. The selectivity index (SI) is the selectivity of the inhibitor for the MAO-B isoform and is given as the ratio of the IC_{50} value for the inhibition of MAO-A versus the IC_{50} value for the inhibition of MAO- B. A higher selectivity index value indicates that an inhibitor is selective for the MAO-B isoenzyme.

Table 4.1. The IC_{50} values for the inhibition of recombinant human MAO-A and –B by compounds **1**-**10**[a]

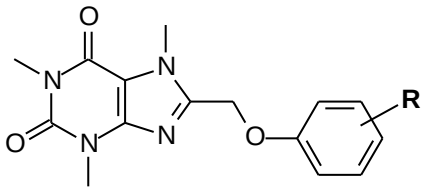

Compd.	R	MAO-A IC_{50} (µM)	MAO-B IC_{50} (µM)	SI[b]
1	H	21.1 ± 3.23	5.78 ± 0.935	3.7
2	3-Cl	No inhibition	0.334 ± 0.010	–
3	3-Br	34.0 ± 31.5	0.148 ± 0.002	229.7
4	3-F	13.2 ± 7.74	1.61 ± 0.723	8.2
5	3-CF_3	4.59 ± 1.06	0.641 ± 0.010	7.1
6	3-CH_3	18.8 ± 1.52	1.23 ± 0.088	15.3
7	3-OCH_3	No inhibition	1.96 ± 0.065	–
8	4-Cl	20.4 ± 7.27	0.250 ± 0.040	81.6
9	4-Br	10.7 ± 2.89	0.189 ± 0.018	56.6
10	4-F	8.22 ± 0.336	0.825 ± 0.044	9.9

[a] All values are expressed as the mean ± SD of duplicate determinations.

[b] The selectivity index is the selectivity for the MAO-B isoform and is given as the ratio of IC_{50}(MAO-A)/IC_{50}(MAO-B).

As shown in Table 4.1 the 8-(phenoxymethyl)caffeine analogues (**1**-**10**) evaluated in this study were inhibitors of both human MAO-A and -B. The only exceptions were compounds **2** and **7** which were found not to be MAO-A inhibitors. The following general observations may be made from the IC_{50} values given in table 4.1:

- **2** and **7** are selective for MAO-B and showed no inhibition for MAO-A.
- **5** is the most potent MAO-A inhibitor with an IC_{50} value of 4.59 µM. This compound also exhibits a relative low degree of isoform selectivity (7 fold).
- **3** and **9** are the most potent MAO-B inhibitors with IC_{50} values in the nano-molar range, 0.148 µM and 0.189 µM, respectively. These two inhibitors also exhibit a high degree of selectivity for MAO-B with SI values of 229.7 and 56.6 for **3** and **9**, respectively. Both these inhibitors are substituted with a bromine on the 8-(phenoxymethyl)caffeine phenyl ring which shows that bromine substitution is most favourable for MAO-B inhibition among the substituents evaluated in this study.
- **3** is approximately half as potent as an MAO-B inhibitor as safinamide (IC_{50} = 0.08 µM), an MAO-B inhibitor currently in clinical trials for the treatment of PD (Strydom *et al*., 2010).
- Of importance is the observation that **1** is the weakest MAO-B inhibitor among the compounds evaluated. This suggests that substitution on the phenyl ring of the 8-(phenoxymethyl)caffeine analogues enhances the MAO-B inhibition potencies.
- Interestingly, the analogues bearing methyl and methoxy substituents on the phenyl ring of the phenoxymethyl substituent are relatively weak MAO-B inhibitors. Since the methyl and methoxy groups are electron donating/releasing groups it may be concluded that electron withdrawing functional groups on the phenyl ring of the phenoxymethyl substituent are more optimal for MAO-B inhibition. In accordance with this view, the 8-(phenoxymethyl)caffeine analogues bearing electron withdrawing functional groups (Cl, Br, F and CF_3) are all potent MAO-B inhibitors with IC_{50} values in the nM range. The only exception is the 8-(phenoxymethyl)caffeine analogue bearing F at C3 which is slightly less potent than the corresponding analogue bearing a CH_3.

Table 4.2. A comparison of the IC_{50} values for the inhibition of MAO-B of the 8-(phenoxymethyl)caffeine analogues bearing Cl, Br, F and CF_3 substituents on C3 of the phenyl ring with the analogue bearing CH_3.

C3 Substituent	IC_{50} value (μM)	Ratio CH_3/X^a
CH_3	1.23	-
Cl	0.334	3.68
Br	0.148	8.31
F	1.61	0.76
CF_3	0.641	1.92

[a]The ratio of $IC_{50}(CH_3)/IC_{50}$(Cl, Br, F or CF_3)

Table 4.3. A comparison of the IC_{50} values for the inhibition of MAO-B of the 8-(phenoxymethyl)caffeine analogues bearing Cl, Br, F and CF_3 substituents on C3 of the phenyl ring with the analogue bearing OCH_3.

C3 Substituent	IC_{50} value (μM)	Ratio OCH_3/X^a
OCH_3	1.96	-
Cl	0.334	5.87
Br	0.148	13.26
F	1.61	1.22
CF_3	0.641	3.05

[a]The ratio of $IC_{50}(OCH_3)/IC_{50}$(Cl, Br, F or CF_3)

— It is important to note that all of the inhibitors evaluated in this study are MAO-B selective. It may therefore be concluded that, in future studies, 8-(phenoxymethyl)caffeine analogues may be used as a lead for the development of MAO-B selective inhibitors.

— Interestingly, for both the 8-(phenoxymethyl)caffeine analogues bearing C3 and C4 halogen substituents, the bromine substituted homologues are the most potent MAO-B inhibitors, followed by the chlorine an then the fluorine substituted homologues. Since the size and degree of steric hindrance of bromine is the largest followed by chlorine and then the fluorine, it may be concluded that larger phenyl substituents with a higher degree of steric hindrance is required for more potent inhibition of MAO-

B. Therefore, this study recommends that, in future studies, 8-(phenoxymethyl)caffeine analogues bearing an iodine on C3 and C4 of the phenoxymethyl phenyl ring should be synthesized and examined as an MAO-B inhibitor. The iodine containing analogue may possibly also be a potent inhibitor of MAO-B, since iodine has a larger steric volume than bromine, chlorine and fluorine. Iodine, however, has a relative low electronegativity while a higher degree of electronegativity seems to be a requirement for potent MAO-B inhibition (see argument above).

Table 4.4. A comparison of the IC_{50} values for the inhibition of MAO-B of the 8-(phenoxymethyl)caffeine analogues bearing Cl, Br and F substituents on C3 of the phenyl ring with the unsubstituted analogue.

C3 Substituent	IC_{50} value (μM)	Ratio H/X[a]
H	5.78	-
Cl	0.334	17.31
Br	0.148	39.04
F	1.61	3.59

[a]The ratio of IC_{50}(H)/IC_{50}(Cl, Br or F)

Table 4.5. A comparison of the IC_{50} values for the inhibition of MAO-B of the 8-(phenoxymethyl)caffeine analogues bearing Cl, Br, and F substituents on C4 of the phenyl ring with the unsubstituted analogue.

C4 Substituent	IC_{50} value (μM)	Ratio H/X[a]
H	5.78	-
Cl	0.250	23.12
Br	0.189	30.58
F	0.825	7.01

[a]The ratio of IC_{50}(H)/IC_{50}(Cl, Br, F or CF_3)

— The importance of a higher degree of substituent volume and steric hindrance for MAO-B inhibition potency is also apparent when comparing the 8-(phenoxymethyl)caffeine analogues bearing a methyl group and a methoxy group on the phenyl ring with the unsubstituted analogue. Both the methyl and methoxy substituted analogues are better inhibitors than the unsubstituted analogue. Since

both the methyl and methoxy adds volume and steric bulk to the 8-(phenoxymethyl)caffeine structure, it may be concluded that these physicochemical properties are important for MAO-B inhibition.

Table 4.6. A comparison of the IC_{50} values for the inhibition of MAO-B of the 8-(phenoxymethyl)caffeine analogues bearing CH_3 and OCH_3 substituents on C3 of the phenyl ring with the unsubstituted analogue.

C3 Substituent	IC_{50} value (μM)	Ratio H/X[a]
H	5.78	-
CH_3	1.23	4.70
OCH_3	1.96	2.95

[a]The ratio of IC_{50}(H)/IC_{50}(CH_3 or OCH_3)

— The 8-(phenoxymethyl)caffeine analogues bearing chlorine and fluorine substituents at C4 of the phenyl ring are more potent MAO-B inhibitors than the C3 substituted analogues. The analogues bearing bromine at C4 of the phenyl ring is slightly less potent than the analogues bearing bromine at C3. Based on the limited data available, it may be speculated that *para* substituents on the phenyl ring are in general slightly more optimal for MAO-B inhibition than *meta* substituents.

Table 4.7. A comparison of the IC_{50} values for the inhibition of MAO-B of the 8-(phenoxymethyl)caffeine analogues containing C3 substituents on the phenyl ring with those bearing C4 substituents.

Substituent	C3 Substituent IC_{50} value (μM)	C4 Substituent IC_{50} value (μM)	Ratio C3/C4[a]
Cl	0.334	0.250	1.34
Br	0.148	0.189	0.78
F	1.61	0.825	1.95

[a]The ratio of IC_{50}(C3 substituent)/IC_{50}(C4 substituent)

4.3.5. Comparison of the MAO inhibition potential of the 8-(phenoxymethyl)caffeines with those of the 8-benzyloxycaffeines

As mentioned in the objectives, one aim of the current study is to compare the MAO inhibition potencies of the 8-(phenoxymethyl)caffeine analogues to those obtained previously for a series of C3 substituted 8-benzyloxycaffeine analogues (Strydom *et al*., 2010). Shown below are IC_{50} values of the 8-benzyloxycaffeine analogues for the inhibition of recombinant human MAO-A and -B.

Table 4.8. The IC_{50} values for the inhibition of recombinant human MAO-A and –B by 8-benzyloxycaffeine analogues (Strydom *et al.,* 2010).

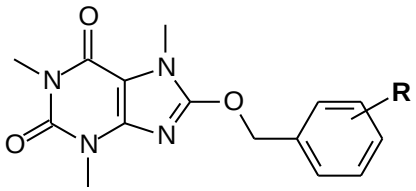

Compd.	R	MAO-A IC_{50} (µM)	MAO-B IC_{50} (µM)	SI[a]
11	3-H	1.24	1.77	0.7
12	3-Cl	0.666	0.107	6.22
13	3-Br	0.941	0.068	13.84
14	3-F	1.07	0.542	1.98
15	3-CF_3	3.72	0.152	24.8
16	3-CH_3	0.397	0.546	0.73
17	3-OCH_3	3.15	1.01	3.12

[a] The selectivity index is the selectivity for the MAO-B isoform and is given as the ratio of IC_{50}(MAO-A)/IC_{50}(MAO-B).

Compared to the IC_{50} values of the 8-(phenoxymethyl)caffeine analogues listed in Table 4.8, the following observation were made:

- Compared to the 8-(phenoxymethyl)caffeine analogues, the 8-benzyloxycaffeines are more potent MAO-A inhibitors. The benzyloxy side chain is therefore better able to enhance the MAO-A inhibition potency than the phenoxymethyl side chain. This shows that though structurally similar, the biological activities of the benzyloxy and phenoxymethyl side chains differ significantly.

  Table 4.9. A comparison of the IC_{50} values for the inhibition of MAO-A of the 8-(phenoxymethyl)caffeine analogues with the 8-benzyloxycaffeine analogues.

C3 substituent	**IC_{50} (µM)**		**Ratio**
	8-Benzyloxy caffeines	8-(Phenoxymethyl) caffeines	(Phenoxymethyl) caffeines/ Benzyloxycaffeines
3-H	1.24	21.1	17.02
3-Cl	0.666	-	-
3-Br	0.941	34	36.13
3-F	1.07	13.2	12.33
3-CF_3	3.72	4.59	1.22
3-CH_3	0.397	18.8	47.35
3-OCH_3	3.15	-	-

- Since the 8-benzyloxycaffeines are more potent MAO-A inhibitors than the 8-(phenoxymethyl)caffeine analogues, they are in general less selective for the MAO-B isoform. In fact, 8-benzyloxycaffeine and 8-(3-methylbenzyloxy)caffeine is slightly MAO-A selective.

- The 8-benzyloxycaffeine analogues are in general more potent inhibitors of MAO-B than the respective 8-phenoxymethylcaffeine analogues. For example, the most potent benzyloxycaffeine, **13** has an IC_{50} value of 0.068 µM while the most potent 8-(phenoxymethyl)caffeine analogue, compound **3**, has an IC_{50} value of 0.148 µM.

- As observed for the 8-(phenoxymethyl)caffeine analogues the analogues bearing methyl and methoxy substituents on the phenyl ring of the C8 side chain are relatively weak MAO-B inhibitors while analogues bearing electron withdrawing functional groups (Cl, Br, F and CF_3) are all potent MAO-B inhibitors. Electron withdrawing functional groups are therefore required for potent MAO-B inhibition by both the 8-(phenoxymethyl)caffeine and 8-benzyloxycaffeine analogues.

Table 4.10. A comparison of the IC_{50} values for the inhibition of MAO-B of the 8-benzyloxycaffeine analogues bearing Cl, Br, F and CF_3 substituents on C3 of the phenyl ring with the analogue bearing CH_3.

C3 Substituent	IC_{50} value (μM)	Ratio CH_3/X[a]
CH_3	0.546	-
Cl	0.107	5.10
Br	0.068	8.03
F	0.542	1.01
CF_3	0.152	3.60

[a]The ratio of $IC_{50}(CH_3)/IC_{50}$(Cl, Br, F or CF_3)

Table 4.11. A comparison of the IC_{50} values for the inhibition of MAO-B of the 8-benzyloxycaffeine analogues bearing Cl, Br, F and CF_3 substituents on C3 of the phenyl ring with the analogue bearing OCH_3.

C3 Substituent	IC_{50} value (μM)	Ratio OCH_3/X[a]
OCH_3	1.01	-
Cl	0.107	9.44
Br	0.068	14.85
F	0.542	1.86
CF_3	0.152	6.64

[a]The ratio of $IC_{50}(OCH_3)/IC_{50}$(Cl, Br, F or CF_3)

- As observed for the 8-(phenoxymethyl)caffeine analogues among the halogen substituted analogues the bromine substituted benzyloxycaffeine is the most potent MAO-B inhibitor, followed by the chlorine and then the fluorine substituted

benzyloxycaffeines. Therefore, phenyl substituents with a higher degree of steric hinderance are required for more potent inhibition of MAO-B by both the 8-phenoxymethylcaffeine and 8-benzyloxycaffeine analogues.

Table 4.12. A comparison of the IC_{50} values for the inhibition of MAO-B of the 8-benzyloxycaffeine analogues bearing Cl, Br and F substituents on C3 of the phenyl ring with the unsubstituted analogue.

C3 Substituent	IC_{50} value (μM)	Ratio H/X[a]
H	1.77	-
Cl	0.107	16.54
Br	0.068	26.03
F	0.542	3.27

[a]The ratio of IC_{50}(H)/IC_{50}(Cl, Br or F)

- The 8-benzyloxycaffeine analogues bearing a methyl group and a methoxy group on the phenyl ring are better inhibitors than the unsubstituted analogue. This is similar to the trend observed with the 8-(phenoxymethyl)caffeine analogues and suggests that a higher degree of substituent volume and steric hinderance is required for enhanced MAO-B inhibition potency

Table 4.13. A comparison of the IC_{50} values for the inhibition of MAO-B of the 8-benzyloxycaffeine analogues bearing CH_3 and OCH_3 substituents on C3 of the phenyl ring with the unsubstituted analogue.

C3 Substituent	IC_{50} value (μM)	Ratio H/X[a]
H	1.77	-
CH_3	0.546	3.24
OCH_3	1.01	1.75

[a]The ratio of IC_{50}(H)/IC_{50}(CH_3 or OCH_3)

4.3.6 Hansch-type structure-activity relationships studies

As seen from the results of the MAO inhibition studies, interesting structure-activity relationships exist between the experimentally determined IC_{50} values and the substituent on the phenyl ring of the 8-(phenoxymethyl)caffeine analogues. In this section of the study, selected physicochemical properties of the substituents on C3 of the phenyl ring will be correlated with the IC_{50} values for the inhibition of MAO-B. The relationship between MAO inhibition and the physiochemical properties of the substituents on the phenyl rings of the inhibitors may be described by the Hansch-type QSAR study. Five parameters (V_w, E_s, π, σ and F) are frequently used to describe the physicochemical properties of a substituent at the meta or para position of a phenyl ring of a biological active molecule. These parameters were selected for the current study since the values of these parameters are experimentally determined values and not calculated values. The bulkiness of a substituent is described by the Van der Waals volume (V_w) and the Taft steric parameter (E_s) while the lipophilicity is described by the Hansch constant (π). The way in which a drug interacts with a receptor is greatly influenced by these steric parameters. The electronic properties of the substituents are described by Swain-Lupton constant (F) and the Hammett constant (σ). A model system, where the effect of a substituent on the ionization of benzoic acids was measured, was used to calculate the values of the electronic parameters of the substituents. Electronic effects are frequently very influential on the biological avtivities of organic molecules (Vlok *et al*., 2006).

Table 4.14. The values of the physicochemical parameters (V_w, E_s, Π, σ and F) used for the Hansch-type QSAR study.

	V_w	E_s	Π	σ	F
3-H	0.08	0	0	0	0
3-Cl	1.07	-0.97	0.71	0.37	0.42
3-Br	1.32	-1.16	0.86	0.39	0.45
3-F	0.36	-0.46	0.14	0.34	0.45
3-CF_3	1.11	-2.4	0.88	0.43	0.38
3-CH_3	1.01	-1.24	0.56	-0.07	0.01
3-OCH_3	1.49	-0.55	-0.02	0.12	0.29

All values of the selected parameters used were obtained from literature (Hansch *et al.,* 1995, Van de Waterbeemb *et al.,* 1987).

In a Hansch-type QSAR study the logarithm of the measured activities ($logIC_{50}$) of a series inhibitors are correlated with the substituent descriptor values by means of a linear ($y = ax + c$) or multivariate linear ($y = ax, + bx_2 + c$) equation. The x-axis equals the V_w, E_s, Π, σ and F values and the y-axis equals the $logIC_{50}$ value. This regression analysis is carried out to calculate the influence of the substituent parameters on the inhibition potency of the inhibitor and the correlation constant (R^2) is calculated. A correlation constant (R^2) of 1 leads to the conclusion that there is an exact correlation between the inhibitor's potency and the physiochemical parameter used. Therefore the closer the R^2 is to 1, the better the correlation and it is therefore possible to predict the influence of different substituent's on an inhibitor`s potency (Gnerre *et al*., 2000). The correlation constant (R^2) is related to the error variance by a *F* value and the higher the *F* value the better the fit. The critical *F* value (F_{max}) can be calculated and if the *F* value of the correlation is higher than the critical *F* value, the correlation is deemed significant (Livingstone & Salt, 2005). The critical F_{max} value for 95% significance for models containing seven $logIC_{50}$ values and two out of a possible five parameters (V_W, E_S,Π, σ and F) was calculated to be 30.18 and where only one parameter was used, the F_{max} value was 25.32 (Strydom *et al.,* 2010; Livingstone & Salt, 2005).

As mentioned above, the Hansch-type SAR analysis was carried out for the seven 8-(phenoxymethyl)caffeine analogues containing substituents at C3 of the phenyl ring. The statistical analysis was carried out with the Statistica software (version 10; StatSoft Inc.). Preliminary results showed that there is no correlation between the physicochemical parameters of the substituents and the MAO-A inhibition potencies. For this reason, only the results obtained with the MAO-B inhibition potencies are presented below. Also, the SAR analysis was not carried out for the 8-(phenoxymethyl)caffeine analogues containing C4 substituents on the phenyl ring, due the small number of inhibitors in this series. As a rule of thumb, 5 compounds are needed for each term in the linear equation. Based on the F_{max} values, a meaningful correlation can however be generated with a smaller amount of test compounds.

The results of the statistical analysis for the inhibition of recombinant human MAO-B by the 8-(phenoxymethyl)caffeine analogues containing substituents at C3 of the phenyl ring are shown in table 4.15.

Table 4.15. Correlations of recombinant human MAO-B inhibition ($logIC_{50}$) by 8-(phenoxymethyl)caffeine analogues with steric, electronic and hydrophobic descriptors of the substituents at C3 of the phenyl ring[a].

Parameter	Slope	y-intercept	R^2	*F*	Significance[b]
σ	**-1.785 ± 0.827**	**0.381 ± 0.243**	**0.48**	**4.66**	**0.083**
F	**-1.784 ± 0.871**	**0.488 ± 0.296**	**0.45**	**4.18**	**0.096**
V_W	**-0.650 ± 0.357**	**0.577 ± 0.369**	**0.39**	**3.31**	**0.128**
π	**-1.136 ± 0.303**	**0.486 ± 0.175**	**0.73**	**14.06**	**0.013**
E_S	**0.389 ± 0.252**	**0.356 ± 0.303**	**0.32**	**2.37**	**0.183**
σ + π	**-0.974 ± 690** **-0.906 ± 0.355**	**0.563 ± 0.183**	**0.80**	**8.15**	**0.31** **0.06**
***F* + π**	**-1.05 ± 0.515** **-0.928 ± 0.258**	**0.695 ± 0.171**	**0.87**	**13.6**	**0.11** **0.023**

[a] The logarithm of the IC_{50} values (expressed in µM) was used in the linear regression analysis.

[b] The significance is the fractional probability that the coefficient of the added variable is zero.

The results show that the π lipophilicity constant has the best correlation with the $logIC_{50}$ values while and the electronic parameter, σ, also showed a relatively good correlation with the inhibition potencies ($logIC_{50}$). For the correlation between π and $LogIC_{50}$ an R^2 value of 0.73 and an *F* value of 14.06 (F_{max} = 25.32) was calculated. The best correlations were however obtained from a combination of two parameters. The two parameter correlation of F and π with the $logIC_{50}$ values yielded the best correlation with a R^2 of 0.87 and an *F* of 13.6 (F_{max} = 30.18) (Fig 4.3). Since the calculated *F* value is lower than the F_{max} value, the correlation is not statistically significant. The probability that F and π are zero for this correlation is 11% and 2.3% respectively. The best mathematical description for the binding affinity of C3 substituted, 8-phenoxymethylcaffeine analogues to recombinant MAO-B is therefore:

$$\text{Log } IC_{50} = -1.05(\pm 0.515)F - 0.928(\pm 0.258)\pi + 0.695(\pm 0.171)$$

$$R^2 = 0.87 \text{ and } F = 13.6$$

(1)

This equation is graphically represented in figure 4.3.

Fig. 4.3. Correlations of the log IC_{50} values for the inhibition of recombinant human MAO-B by C3 substituted 8-(phenoxymethyl)caffeine analogues with the Hansch constant (π). The π values were adjusted by the contribution of the Swain-Lupton constant (F) as indicated on the x-axis titles. The linear regression line is a representation of equation 1.

The two parameter correlation of of π and σ with the logIC_{50} values also showed a good correlation with an R^2 of 0.80 and an *F* value of 8.15 (F_{max} = 30.18). Although the statistical *F* value is lower than the F_{max}, the correlation supports the findings of the linear equation given above. These are:

- The negative signs of the *F* and σ_m parameter coefficients indicate that the inhibition potencies of compounds **1–7** towards human MAO-B may be enhanced by substitution with more electron withdrawing groups at C3 of the phenoxymethyl phenyl ring. Larger values of F and σ_m indicate a higher degree of electron withdrawal by the functional group. This finding is similar to the results of the QSAR study carried out with the 8-benzyloxycaffeine analogues (Strydom *et al*., 2010). The logIC_{50} values of the 8-benzyloxycaffeine analogues also correlated with the F and σ_m electronic parameters and the signs of these parameter coefficients were also negative. The best mathematical description of the inhibition of human MAO-B by the 8-benzyloxycaffeine analogues were:

$\log IC_{50} = -1.15F - 1.04\pi + 0.30$ ($R^2 = 0.89$ and $F = 25.4$)

- The negative signs of the π parameter coefficient indicate that the inhibition potencies of compounds **1–7** towards human MAO-B may be enhanced by substitution with more lipophilic functional groups on C3 of the phenoxymethyl phenyl ring. Larger values of π indicate a higher degree of lipophilicity of the functional group.

- In this study the best linear equation that correlates the $\log IC_{50}$ values to the F and π parameter coefficients ($\text{Log}IC_{50} = -1.05F - 0.928\pi + 0.695$) was derived from 7 compounds. Although the correlation is not significant (as judged by the statistical F value), the addition of at least 3 more analogues would improve the model. This study suggests that the 8-(phenoxymethyl)caffeine analogues containing the following 3 substituents on C3 of the phenoxymethyl phenyl ring be synthesized and evaluated as MAO-B inhibitors in future studies. The theoretical IC_{50} values, calculated according to the equation cited above, are also given:

Table 4.16. The substituents on C3 of the phenoxymethyl phenyl ring of the 8-(phenoxymethyl)caffeine analogues that may be examined in future studies. For each substituent the respective F and π parameter values are provided together with the theoretical IC_{50} values for the inhibition of human MAO-B.

	F	**π**	**Calculated IC_{50} (μM)**
I	0.42	1.12	0.164
NO_2	0.65	-0.28	1.87
SO_2CF_3	0.74	0.55	0.256

4.4 Time-dependent studies

4.4.1 Introduction

Also known as reversibility studies, time-dependent studies evaluate whether an inhibitor binds covalently (irreversible) or non-covalently (reversible) to the enzyme. For the time-dependent studies an assay where the enzyme activity measurements are based on the extent to which kynuramine is oxidized to 4-hydroxyquinoline by the MAO isoforms (Novaroli *et al*., 2005) (Fig. 4.4) will be employed. The inhibitor and the enzyme (MAO-A or –B) will be combined and incubated for different periods of time (0, 15, 30, 60 minutes). The substrate (kynuramine) will subsequently be added and the reactions will be incubated for a further 15 min. The MAO-catalysed 4-hydroxyquinoline formation will then be measured fluorometrically at excitation and emission wavelengths of 310 nm and 400 nm, respectively. An inhibitor is reversible if the amount of 4-hydroxyquinoline generated by MAO over the 4 time periods remains unchanged.

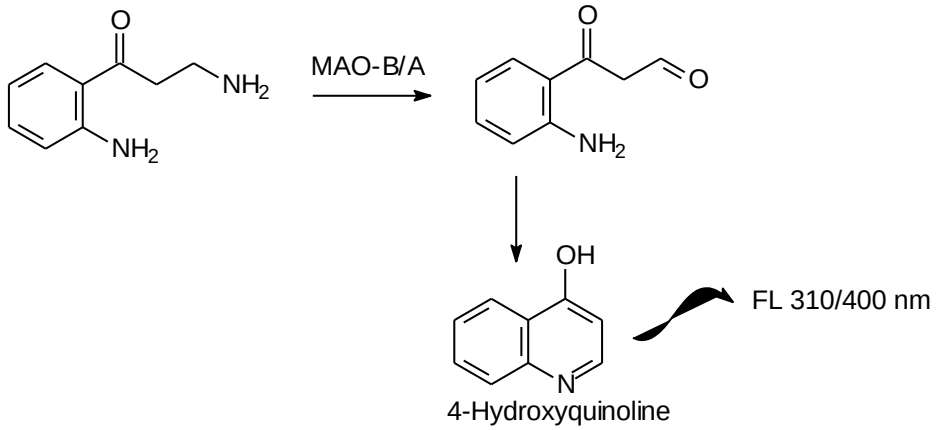

Fig. 4.4. Reaction scheme for the oxidation of kynuramine to 4-hydroxyquinoline by MAO-A and -B.

4.4.2 Method

The respective MAO preparations were preincubated for periods of 0, 15, 30, 60 min at 37 °C with **3** and **5** at concentrations of 0.30 µM and 9.7 µM (approximately 2 fold the measured IC_{50} value) for human MAO-B and human MAO-A, respectively (Manley-King *et al.,* 2009; Ogunrombi *et al.,* 2008). For this purpose, concentrations of 0.03 mg/mL for both human MAO-A and –B were used. The incubations were carried out in potassium phosphate buffer (100 mM, pH 7.4, made isotonic with KCl) for studies with the recombinant human enzymes. A final concentration of 45 µM kynuramine for human MAO-A and 30 µM kynuramine for human MAO-B were then incubated with the preincubated enzyme preparations at 37 °C for 15 min. The final volumes of these incubations were 500 µl and the final concentrations of **3** and **5** were 0.15 µM and 4.35 µM, respectively. The final concentrations of the enzyme preparations were 0.015 mg/ml human MAO-A and –B. The reactions with the recombinant human enzymes were terminated with 400 µl NaOH (2 M). A volume of 1000 µl distilled water was added to the incubations. The rates of formation of 4-hydroxyquinoline were measured at excitation and emission wavelengths of 310 and 400 nm, respectively. Quantitative estimations of 4-hydroxyquinoline were made by means of a linear calibration curve ranging from 0.188–6.25 µM. Each calibration standard was prepared to a final volume of 500 µL in potassium phosphate buffer and also contained 400 µL NaOH (2 N) and 1000 µL distilled water. All measurements were carried out in triplicate and are expressed as mean ± standard error of the mean (SEM).

4.4.3 Results

Panel A

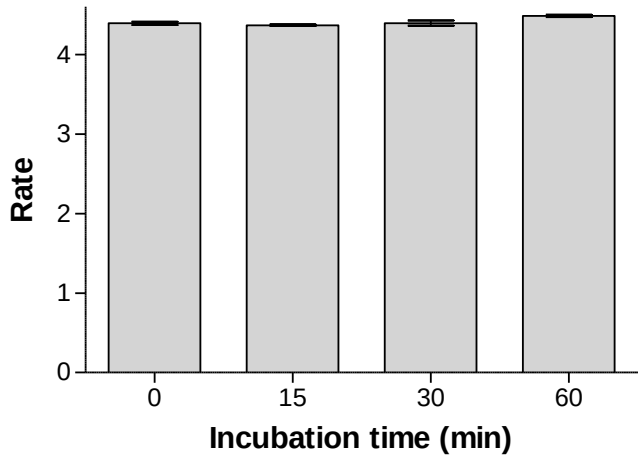

Panel B

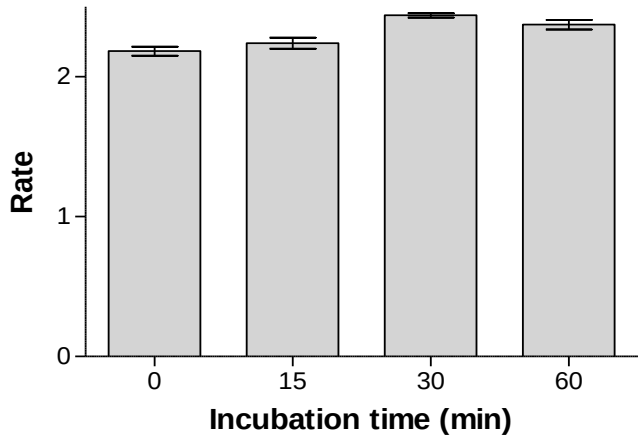

Fig. 4.5. Time-dependant inhibition of recombinant human MAO-A (Panel A) and recombinant human MAO-B (Panel B) by **5** and **3**, respectively. The enzymes were preincubated for various periods of time (0–60 min) with **5** (MAO-A) and **3** (MAO-B) at concentrations of 9.7 µM and 0.3 µM, respectively. The concentrations of the enzyme substrate, kynuramine, were 45 and 30 µM for the studies with MAO-A and MAO-B, respectively. The catalytic rates are expressed as nmoles 4-hydroxyquinoline formed/min/mg protein.

As shown in Fig 4.5, there is no time-dependent reduction in the rates of MAO-A and –B catalysed oxidation of kynuramine when compound **5** and **3** are preincubated with the MAO-A and –B, respectively, for various periods of time. From this result it may be concluded that the inhibition of MAO-A and –B is reversible, at least for the time period (60 min) and at the inhibitor concentrations (2 × IC_{50}) evaluated.

4.5 Mode of inhibition - Construction of Lineweaver-Burke plots

4.5.1 Introduction

Using a set of Lineweaver–Burke plots, the mode of inhibition may be examined. For this purpose, an assay with the same principles as the assay used for time-dependent studies will be employed. With this procedure the MAO-B catalysed formation of 4-hydroxyquinoline from kynuramine will be measured in the presence of one selected inhibitor (**3**) (Novaroli *et al*., 2005) (Fig. 4.6). Lineweaver–Burke plots will be constructed by plotting the initial rates of oxidation at four different substrate concentrations in the absence and presence of three different concentrations of the inhibitor. As enzyme source, recombinant human MAO- B will be used.

4.5.2 Method

Compound **3,** at concentrations of 0, 0.0375, 0.075 and 0.15 µM was selected as inhibitor, because **3** was found to be the most potent inhibitor of the test series. Kynuramine (at 15, 30, 60 and 90 µM) served as substrate. The 16 different incubations containing different substrate and inhibitor concentrations were pre-warmed for 15 minutes and human MAO-B (0.015 mg/ml) was added. After 20 minutes of incubation the reactions were stopped with the addition of 400 ml NaOH (2N) and 1000 µL water. The amount of fluorescence, which represents the amount of 4-hydroxyquinoline formed, was measured fluorometrically at excitation and emission wavelengths of 310 and 400 nm, respectively. Quantitative estimations of 4-hydroxyquinoline were made by means of a linear calibration curve ranging from 0.188–6.25 µM. Each calibration standard was prepared to a final volume of 500 µL in potassium phosphate buffer and also contained 400 µL NaOH (2 N) and 1000 µL distilled water. Linear regression analysis was performed using the SigmaPlot software package (Systat Software Inc.).

4.5.3 Results – Lineweaver-Burke plot

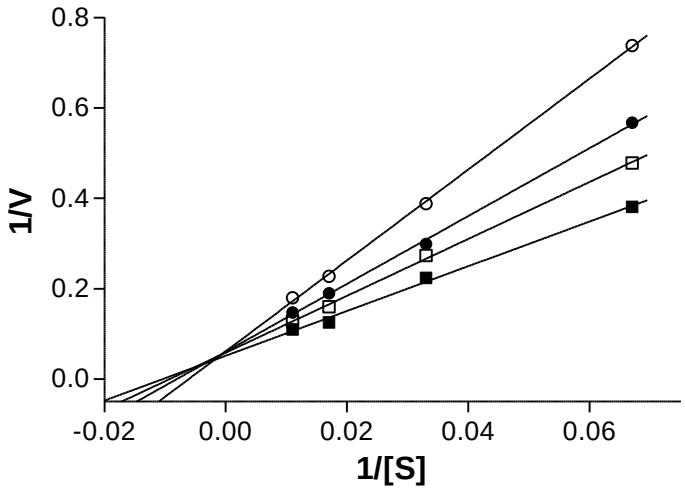

Fig. 4.6. Lineweaver-Burk plots of the recombinant human MAO-B catalyzed oxidation of kynuramine in the absence (filled squares) and presence of various concentrations **3**. For the studies with MAO-B the concentrations of **3** were: 0.0375 µM (open squares), 0.075 µM (filled circles), 0.15 µM (open circles). The rates (V) are expressed as nmol product formed/min/mg protein.

As can be seen from Figure 4.6, the Lineweaver-Burke plots intersect on the y-axis. This is indicative that the inhibitor is a competitive inhibitor. Since competitive inhibitors interact reversibly with the target enzyme, this is further support that the 8-(phenoxymethyl)caffeine analogues are reversible inhibitors of MAO-B.

4.6 Conclusion

This section demonstrates that 8-(phenoxymethyl)caffeine analogues are inhibitors of MAO-A and –B. The inhibitors display moderately potent inhibition activities towards human MAO-A with IC_{50} values ranging from 4.59 µM to 34.0 µM. The 8-(phenoxymethyl)caffeine analogues exhibit selectivity for the MAO-B isoenzyme, and among the test compounds, several highly potent inhibitors were identified. The most potent inhibitor was 8-(3-bromophenoxymethyl)caffeine with an IC_{50} value of 0.148 µM toward human MAO-B. This study also shows that two selected analogues bind reversibly to MAO-A and –B, respectively, and that the mode of MAO-B inhibition is competitive for one representative compound.

Qualitative inspection of the results revealed interesting structure-activity relationships. For example, for the 8-(phenoxymethyl)caffeine analogues bearing both the C3 and C4 substituents on the phenyl ring, the MAO-B activity significantly increases with halogen substitution. In addition, increased electronegativity of the halogen substituent lead to increased MAO-B inhibition activity. To quantify these and other apparent relationships, a Hansch-type QSAR study was carried out. The results showed that the $\log IC_{50}$ correlated with the Hansch lipophilicity (π) and the Swain-Lupton electronic (F) constants of the substituents on C3 of the phenoxymethyl phenyl ring. Although, based on an r^2 value of 0.87 and a statistical F value of 13.6, the correlation was judged not to be significant, important conclusions may be drawn from the results. From the QSAR analysis it may be concluded that electron withdrawing substituents at C3 with a high degree of lipophilicity enhance MAO-B inhibition potency. These results are similar to those previously obtained for the series of 8-benzyloxycaffeine analogues. For this series, the MAO-B inhibition potencies correlated with the Hansch lipophilicity (π) and Hammett electronic (σ) constants of the substituents at C3 of the benzyloxy ring. Similarly to the 8-(phenoxymethyl)caffeine analogues, electron withdrawing substituents with a high degree of lipophilicity also enhance the MAO-B inhibition potencies of 8-benzyloxycaffeine analogues. This study propose additional 8-(phenoxymethyl)caffeine analogues that may be investigated in future studies in order to improve the linear QSAR model.

CHAPTER 5

Summary

As mentioned in the introduction, in the current study 8-(phenoxymethyl)caffeine (**1**) and nine 8-(phenoxymethyl)caffeine analogues (**2**-**10**) were synthesized and evaluated as inhibitors of recombinant human MAO-A and –B. Both MAO-A and –B are of pharmacological importance since these enzymes are responsible for the metabolism of monoamine neurotransmitters in the brain. MAO-A is responsible for the oxidation of serotonin and noradrenalin and inhibitors of this enzyme is frequently used to treat depressive illness. MAO-B is a major dopamine metabolizing enzyme in the brain and inhibitors of this enzyme is used in the treatment of neurodegenerative diseases such as PD. MAO-B inhibitors may possess neuroprotective properties in PD by reducing potentially neurotoxic by-products that are associated with the oxidation of dopamine. These are hydrogen peroxide and dopaldehyde. In addition, MAO-B inhibitors may also provide symptomatic relieve, especially when combined with levodopa, since they prevent the metabolism of dopamine and thereby may conserve the dopamine supply in the brain.

The lead compound for the design of new MAO-B inhibitors in the current study was caffeine. Although caffeine is a weak MAO-B inhibitor, substitution at C8 with a variety of substituents has been shown to enhance the MAO-B inhibition potency of caffeine several orders of a magnitude. For example, substitution of caffeine with a benzyloxy substituent at C8 yields compounds which inhibit MAO-B with exceptional potencies (Strydom *et al*., 2008). Studies in our laboratory have shown that a variety of C3-substituted benzyloxy side chains enhance the MAO-B inhibition potency of caffeine. The benzyloxy substituent therefore appears to be particularly useful for MAO-B inhibition. The phenoxymethyl substituent is a close structural analogue of the benzyloxy substituent and may therefore possess similar biological properties. This study examined if C8 substitution of caffeine with a variety of phenoxymethyl substituents also enhances caffeine`s MAO-B inhibition activity to a similar degree than observed with the benzyloxy substituents (Strydom *et al*., 2010). For this purpose 8-(phenoxymethyl)caffeine (**1**) and nine 8-(phenoxymethyl)caffeine analogues (**2**-**10**) were synthesized and evaluated as inhibitors of recombinant human MAO-A and –B. This study examined the effect that a variety of substituents on C3 and C4 of the phenoxymethyl phenyl ring had on the MAO-A and –B inhibition potencies of 8-(phenoxymethyl)caffeine. The MAO-A and –B inhibition potencies of the 8-(phenoxymethyl)caffeine analogues were subsequently compared to that of the previously studied 8-benzyloxycaffeine analogues.

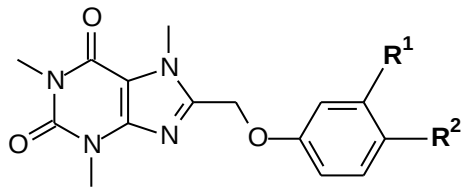

Compound	R^1	R^2
1	H	H
2	Cl	H
3	Br	H
4	F	H
5	CF_3	H
6	CH_3	H
7	OCH_3	H
8	H	Cl
9	H	Br
10	H	F

Fig. 5.1. The structures of the compounds examined in this study.

Chemistry: 8-(Phenoxymethyl)caffeine (**1**) and the nine 8-(phenoxymethyl)caffeine analogues (**2**-**10**) were successfully synthesized by reacting 1,3-dimethyl-5,6-diaminouracil and the appropriate substituted phenoxyacetic acid in the presence of the carbidiimide dehydrating agent EDAC. In six instances, the required phenoxyacetic acids are not commercially available and were successfully prepared from the corresponding phenol. The structures of the target inhibitors were verified by NMR and MS analysis. Both the ^{1}H NMR and ^{13}C NMR spectra corresponded with the proposed structures and the expected exact masses were also recorded for each compound. HPLC analysis revealed a single peak for each compound analyzed which indicates a high degree of purity for each compound.

MAO inhibition studies: The 8-(phenoxymethyl)caffeine analogues were evaluated as inhibitors of recombinant human MAO-A and –B. The recombinant human enzymes are commercially available. A fluorometric assay was employed to measure the inhibition potencies of the test compounds, and the activities were expressed as the IC_{50} values. The MAO activity measurements were based on measuring the amount of MAO generated H_2O_2. H_2O_2 reacts with Amplex Red added to the reaction mixtures to form resorufin. The quantity of resorufin in the reactions was subsequently measured fluorometrically since resorufin fluoresces at an excitation wavelength of 560 nm and an emission wavelength of 590 nm (Zhou & Panchuk-Voloshina, 1997).

The results showed that, while the 8-(phenoxymethyl)caffeine analogues also inhibited MAO-A, they were MAO-B selective inhibitors. **3** and **9** were the most potent MAO-B inhibitors with IC_{50} values of 0.148 µM and 0.189 µM, respectively. These two inhibitors also exhibited a high degree of selectivity for MAO-B with SI values of 229 and 56 for **3** and **9**, respectively. Qualitative inspection of the inhibition data revealed that electron withdrawing functional groups on the phenyl ring of the phenoxymethyl substituent are more optimal for MAO-B inhibition. For example, the 8-(phenoxymethyl)caffeine analogues bearing electron withdrawing functional groups (Cl, Br and CF_3) are all potent MAO-B inhibitors with IC_{50} values in the nM range while those bearing methyl and methoxy groups, which are electron donating/releasing groups, were weaker inhibitors with IC_{50} values in the µM range.

Also of interest was the observation that, for the 8-(phenoxymethyl)caffeine analogues bearing halogens on C3 and C4 of the phenoxymethyl phenyl ring, the larger halogen substituents with a higher degree of steric hindrance yielded more potent inhibition. For example, the bromine substituted homologues were the most potent MAO-B inhibitors, followed by the chlorine an then the fluorine substituted homologues. This study recommends that, in future studies, 8-(phenoxymethyl)caffeine analogues bearing larger substituents with a higher degree of steric hindrance on C3 and C4 of the phenoxymethyl phenyl ring should be synthesized as potential MAO-B inhibitors. The importance of a higher degree of substituent volume and steric hindrance for MAO-B inhibition potency was also shown by the observation that the 8-(phenoxymethyl)caffeine analogues bearing a methyl group and a methoxy group on the phenyl ring were better inhibitors than the unsubstituted analogue.

As mentioned above, another aim of this study was to compare the MAO-A and –B inhibition potencies of the 8-(phenoxymethyl)caffeine analogues to that of the previously studied 8-benzyloxycaffeine analogues. The 8-benzyloxycaffeines were found to be more potent MAO-A inhibitors which showed that the benzyloxy side chain is better suited to enhance the MAO-A inhibition potency than the phenoxymethyl side chain. It may be concluded that though structurally similar, the biological activities of the benzyloxy and phenoxymethyl side chains differ significantly. Also, the 8-benzyloxycaffeines were in general less selective for the MAO-B isoform than the 8-(phenoxymethyl)caffeine analogues. As observed for the 8-(phenoxymethyl)caffeine analogues, qualitative inspection of the MAO-B inhibition data for the 8-benzyloxycaffeines revealed that electron withdrawing substituents with a higher degree of steric hindrance were required for potent MAO-B inhibition.

From these observations, it may therefore be concluded that, in future studies, 8-(phenoxymethyl)caffeine analogues may be used as a lead for the development of MAO-B selective inhibitors.

Time-dependency and mode of inhibition: The time-dependency of inhibition of both MAO-A and –B by a selected 8-(phenoxymethyl)caffeine analogues were also evaluated. The results showed that compounds **5** and **3,** when preincubated with the MAO-A and –B, respectively, did not reduce the catalytic rates of MAO-A and –B in a time dependent manner. From this result it was concluded that the inhibition of MAO-A and –B is reversible. For the inhibition of MAO-B by compound **3**, a set of Lineweaver–Burke plots were constructed in order to determine the mode of inhibition. The results showed that the Lineweaver-Burke plots intersected on the y-axis which indicates that this inhibitor is a competitive inhibitor.

Hansch-type SAR study: Based on the inhibition data, interesting structure-activity relationships exist between the experimentally determined IC_{50} values and the substituent on the phenyl ring of the 8-(phenoxymethyl)caffeine analogues. To quantify these, a Hansch-type SAR analysis was carried out for the seven 8-(phenoxymethyl)caffeine analogues containing substituents at C3 of the phenyl ring. The two parameter correlation of π and F with the $\log IC_{50}$ values yielded the best correlation. The R^2 was found to be 0.87 while the statistical *F* value was 13.6 (F_{max} = 30.18). Also, the two parameter correlation of π and σ with the $\log IC_{50}$ values gave a good correlation with an R^2 of 0.80 and an *F* value of 8.15. Since the calculated F values are lower than the F_{max} value, the correlations are not statistically significant. In spite of this, the results supported the qualitative observations made from the inhibition data.

$$\log IC_{50} = -1.05F - 0.928\pi + 0.695 \quad (R^2 = 0.87 \text{ and } F = 13.6)$$

$$\log IC_{50} = -0.974\sigma_m - 0.906\pi + 0.563 \quad (R^2 = 0.80 \text{ and } F = 8.15)$$

The negative signs of the *F* and σ_m parameter coefficients indicate that the inhibition potencies of compounds **1**–**7** towards human MAO-B may be enhanced by substitution with electron withdrawing groups at C3 of the phenoxymethyl phenyl ring. The negative signs of the π parameter coefficient indicate that the inhibition potencies of compounds **1**–**7** towards human MAO-B may be enhanced by substitution with more lipophilic functional groups on C3 of the phenoxymethyl phenyl ring.

Future recommendations: This study recommends that at least 3 more 8-(phenoxymethyl)caffeine analogues containing the following 3 substituents on C3 be synthesized and evaluated as MAO-B inhibitors. The addition of the 3 analogues would improve the Hansch-type SAR model described above. The following 3 8-(phenoxymethyl)caffeine analogues are proposed for future studies. Their theoretical IC_{50} values (calculated according to the best linear predictive equation) are also given:

Table 5.1. Structures of compounds that may be examined in future studies.

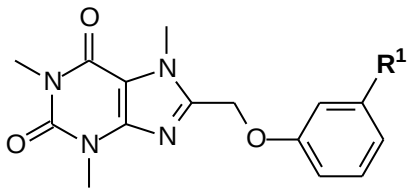

R^1	Calculated IC_{50} (μM)
I	0.164
NO_2	1.87
SO_2CF_3	0.256

Bibliography

Andringa, G. & Cools A. R. (2000). The neuroprotective effects of CGP3466B in the best in vivo model of parkinson's disease, the bilaterally MPTP-treated rhesus monkey. *Journal of neural transmission,* 60: 215–225.

Auluck, P. K., Chan, H. Y., Trojanowski, J. Q., Lee, V. M. & Bonini, N. M. (2002). Chaperone suppression of alpha-synuclein toxicity in a drosophila model for Parkinson's disease. *Science,* 295: 865–868.

Bakhle, Y. S. (1990). Pharmacokinetic and metabolic properties of the lung. *British journal of anesthesia*, 65: 79–93.

Betarbet, R., Sherer, T. B., Di Monte, D. A. & Greenamyre, J. T. (2002). Mechanistic approaches to Parkinson's disease pathogenesis. *Brain pathology,* 12: 499–510.

Binda, C., Li, M., Hubalek, F., Restelli, N., Edmondson, D. & Mattevi, A. (2003). Insights into the mode of inhibition of human mitochondrial monoamine oxidase B from high-resolution crystal structures. *Proceedings of the national academy of sciences of the United States of America,* 100: 9750-9755.

Binda, C., Mattevi, A. & Edmondson, D. (2002a). Structure-function relationships in flavoenzyme-dependent amine oxidations: a comparison of polyamine oxidase and monoamine oxidase. *Journal of biological chemistry,* 277: 23973-23976.

Binda, C., Newton-Vinson, P., Hubalek, F., Edmondson, D. & Mattevi, A. (2002b). Structure of human monoamine oxidase B, a drug target for the treatment of neurological disorders. *Nature structural biology,* 9: 22-26.

Binda, C., Wang, J., Pisani, L., Caccia, C., Carotti, A. & Salvati, P. (2007). Structures of human monoamine oxidase B complexes with selective noncovalent inhibitors: safinamide and coumarin analogues. *Journal of medicinal chemistry,* 50: 5848-5852.

Burke, W. J., Li, S. W., Chung, H. D., Ruggiero, D. A., Kristal, B. S., Johnson, E. M., Lampe, P., Kumar, V. B., Franko, M., Evelyn A. Williams, E. A. & Zahm, D. S. (2004). Neurotoxicity of MAO metabolites of catecholamine neurotransmitters: role in neurodegenerative diseases. *Neurotoxicology,* 25: 101–115.

Castillo, V., Lizcano, J. M. & Unzeta, M. (1999). Presence of SSAO in human and bovine meninges and microvessels. *Neurobiology,* 7: 263–272.

Chen, J. J. & Swope, D. M. (2007). Pharmacotherapy for Parkinson's disease. *Pharmacotherapy,* 27: 161S-173S.

Cohen, G. (2000). Oxidative stress, mitochondrial respiration and Parkinson's disease. *Annals of the New York academy of science*, *899*: 112–120.

Cummings, C. J., Reinstein, E., Sun, Y., Antalffy, B., Jiang, Y., Ciechanover, A., Orr, H. T., Beaudet, A. L. & Zoghbi, H. Y. (1999). Mutation of the E6-AP ubiquitin ligase reduces nuclear inclusion frequency while accelerating polyglutamine-induced pathology in SCA1 mice. *Neuron*, *24*: 879–892.

Cummings, C. J., Sun, Y., Opal, P., Antalffy, B., Mestril, R., Orr, H. T., Dillmann, W. H., & Zoghbi, H. Y. (2001). Over-expression of inducible HSP70 chaperone suppresses neuropathology and improves motor function in SCA1 mice. *Human molecular genetics,* 10: 1511–1518.

Dauer, W. & Przedborski, S. (2003). Parkinson's disease: mechanisms and models. *Neuron, 39*: 889-909.

Dick, F. D., De Palma, G., Ahmadi, A., Scott, N. W., Prescott, G. J., Bennett, J., Semple, S., Dick, S., Counsell, C., Mozzoni, P., Haites, N., Bezzina Wettinger, S., Mutti, A., Otelea, M., Seaton, A., Söderkvist, P. & Felice, A. (2007). Environmental risk factors for parkinson's disease and parkinsonism: the geoparkinson study. *Occupational and environmental medicine*; 64: 666–672.

Dixon, M. (1953). The determination of enzyme inhibitor constants. *Biochemical journal, 55*: 170-171.

Dostert, P. L., Strolin Benedetti, M. & Tipton, K. F. (1989). Interactions of monoamine oxidase with substrates and inhibitors. *Medicinal research reviews*, 19: 45–89

Dowd, J. E. & Riggs, D. S. (1964). A comparison of estimates of Michaelis-Menten kinetic constants from various linear transformations. *Journal of biological chemistry, 240:* 863-869

Edmondson, D., Binda, C. & Mattevi, A. (2007). Structural insights into the mechanism of amine oxidation by monoamine oxidase A and B. *Archives of biochemistry and biophysics,* 464: 269-276.

Edmondson, D., Mattevi, A., Binda, C., Li, M. & Hubalek, F. (2004). Structure and mechanism of monoamine oxidase. *Current medicinal chemistry, 11:* 1983-1993.

Factor, S. (2008). Current status of symptomatic medical therapy in Parkinson's disease. *Neurotherapeutics,* 5: 210-225.

Fernandez, H. & Chen, J. (2007). Monoamine oxidase-B inhibition in the treatment of Parkinson's disease. *Pharmacotherapy, 2*: 174S-185S.

Finberg, J. P. & Youdim, M. B. (1985). Modification of blood pressure and nictitating membrane response to sympathetic amines by selective monoamine oxidase inhibitors, types A and B, in the cat. *British journal of pharmacology,* 85: 541–546.

Fowler, J. S., Volkow, N. D., Wang. G., Pappas, N., Logan, J., Shea, C., Alexoff, D., MacGregor, R. R. Schlyer, D. J., Zezulkova, I. & Wolf, A.P. (1996). Brain monoamine oxidase A inhibition in cigarette smokers. *Proceedings of the national academy of sciences of the United States of America,* 93: 14065–14069

Gnerre, C., Catto, M., Leonetti, F., Weber, P., Carrupt, P. & Altomare, C. (2000). Inhibition of monoamine oxidase by functionalized coumarin derivatives: biological activities, QSAR's, and 3D-QSAR's. *Journal of medicinal chemistry, 43*: 4747-4758.

Grimsby, J., Lan, N. C., Neve, R., Chen, K. & Shih, J. C. (1990). Tissue distribution of human monoamine oxidase A and B mRNA. *Journal of neurochemistry,* 55: 1166-1169.

Grimsby, J., Zentner, M., & Shih, J. C. (1996). Identification of a region important for human monoamine oxidase B substrate and inhibitor selectivity. *Life sciences,* 9: 777–787.

Grunblatt, E., Mandel, S., Jacob-Hirsch, J., Zeligson, S., Amariglo, N., Rechavi, G., Li, J., Ravid, R., Roggendorf, W., RiedererI, P. & Youdim, M.B. (2004). Gene expression profiling of parkinsonian substantia nigra pars compacta; alterationsin ubiquitin-proteasome, heat shock protein, iron and oxidative stress regulated proteins, cell adhesion/cellular matrix and vesicle trafficking genes. *Journal of neural transmission*. 111: 1543–1573.

Hansch, C. & Leo, A. (1995). Exploring QSAR. Fundamentals and applications in chemistry and biology. Washington DC: American Chemical Society. 1-124.

Hayes, N. V. & Branch, G. E. K. (1943). The acidic dissociation constants of phenoxyacetic acid and its derivatives. *Journal of the American chemical society, 65*: 1555-1564.

Healy, D. G., Falchi, M., O'Sullivan, S. S., Bonifati, V., Durr, A., Bressman, S., Brice, A., Aasly, J., Zabetian, C. P., Goldwurm, S., Ferreira, J. J., Tolosa, E., Kay, D. M., Klein, C., Williams, D. R., Marras, C., Lang, A. E., Wszolek, Z. K., Berciano, J., Schapira, A. H., Lynch, T., Bhatia, K. P., Gasser, T., Lees, A. J. & Wood, N. W. International LRRK2 Consortium (2008). Phenotype, genotype, and worldwide genetic penetrance of LRRK2-associated Parkinson's disease: a case-control study. *Lancet neurology,* 7: 583–590.

Holt, A., Sharman, D., Baker, G. & Palcic, M. (1997). A continuous spectophotometric assay for monoamine oxidase and related enzymes in tissue homogenates. *Analytical biochemistry, 244*: 384-392.

Hubalek, F., Binda, C., Khalil, A., Li, M., Mattevi, A., Castagnoli, N. & Edmondson, D. E. (2005). Demonstration of isoleucine 199 as a structural determinant for the selective inhibition of human monoamine oxidase B by specific reversable inhibitors. *Journal of biological chemistry, 280*: 15761-5766.

Inoue, H., Castagnoli, K., Vand der Schyf, C., Mabic, S., Igarashi, K. & Castagnoli, N. J. (1999). Species-dependant differences in monoamine oxidase A and B-catalyzed oxidation of various C4 substituted 1-methyl-4-phenyl-1,2,3,6-tetrahydropyridinyl derivatives. *Journal of pharmacology and experimental therapeutics, 291*: 856-864.

Jalkanen, S. & Salmi, M. (2001). Cell surface monoamine oxidases: enzymes in search of a function. *The EMBO journal, 20*: 3893-3901.

Klinman, J. P. & Mu, D. (1994) Quinoenzymes in biology. *Annual review of biochemistry*, 63: 299-344.

Kragten, E., Lalande, I., Zimmermann, K., Roggo, S., Schindler, P., Müller, D., Van Oostrum, J., Waldmeier, P. & Fürst, P. (1998). Glyceraldehyde-3-phosphate dehydrogenase, the putative target of the antiapoptoticcompounds CGP 3466 and R-(-)-deprenyl. *Journal of biological chemistry*, 273: 5821–5828.

Koelsch, C. F. (1931). The identification of phenols. *Journal of the American chemical society, 53*: 304-305.

Lan, N. C., Chen, C. H. & Shih. J. C. (1989). Expression of functional human monoamine oxidase A and B cDNAs in mammalian cells. *Journal of neurochemistry*, 52: 1652- 1654.

Lees, A. (2005). Alternatives to levodopa in the initial treatment of early Parkinson's disease. *Drugs & aging , 22*: 731-740.

Lees, A. J., Hardy, J. & Revesz, T. (2009). Parkinson's disease. *Lancet*, 373: 2055-2066.

LeWitt, P. & Taylor, D. (2008). Protection Against Parkinson's Disease Progression:Clinical Experience. *Neurotherapeutics: the journal of the American society for experimental neurotherapeutics, 5*: 210-225.

Livingstone, D. J. & Salt, D. W. (2005). Judging the significance of multiple linear regretion models. *Journal of medicinal chemistry,* 48: 661-663.

Manley-King, C.I., Terre'Blanche, G., Castagnoli Jr. N., Bergh, J.J. & Petzer, J.P. (2009). Inhibition of monoamine oxidase B by *N*-methyl-2-phenylmaleimides. *Bioorganic & medicinal chemistry*, 17: 3104-3110.

Maroney A.C., Glicksman M. A., Basma A. N., Walton, K. M., Knight Jr, E., Murphy, C. M., Bartlett, B. A., Finn, J. P., Angeles, T., Matsuda, Y., Neff, N. T. & Dionne, C. A. (1998). Motor neuron apoptosis is blocked by CEP-1347 (KT 7515), a novel inhibitor of the JNK signaling pathway. *Journal of neurosciences*, 18: 104–111.

Meyerson, L., McMurtrey, K. & Davis, V. (1978). A rapid and sensitive potentiometric assay for monoamine oxidase using a ammonia-selective electrode. *Analytical biochemistry, 86*: 287-297.

Meyer-Almes, F. & Auer, M. (2000). Enzyme inhibition assays using fluorescence Correlation spectroscopy: A new algorithm for the derivation of k_{cat}/K_M and K_i values at substrate concentrations much lower than the Michaelis constant. *Biochemistry***,** *39:* 13261-13268

Muller, C.E., Geis, U., Hipp, J., Schobert, U., Frobenius, W., Pawlowski, M., Suzuki, F. & Sandoval-Ramirez, J. (1997). Synthesis and structure-activity relationships of 3,7-dimethyl-1-propargylxanthine derivatives, A_{2A}-selective adenosine receptor antagonists. *Journal of medicinal chemistry,* 40: 4396-4405.

Nagatsu, T. (2004). Progress in monoamine oxidase (MAO) research in relation to genetic engineering. *Neurotoxicology, 25*: 197-217.

Nicotra, A. & Parvez, S. (1999). Methods for assaying monoamine oxidase A and B activity: recent developments. *Biogenic amines, 15*: 307-320.

Novaroli, L., Reist, M., Favre, E., Carotti, A., Catto, M. & Carrupt, P. (2005). Human recombinant monoamine oxidase B as reliable and efficient enzyme source for inhibitor screening. *Bioorganic & medicinal chemistry*, *13: 6212-6217*

O'Brien, E., Kiely, K. & Tipton, K. (1978). A discontinuous luminometric assay for monoamine oxidase using an ammonia-selective electrode. *Analytical biochemistry, 86*: 287-297.

Ogunrombi, M.O., Malan, S.F., Terre'Blanche, G., Castagnoli Jr. N., Bergh, J.J. & Petzer, J.P. (2007). Neurotoxicity studies with the monoamine oxidase B substrate 1-methyl-3-phenyl-3-pyrroline. *Life sciences*, 81: 458-467.

Ogunrombi, M.O., Malan, S.F., Terre'Blanche, G., Castagnoli Jr. N., Bergh, J.J. & Petzer, J.P. (2008). Structure–activity relationships in the inhibition of monoamine oxidase B by 1-methyl-3-phenylpyrroles. *Bioorganic & medicinal chemistry*, 16: 2463-2472.

O'Sullivan, J., Unzeta, M., Healy, J., O'Sullivan, M.I., Davey, G. & Tipton, K.F. (2004). Semicarbazide-sensitive amine oxidases: enzymes with quite a lot to do. *Neurotoxicology*, 25: 303-315.

Paisan-Ruiz, C., Jain, S., Evans E. W., Gilks, W. P., Simón, J., van der Brug, M., López de Munain, A., Aparicio, S., Gil, A. M., Khan, N., Johnson, J., Martinez, J. R., Nicholl, D., Carrera, I. M., Pena, A. S., de Silva, R., Lees, A., Martí-Massó, J. F., Pérez-Tur, J., Wood, N. W., Singleton, A. B. (2004). Cloning of the gene containing mutations that cause PARK8-linked Parkinson's disease. *Neuron*, 44: 595–600.

Parkinson Study Group (1996). Impact of deprenyl andtocopherol treatment on Parkinson's disease in DATATOP subjects not requiring levodopa. *Annals of Neurology.* 39: 29–36.

Parkinson Study Group (2000a). A randomized controlled trial comparing pramipexole with levodopa in early Parkinson's disease: design and methods of the CALM-PD Study. *Clinical neuropharmacology*, 23: 34–44.

Parkinson Study Group (2002). Dopamine transporter brain imaging toassess the effects of pramipexole vs levodopa on Parkinson disease progression. *Journal of the American medical association*, 287:1653–1661.

Parkinson Study Group (2004). The safety and tolerability of a mixed lineage kinase inhibitor (CEP-1347) in PD. *Neurology*, 62:330–332.

Papesch, V. & Schroeder, E. F. (1951). Synthesis of 1-mono- and 1,3-disubstituted 6-aminouracils. Diuretic activity. *Journal of organic chemistry*, 16: 1879-1890.

Pinna, A., Wardas, J., Simola, N. & Morelli, M. (2005). New therapies for the treatment of Parkinson's disease: adenosine A_{2A} receptor antagonists. *Life sciences,* 77: 3259-3267.

Pretorius, J., Malan, S.F., Castagnoli, N., Jr., Bergh, J.J. & Petzer, J.P. (2008). Dual inhibition of monoamine oxidase B and antagonism of the adenosine A_{2A} receptor by (E,E)-8-(4-phenylbutadien-1-yl)caffeine analogues. *Bioorganic & medicinal chemistry*, 16: 8676-8684.

Przedborski, S. (2005). Pathogenesis of nigral cell death in Parkinson's disease. *Parkinsonism and related disorders , 11*: S3-S7.

Riederer, P., Danielczyk, W. & Grunblatt, E. (2004a). Monoamine oxidase-B inhibition in Alzheimer's disease. *Neurotoxicology, 25*: 271-277.

Riederer, P., Lachenmayer, L. & Laux, G. (2004b). Clinical applications of MAO-inhibitors. *Current medicinal chemistry, 11*: 2033-2043.

Rodwell, V. W. (1993). Enzymes: Kinetics. *In:* Murray, R.K., Granner, D.K., Mayes, P.A., & Rodwell, V.W. (eds) *Harper's biochemistry. 23rd edition*. New Jersey. Appleton & Lange, :60-70.

Salach, J. & Weyler, W. (1987). Preperation of the flavin-containing aromatic amine oxidases of human placenta and beef liver. *Methods in enzymology, 142*: 627-637.

Shih, J., Chen, K. & Ridd, M. (1999). Monoamine oxidase: from genes to behaviour. *Annual review of neuroscience , 22*: 197-217.

Shimada, J., Suzuki, F., Nonaka, H. & Ishii, A. (1992). 8-Polycycloalkyl-1,3-dipropylxanthines as potent and selective antagonists for A1-adenosine receptors. *Journal of medicinal chemistry*, 35: 924–930.

Selley, M. L. (2005) Simvastatin prevents 1-methyl-4-phenyl-1,2,3,6-tetrahydropyridine induced striatal dopamine depletion and protein tyrosine nitration in mice, *Brain research*, 10: 1–6.

Singer, T., Ramsay, R., McKeown, K., Trevor, A. & Castagnoli, N. J. (1988). Mechanism of the neurotoxicity of 1-methyl-4-phenylpyridinium (MPP^+), the toxic bioactivation product of 1-methyl-4-phenyl-1,2,3,6-tetrahydropyridine by monoamine oxidase inhibitors. *Nature, 49*: 17-23.

Smeyne, R. & Jackson-Lewis, V. (2004). The MPTP model of Parkinson's disease. *Molecular brain research, 134*: 57-66.

Son, S., Ma, J., Kondou, Y., Yoshimura, M., Yamashita, E. & Tsukihara, T. (2008). Structure of human monoamine oxidase A at 2.2-Å resolution: the control of opening the entry for substrates/inhibitors. *Proceedings of the national academy of sciences of the United States of America,* 105: 5739-5744.

Speer, J. H. & Raymond, A. L. (1953). Some alkyl homologues of theophyline. *Journal of the American chemistry society*, 75: 114-115.

Standaert, D. G. & Young, A. B. (2006). Treatment of central nervous system degenerative disorders: Parkinson's disease. *In:* Brunton, L. L., Lazo, J. S. & Parker, K. L. (eds). *Goodman & Gilman's: The pharmacological basis of therapeutics 10th edition*: New York. McGraw-Hill, :529-533.

Strydom, B., Malan, S. F., Castagnoli Jr. N., Bergh, J. J. & Petzer, J. P. (2010). Inhibition of monoamine oxidase by 8-benzyloxycaffeine analogues. *Bioorganic & medicinal chemistry*, 18: 1018-1028.

Suzuki, F., Shimada, J., Mizumoto, H., Karasawa, A., Kubo, K., Nonaka, H., Ishii, A. & Kawakita, T. (1992). Adenosine A1 antagonists. 2. Structure-activity relationships on diuretic activities and protective effects against acute renal failure. *Journal of medicinal chemistry*, 35: 3066–3075.

Tanner, C. M. (2003). Is the cause of Parkinson's disease environmental or hereditary? Evidence from twin studies. *Advances in neurology,* 91: 133–142.

Taylor, K. S., Counsell, C. E., Gordon, J. C. & Harris, C. E. (2005). Screening for undiagnosed parkinsonism among older people in general practice. *Age ageing,* 34: 501–04.

The NINDS NET-PD Investigators (2006). A randomized, double-blind, futility clinical trial of creatine and minocycline in early Parkinson disease. *Neurology*, 66: 664–671.

Traube, W. (1900). Der synthetische aufbau der harnsaure, des xanthenes, theobromins, theophyllins und caffeine aus der cyanessigsaure. *Chemische berichte*, 33: 3035-3056.

Van de Waterbeemb, H. & Testa, B. (1987). The parametrization of lipophilicity and other structural properties in drug design. *Advances in drug research.* London: Academic press. 85-225.

Wahner, A. D., Bronstein, J. M., Y.M. Bordelon, Y. M., & Ritz, B. (2008). Statin use and the risk of Parkinson disease, *Neurology*, 70: 1418–1422.

Warrick, J. M., Chan, H. Y., Gray-Board, G. L., Chai, Y., Paulson, H. L. & Bonini, N. M. (1999). Suppression of polyglutamine-mediated apoptotic neurodegeneration in Drosophila by the molecular chaperone HSP70. *Nature. Genetics, 23*: 425–428.

Weyler, W., Titlow, C. C. & Salach J. I. (1990). Catalytically active monoamine oxidase type A from human liver expressed in Saccharomyces cerevisiae contains covalent FAD. *Biochemical and Biophysical research communications*, 173: 1205-1211.

Wolozin, B., Wang, S. W., Li, N. C., Lee, A., T.A. Lee, T. A. & Kazis, L. E. (2007). Simvastatin is associated with a reduced incidence of dementia and Parkinson's disease. *BMC medicine*, 5: 20.

Vatassery, G. T., Fahn, S., Kuskowski, M. A.; Parkinson Study Group (1998). Alpha tocopherol in CSF of subjects taking high-dose vitamin E in the DATATOP study. *Neurology*, 50: 1900–1902.

Vlok, N., Malan, S., Castagnoli, N. J., Bergh, & Petzer, J. J. (2006). Inhibition of monoamine oxidase B by analogues of the adenosine A_{2A} receptor antagonist (E)-8-(3-chlorostyryl)caffeine(CSC). *Bioorganic & medicinal chemistry, 14*: 3512-3521.

Yacoubian, T. A. & Standaert, D. G. (2009). Targets for neuroprotection in Parkinson's disease. *Biochimica et biophysica acta,* 1792: 676-687.

Youdim, M. & Bakhle, Y. (2006). Monoamine oxidase: isoforms and inhibitors in Parkinson's disease and depressive illness. *British journal of pharmacology, 147*: S287-S296.

Youdim, M., Edmondson, D. & Tipton, K. (2006). The therapeutic potential of monoamine oxidase inhibitors. *Nature reviews. Neuroscience, 7*: 295-309.

Youdim, M. B. H., Finberg, J. P. M. & Tipton, K. F. (1988). Monoamineoxidase*. In:* Trendelenburg, U. & Weiner, U. (eds) *Catecholamine II.* Berlin, Springer-verlag, :119–192.

Zhao, G., Yu, T., Wang, X., & Jing, Y. (2005). Synthesis and structure–activity relationship of ethacrynicacid analogues on glutathione-s-transferase P1-1 activity inhibition. *Bioorganic & medicinal chemistry, 13*: 4056-4062.

Zhou, J., Zhong, B. & Silverman, R. (1996). Direct continuous fluorometric assay for monoamine oxidase. *Analytical biochemistry, 234*: 9-12.

Zhou, M. & Panchuk-Voloshina, N. (1997). A one-step fluorometric method for the continuous measurement of monoamine oxidase activity. *Analytical biochemistry*, 253: 169-174.

Addendum

S1: HPLC traces of the following new/unknown compounds

- 8-Phenoxymethylcaffeine (**1**)
- 8-(3-Chlorophenoxymethyl)caffeine (**2**)
- 8-(3-Bromophenoxymethyl)caffeine (**3**)
- 8-(3-Fluorophenoxymethyl)caffeine (**4**)
- 8-(3-Trifluoromethylphenoxymethyl)caffeine (**5**)
- 8-(3-Methylphenoxymethyl)caffeine (**6**)
- 8-(3-Methoxyphenoxymethyl)caffeine (**7**)
- 8-(4-Chlorophenoxymethyl)caffeine (**8**)
- 8-(4-Bromophenoxymethyl)caffeine (**9**)
- 8-(4-Fluorophenoxymethyl)caffeine (**10**)

Method: To determine the purity of the previously unreported compounds (**1-10**), HPLC analyses were carried out. HPLC analyses were performed with an Agilent 1100 HPLC system equipped with a quaternary pump and an Agilent 1100 series diode array detector. A Venusil XBP C18 column (4.60 $\times$ 150 mm, 5 µm) was used and the mobile phase consisted initially of 30% acetonitrile and 70% MilliQ water at a flow rate of 1 mL/min. At the start of each HPLC run a solvent gradient program was initiated by linearly increasing the composition of the acetonitrile in the mobile phase to 85% acetonitrile over a period of 5 min. Each HPLC run lasted 15 min and a time period of 5 min was allowed for equilibration between runs. A volume of 20 µL of solutions of the test compounds in acetonitrile (1 mM) was injected into the HPLC system and the eluent was monitored at wavelengths of 210, 254 and 300 nm.

8-Phenoxymethylcaffeine (1)

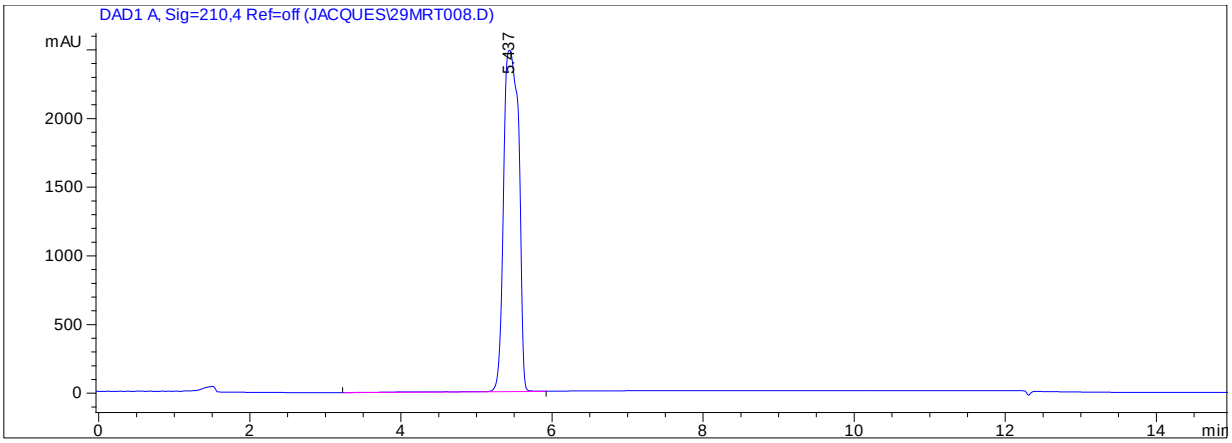

8-(3-Chlorophenoxymethyl)caffeine (2)

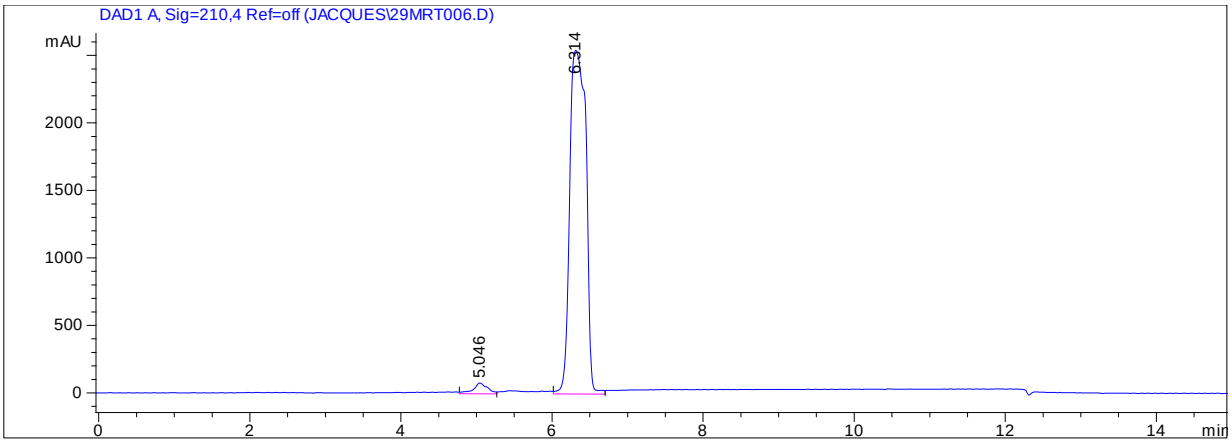

8-(3-Bromophenoxymethyl)caffeine (3)

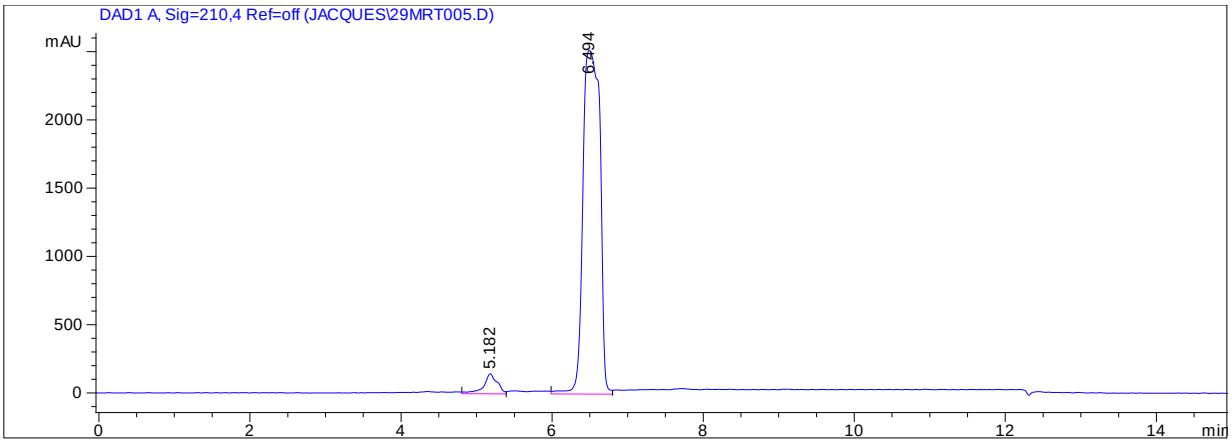

8-(3-Fluorophenoxymethyl)caffeine (4)

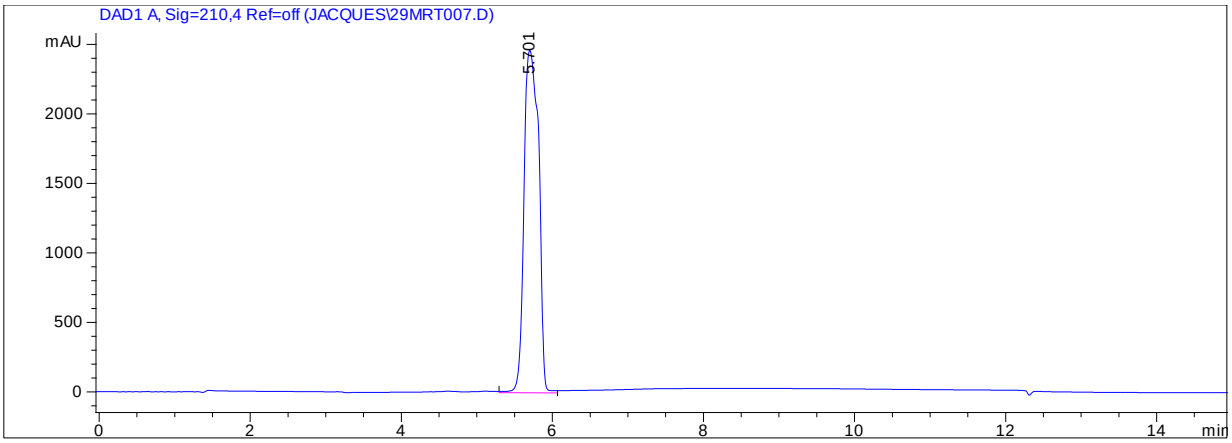

8-(3-Trifluoromethylphenoxymethyl)caffeine (5)

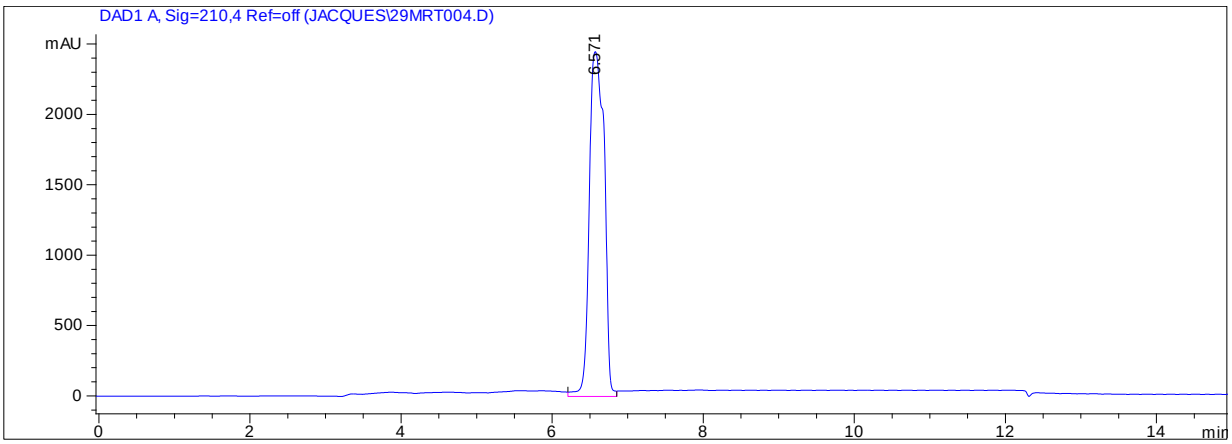

8-(3-Methylphenoxymethyl)caffeine (6)

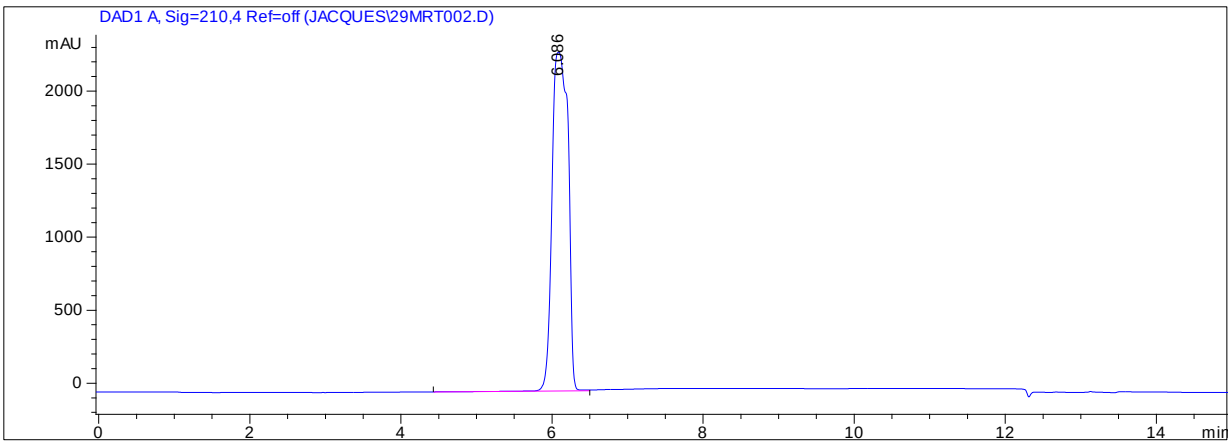

8-(3-Methoxyphenoxymethyl)caffeine (7)

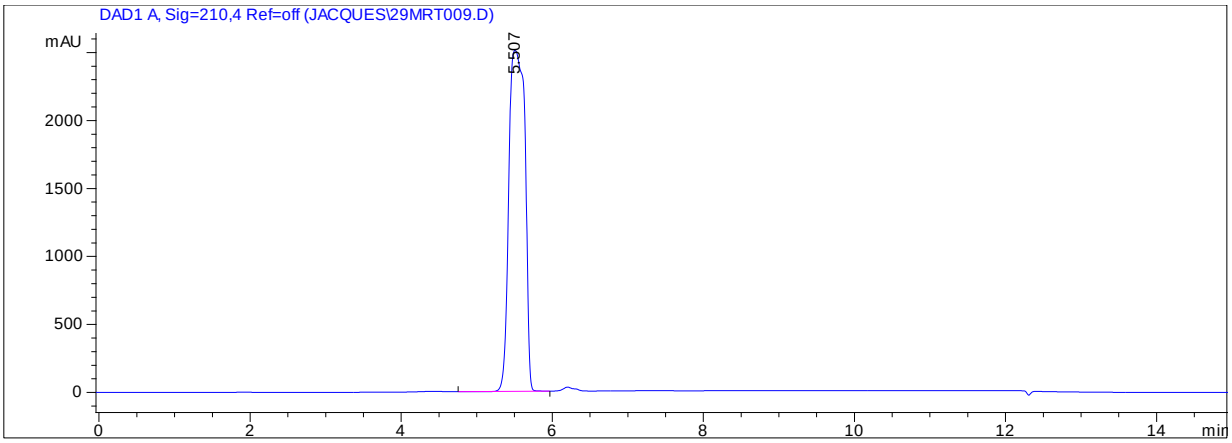

8-(4-Chlorophenoxymethyl)caffeine (8)

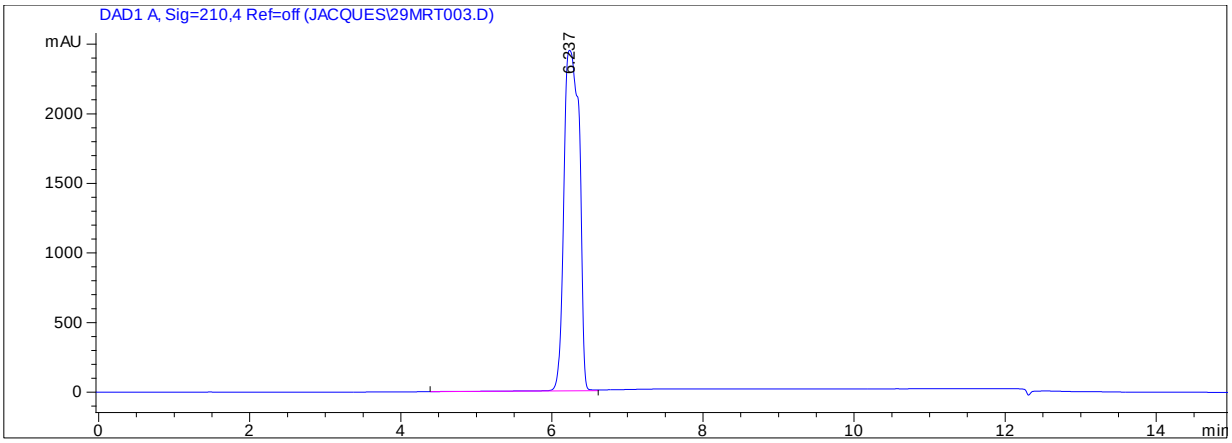

8-(4-Bromophenoxymethyl)caffeine (9)

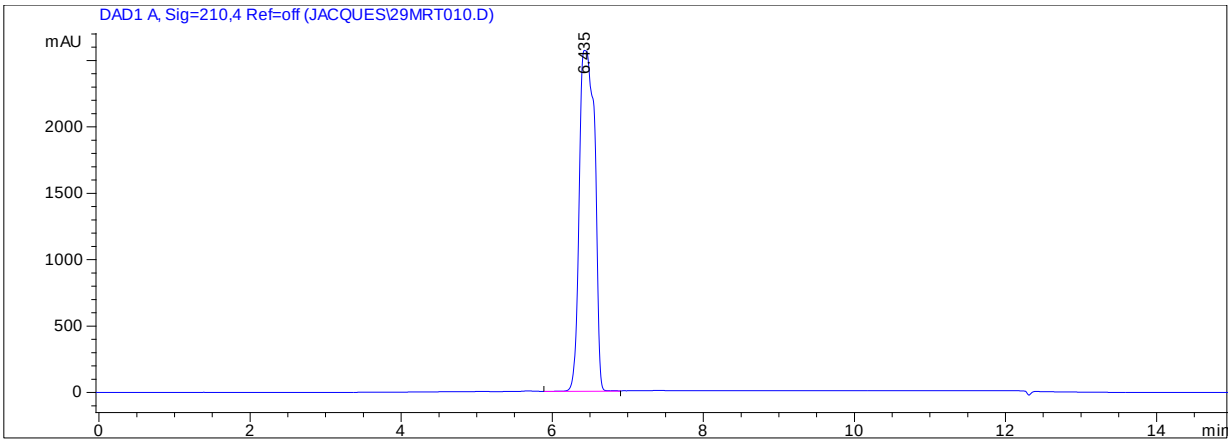

8-(4-Fluorophenoxymethyl)caffeine (10)

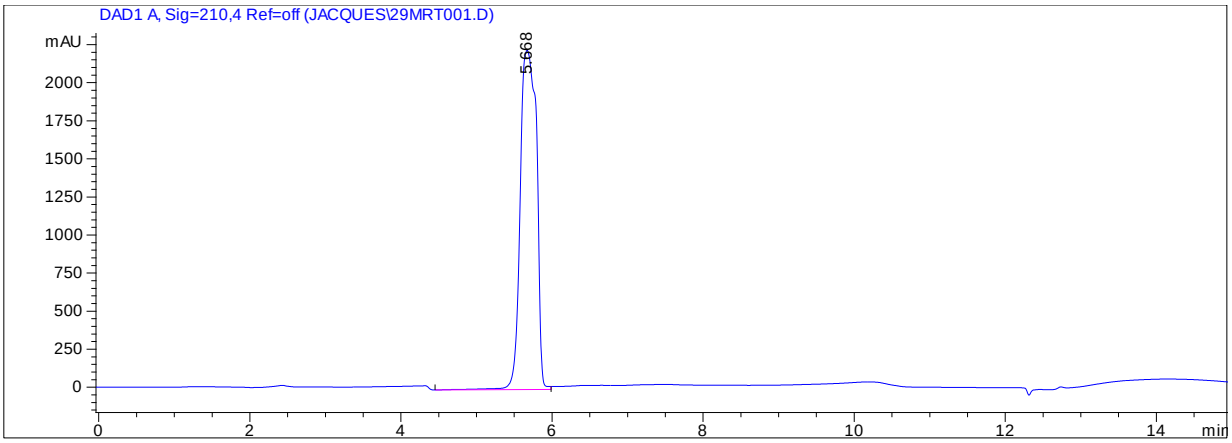

Acetonitrile solvent

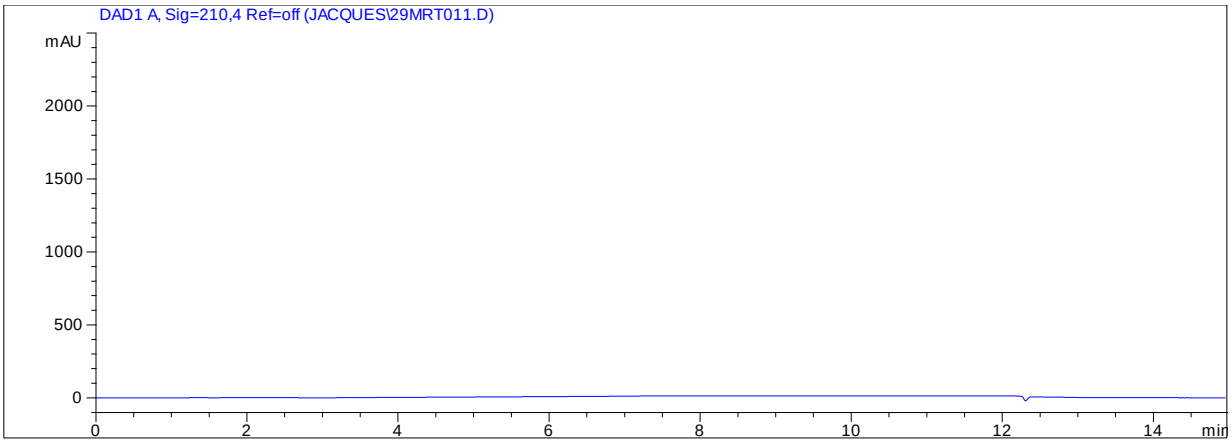

S2: ^{1}H NMR and ^{13}C NMR spectra of the following new/unknown compounds

- 8-Phenoxymethylcaffeine (**1**)
- 8-(3-Chlorophenoxymethyl)caffeine (**2**)
- 8-(3-Bromophenoxymethyl)caffeine (**3**)
- 8-(3-Fluorophenoxymethyl)caffeine (**4**)
- 8-(3-Trifluoromethylphenoxymethyl)caffeine (**5**)
- 8-(3-Methylphenoxymethyl)caffeine (**6**)
- 8-(3-Methoxyphenoxymethyl)caffeine (**7**)
- 8-(4-Chlorophenoxymethyl)caffeine (**8**)
- 8-(4-Bromophenoxymethyl)caffeine (**9**)
- 8-(4-Fluorophenoxymethyl)caffeine (**10**)

Proton (^{1}H) and carbon (^{13}C) NMR spectra were recorded on a Bruker Avance III 600 spectrometer at frequencies of 600 MHz and 150 MHz, respectively. All NMR measurements were conducted in $CDCl_3$.

^{1}H-NMR and ^{13}C-NMR

8-Phenoxymethylcaffeine (1)

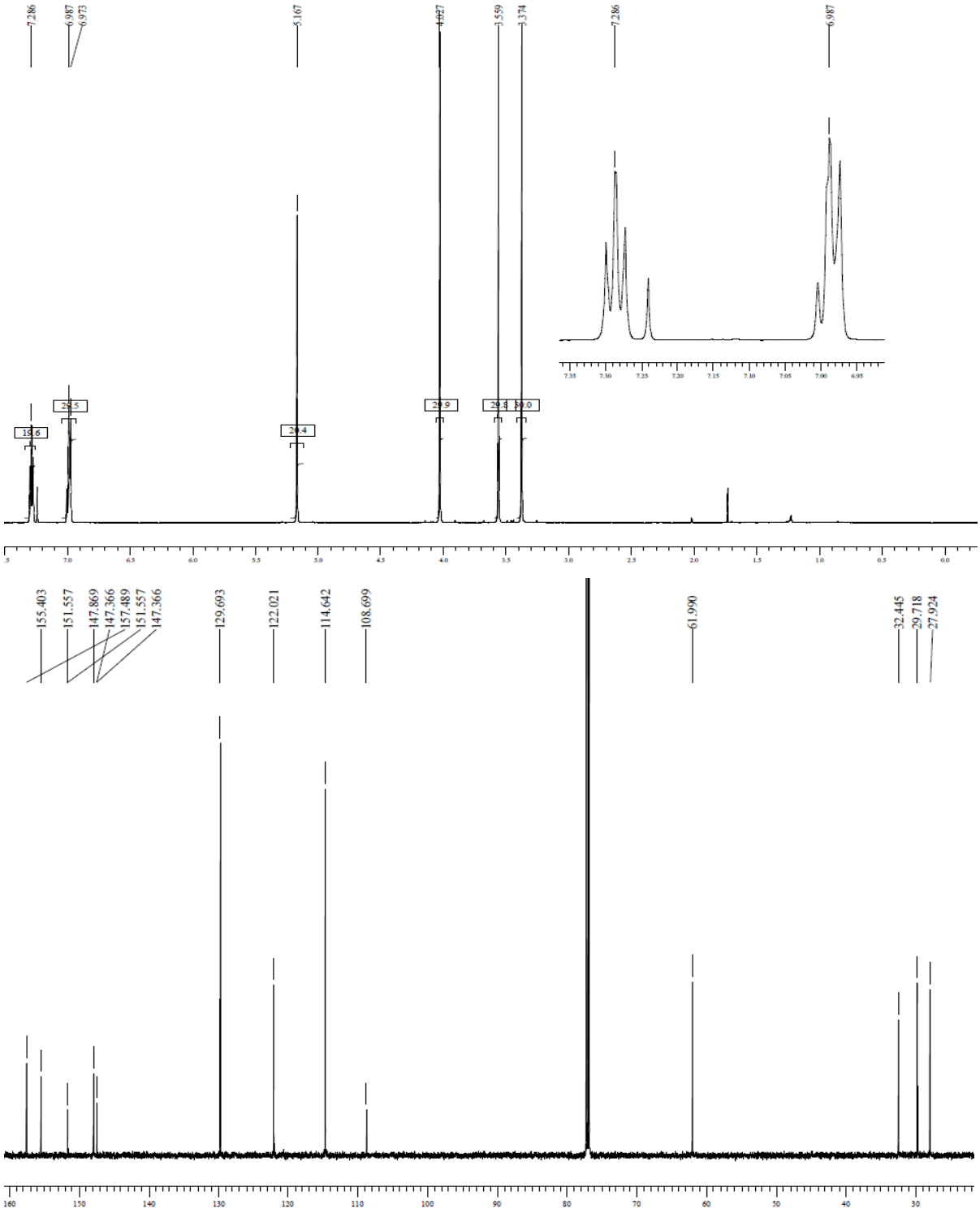

^{1}H-NMR and ^{13}C-NMR

8-(3-Chlorophenoxymethyl)caffeine (2)

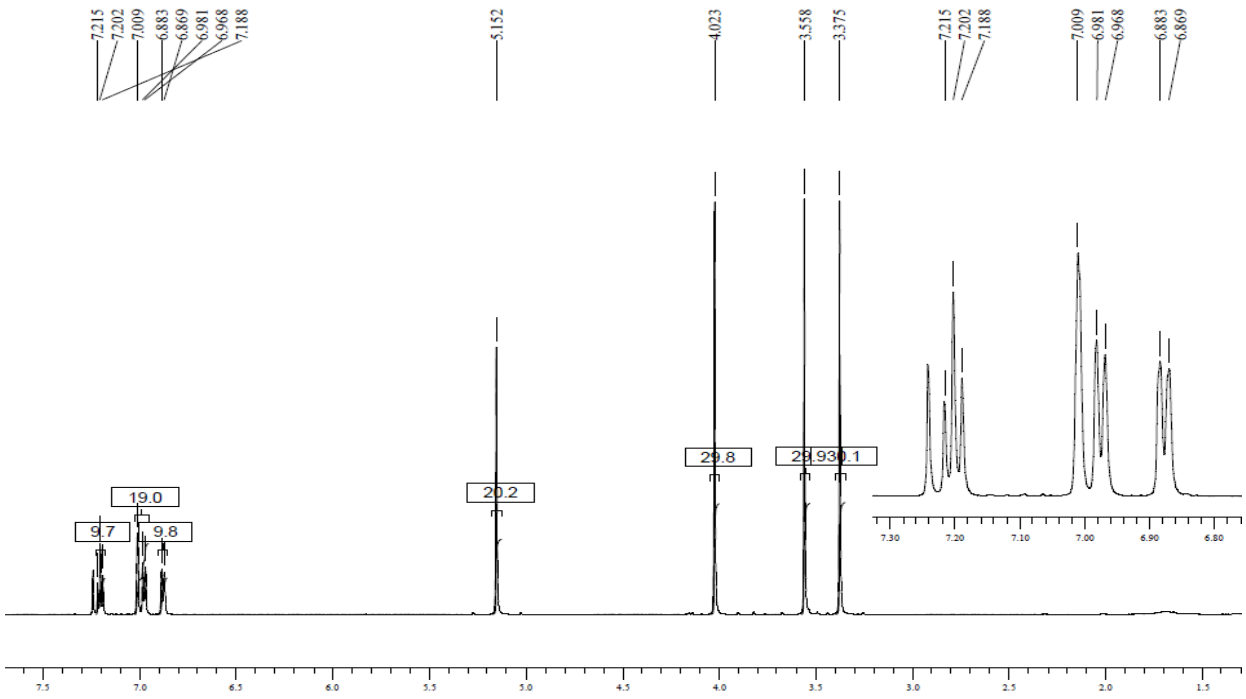

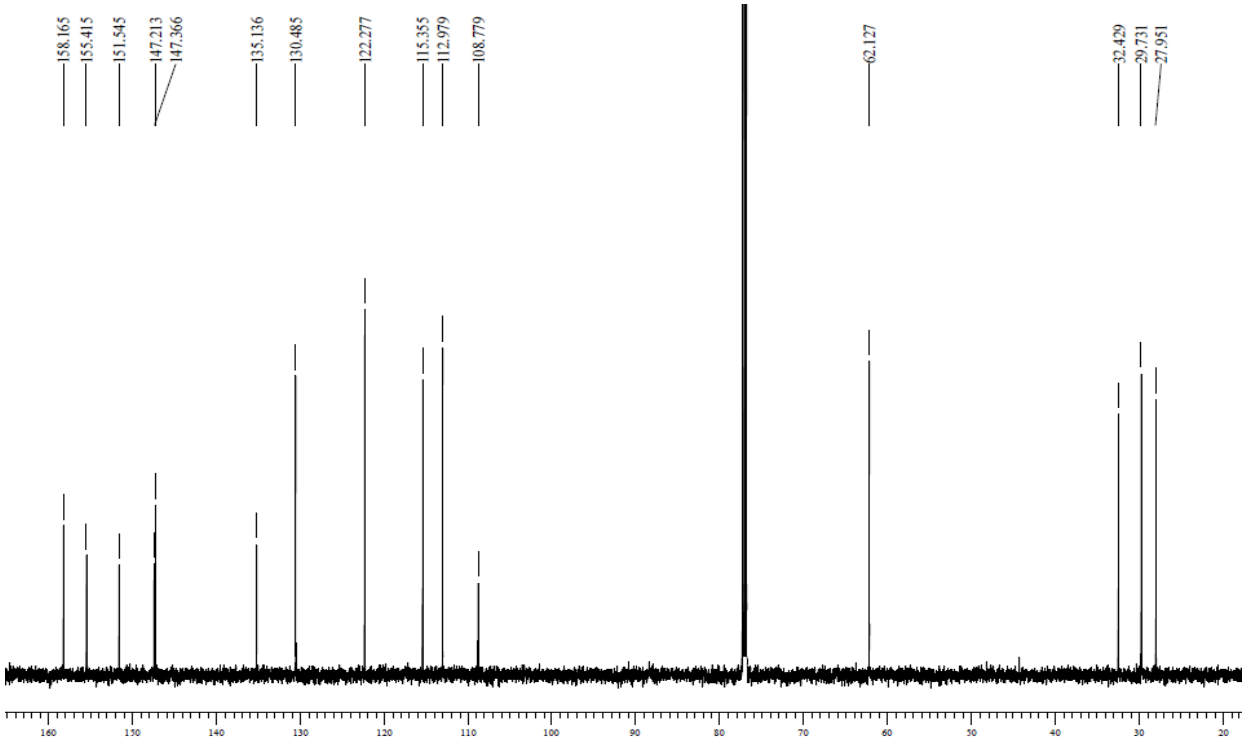

^{1}H-NMR and ^{13}C-NMR

8-(3-Bromophenoxymethyl)caffeine (3)

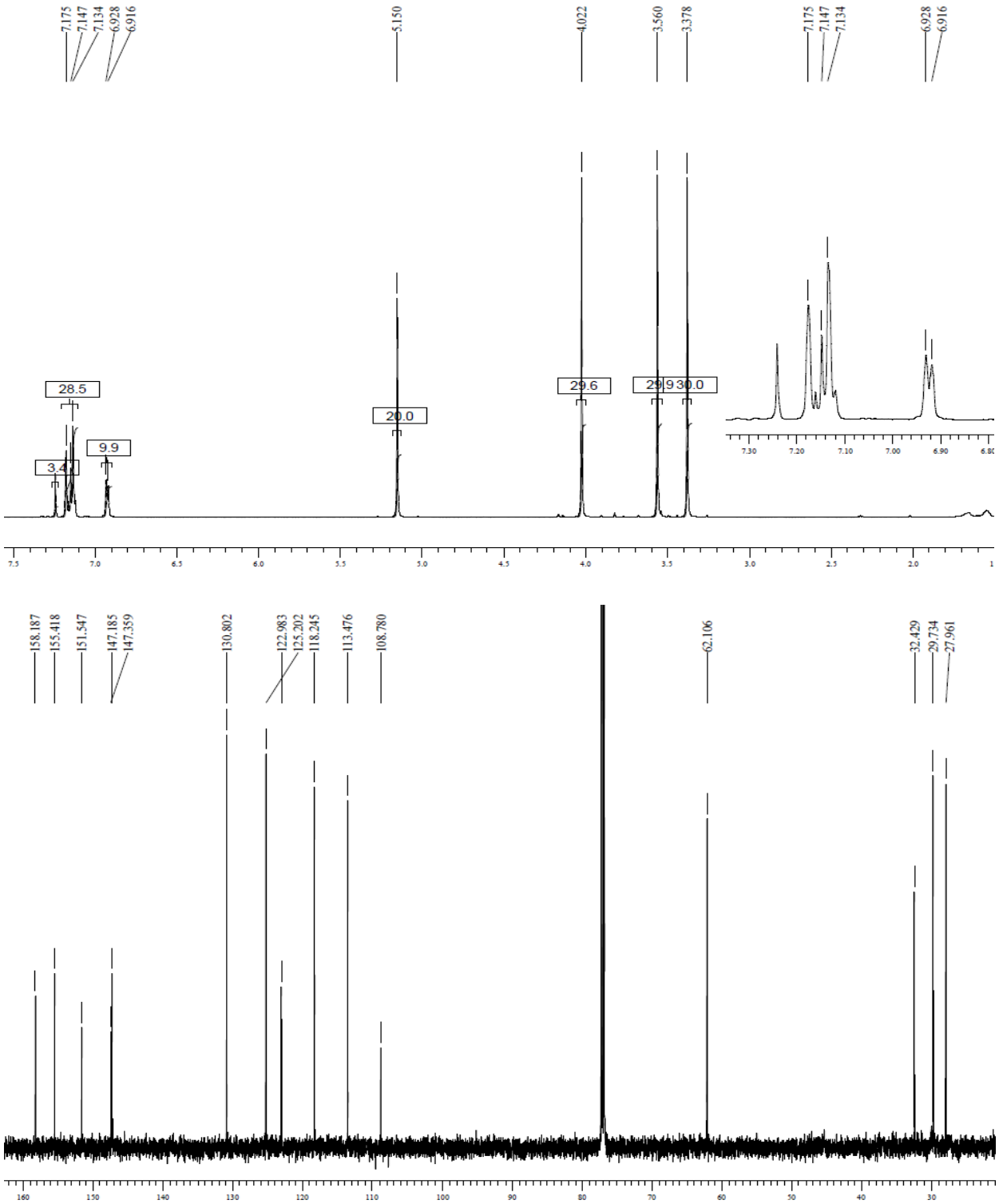

^{1}H-NMR and ^{13}C-NMR

8-(3-Fluorophenoxymethyl)caffeine (4)

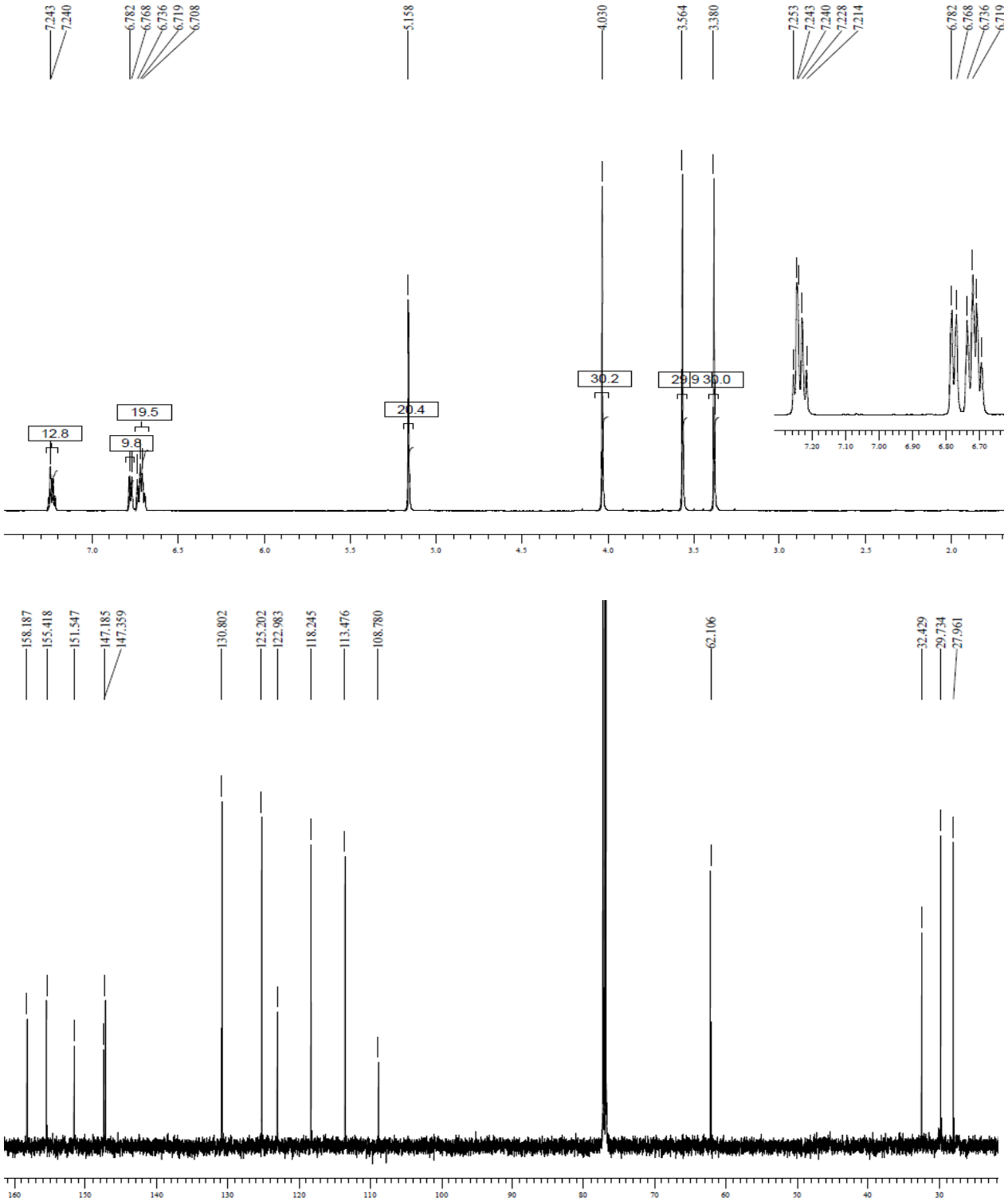

^{1}H-NMR and ^{13}C-NMR

8-(3-Trifluorophenoxymethyl)caffeine (5)

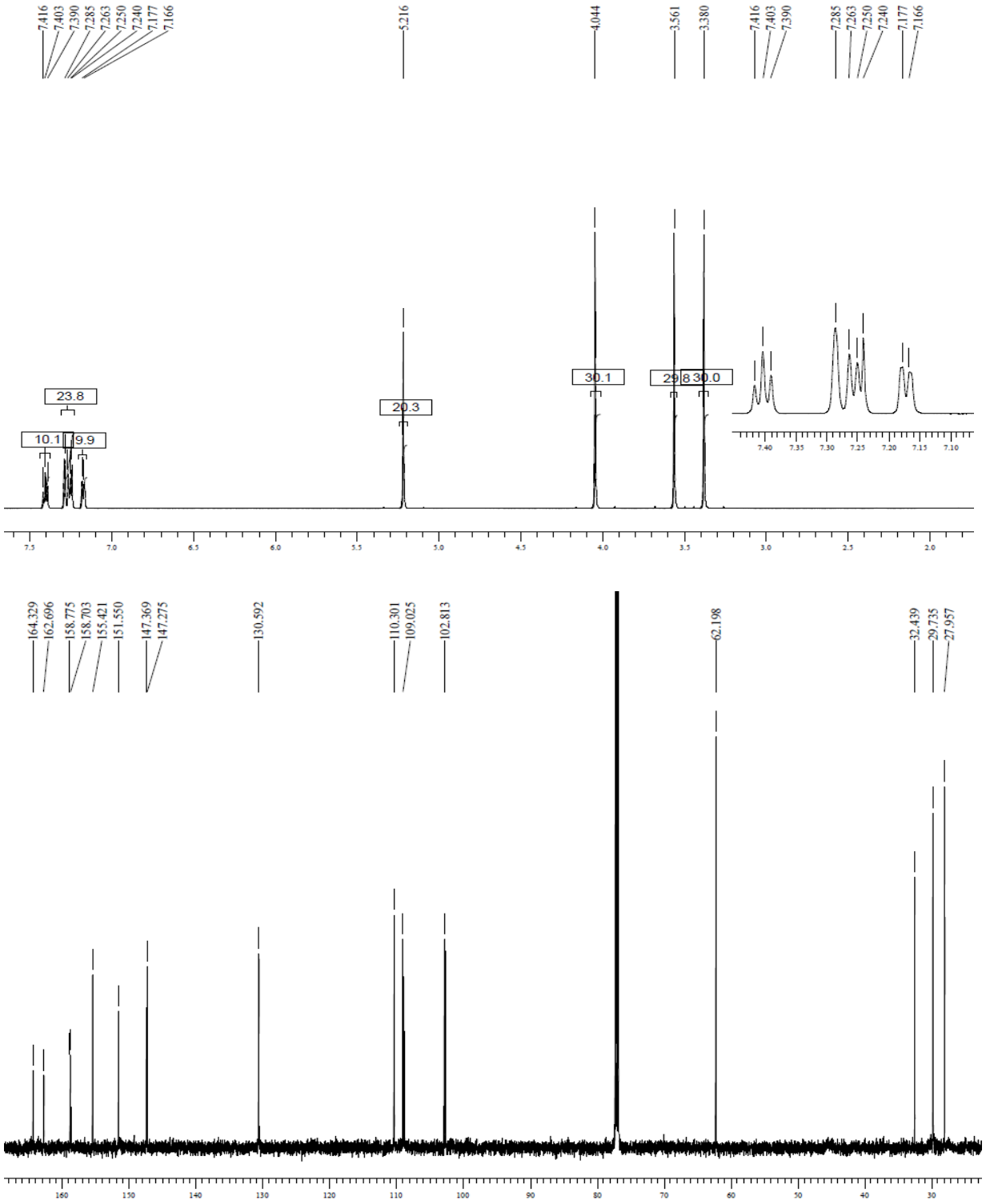

^{1}H-NMR and ^{13}C-NMR

8-(3-Methylphenoxymethyl)caffeine (6)

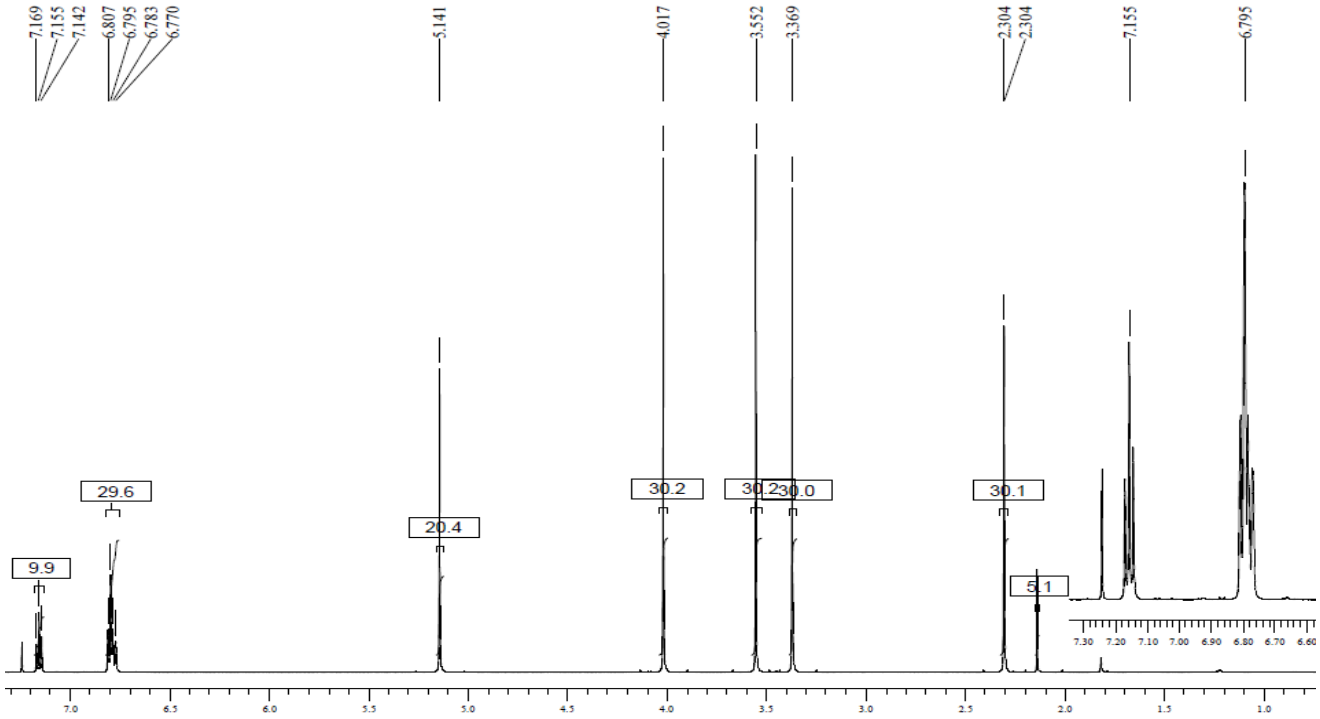

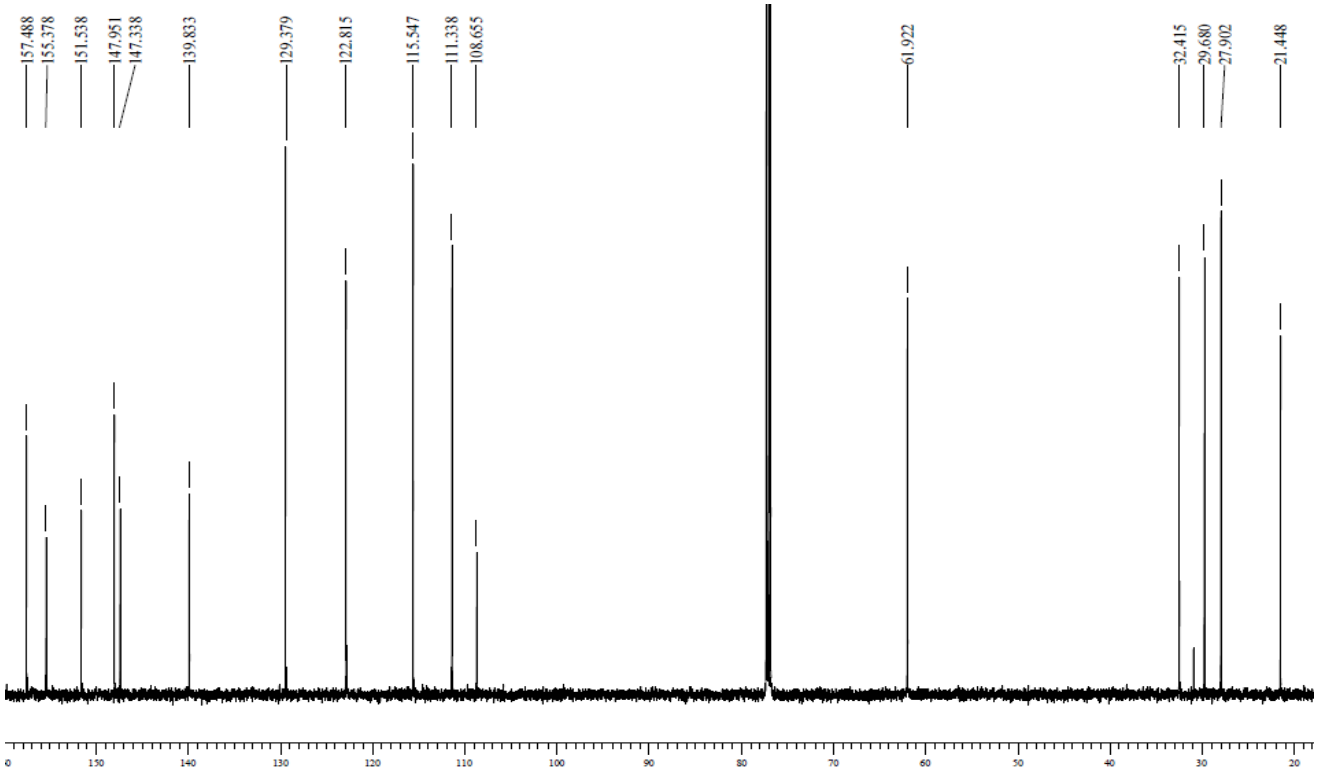

^{1}H-NMR and ^{13}C-NMR

8-(3-Methoxyphenoxymethyl)caffeine (7)

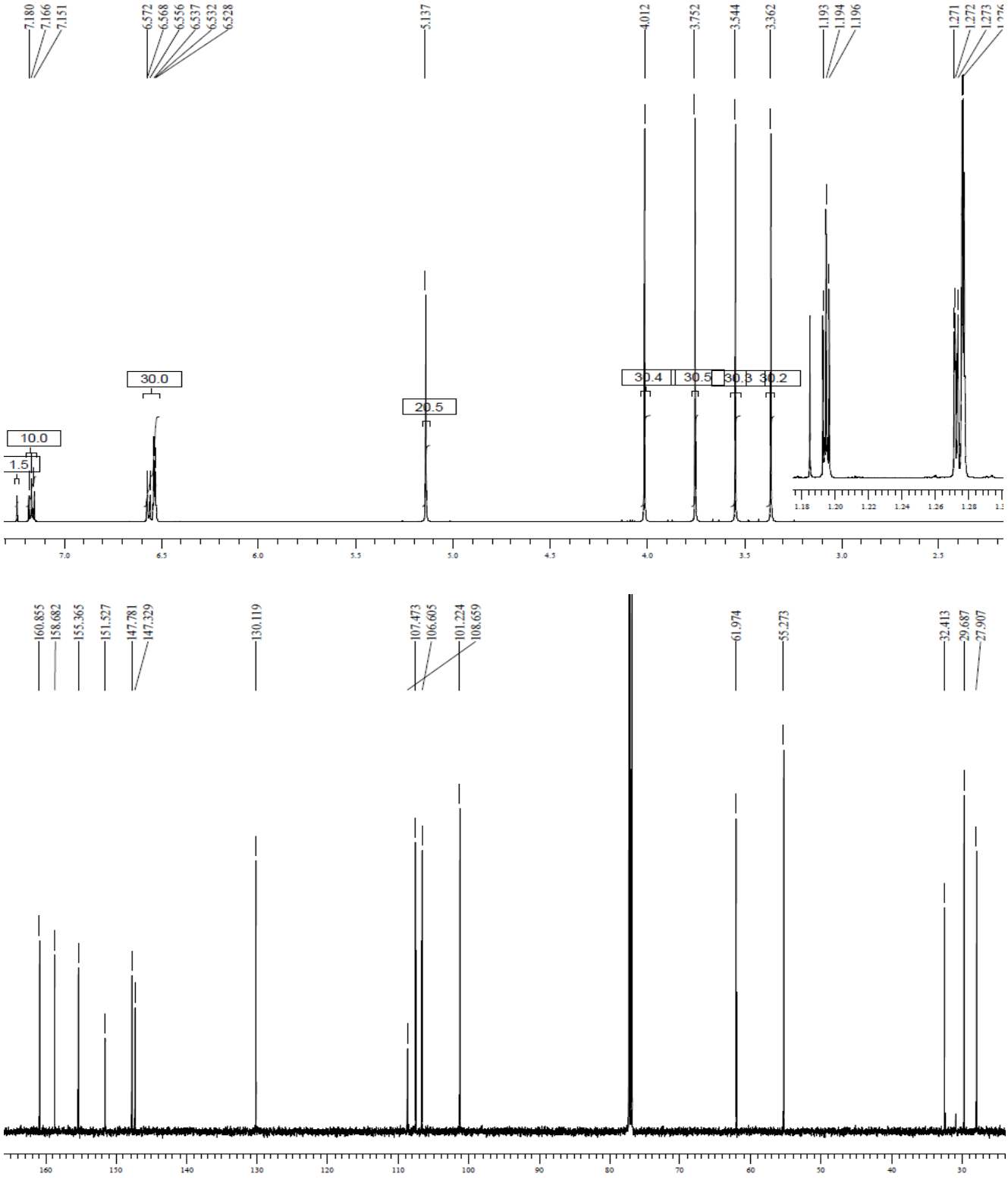

^{1}H-NMR and ^{13}C-NMR

8-(4-Chlorophenoxymethyl)caffeine (8)

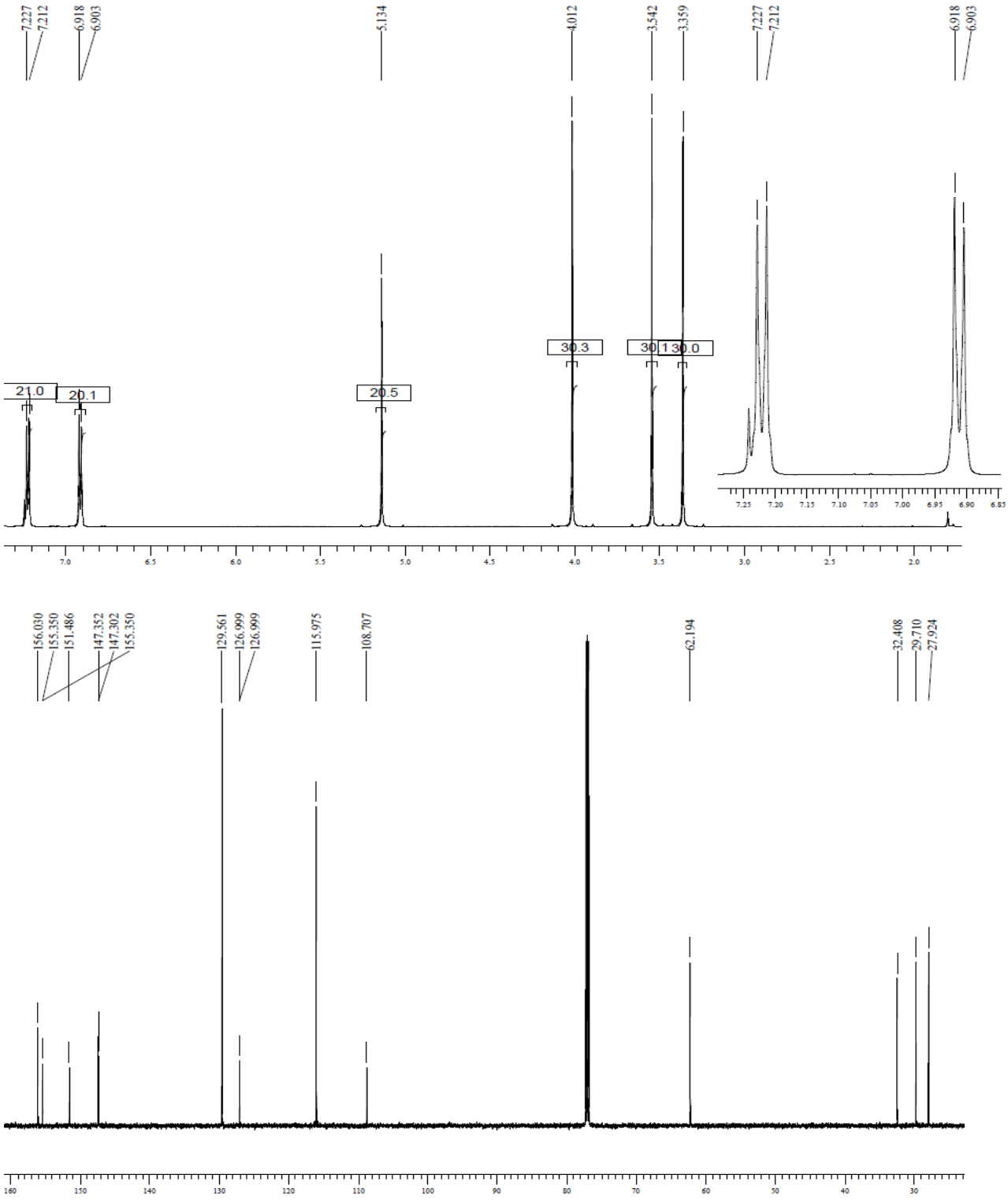

^{1}H-NMR and ^{13}C-NMR

8-(4-Bromophenoxymethyl)caffeine (9)

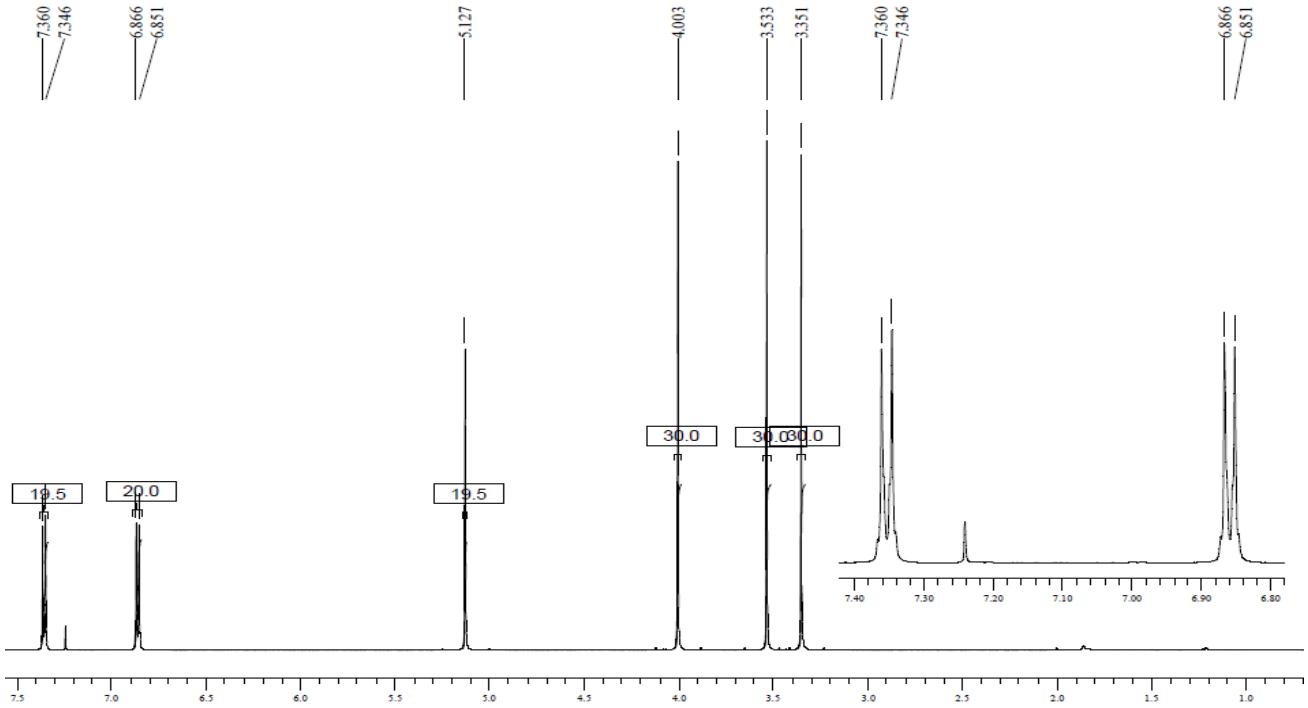

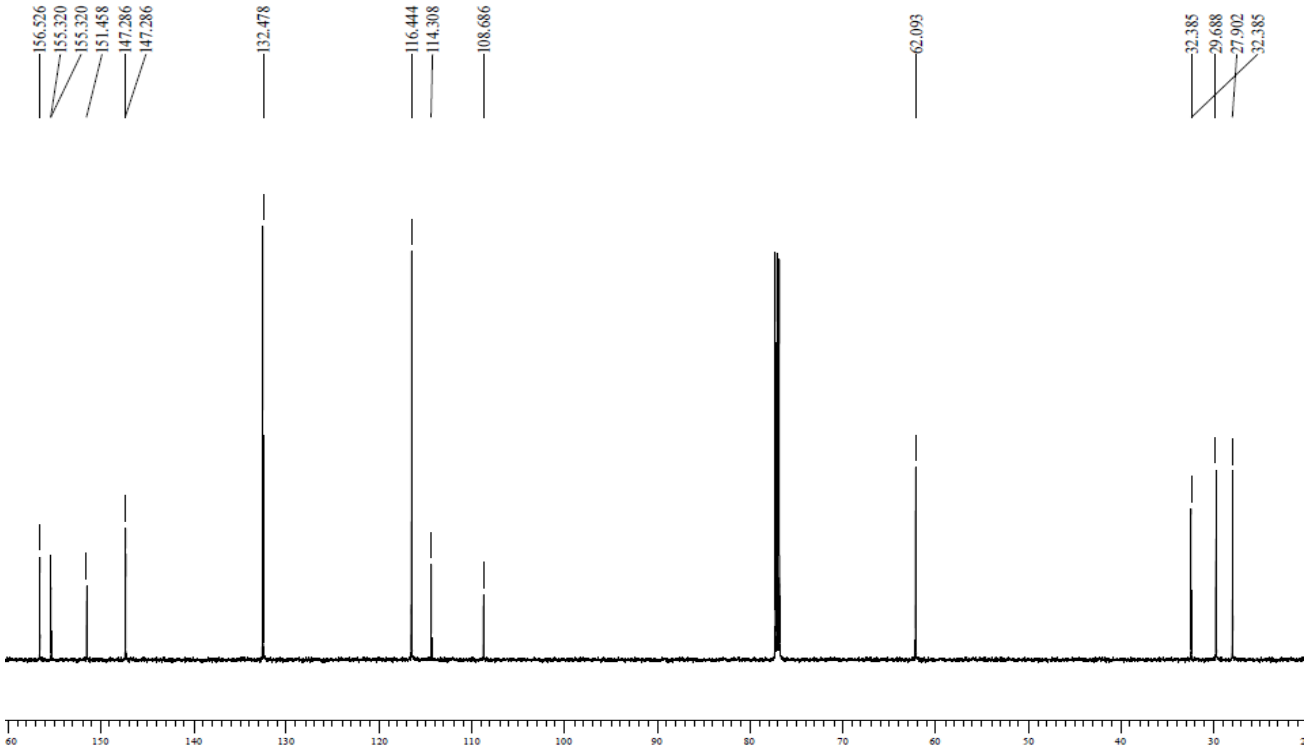

^{1}H-NMR and ^{13}C-NMR

8-(4-Fluorophenoxymethyl)caffeine (10)

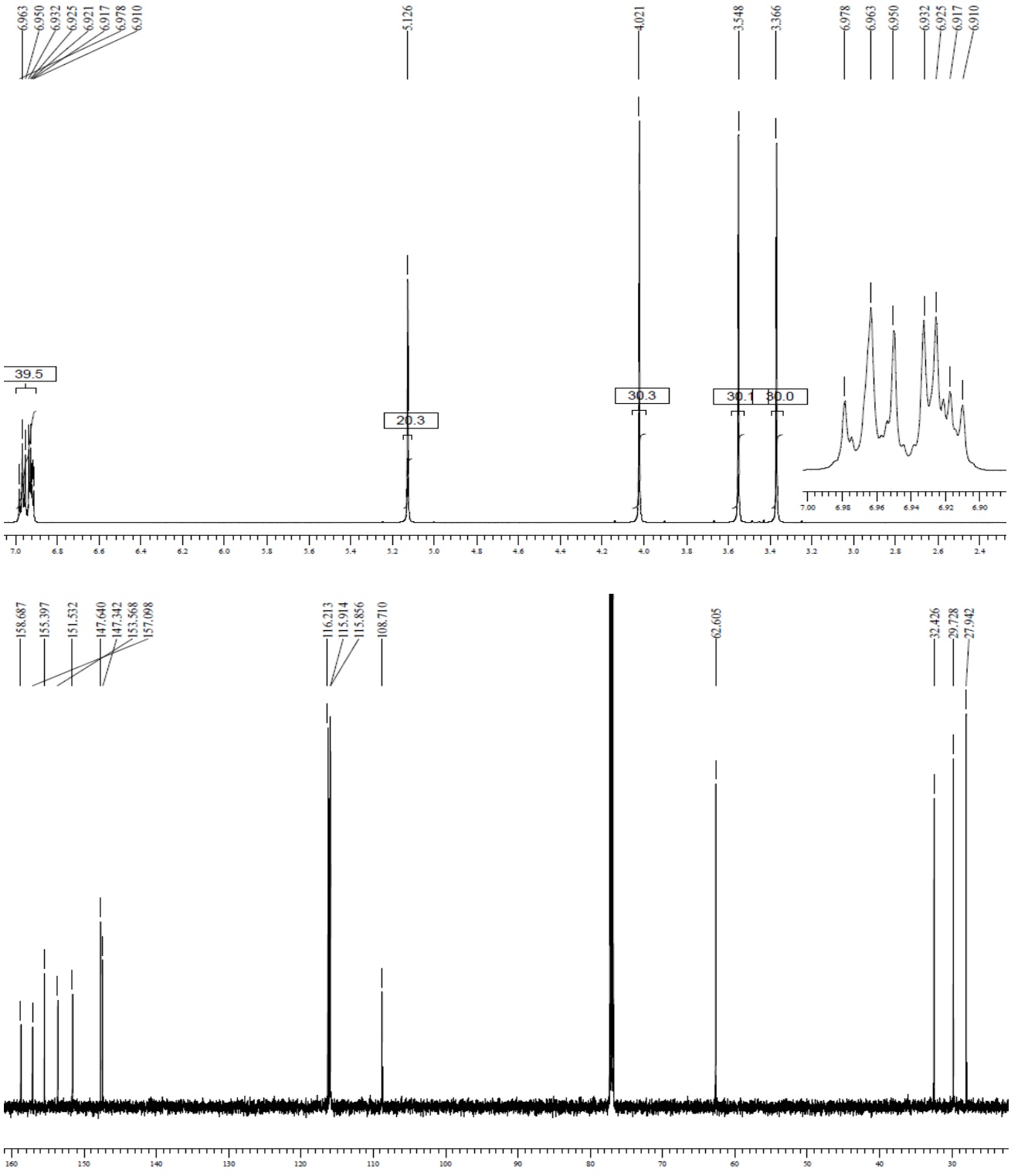

S3: Mass spectra of the following new/unknown compounds

- 8-Phenoxymethylcaffeine (**1**)
- 8-(3-Chlorophenoxymethyl)caffeine (**2**)
- 8-(3-Bromophenoxymethyl)caffeine (**3**)
- 8-(3-Fluorophenoxymethyl)caffeine (**4**)
- 8-(3-Trifluoromethylphenoxymethyl)caffeine (**5**)
- 8-(3-Methylphenoxymethyl)caffeine (**6**)
- 8-(3-Methoxyphenoxymethyl)caffeine (**7**)
- 8-(4-Chlorophenoxymethyl)caffeine (**8**)
- 8-(4-Bromophenoxymethyl)caffeine (**9**)
- 8-(4-Fluorophenoxymethyl)caffeine (**10**)

8-Phenoxymethylcaffeine (1)

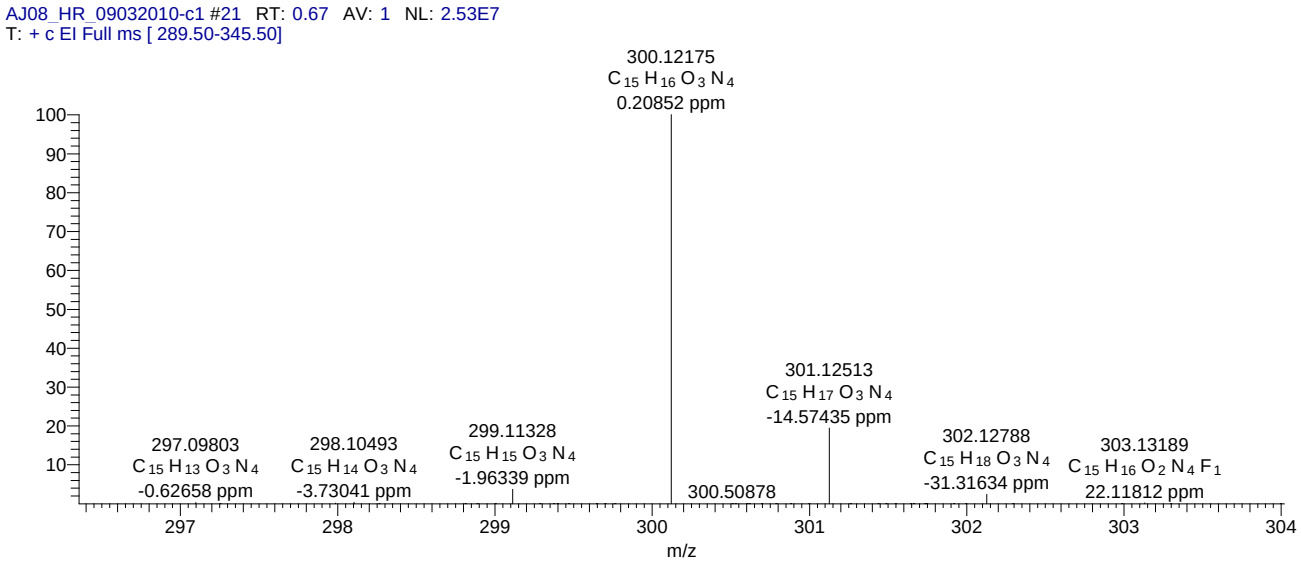

8-(3-Chlorophenoxymethyl)caffeine (2)

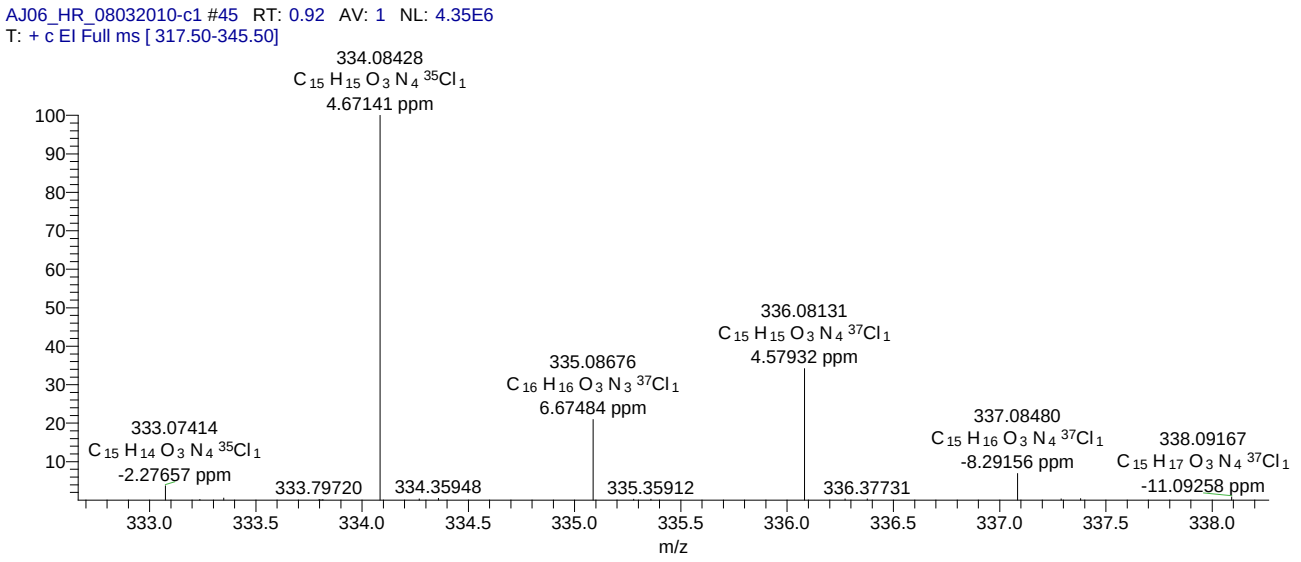

8-(3-Bromophenoxymethyl)caffeine (3)

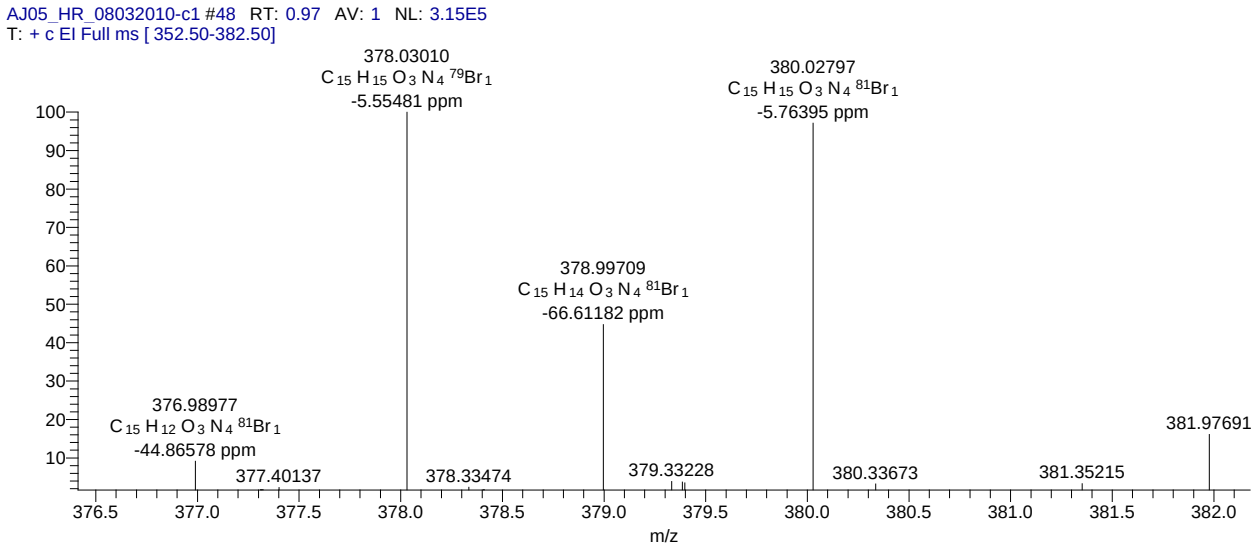

8-(3-Fluorophenoxymethyl)caffeine (4)

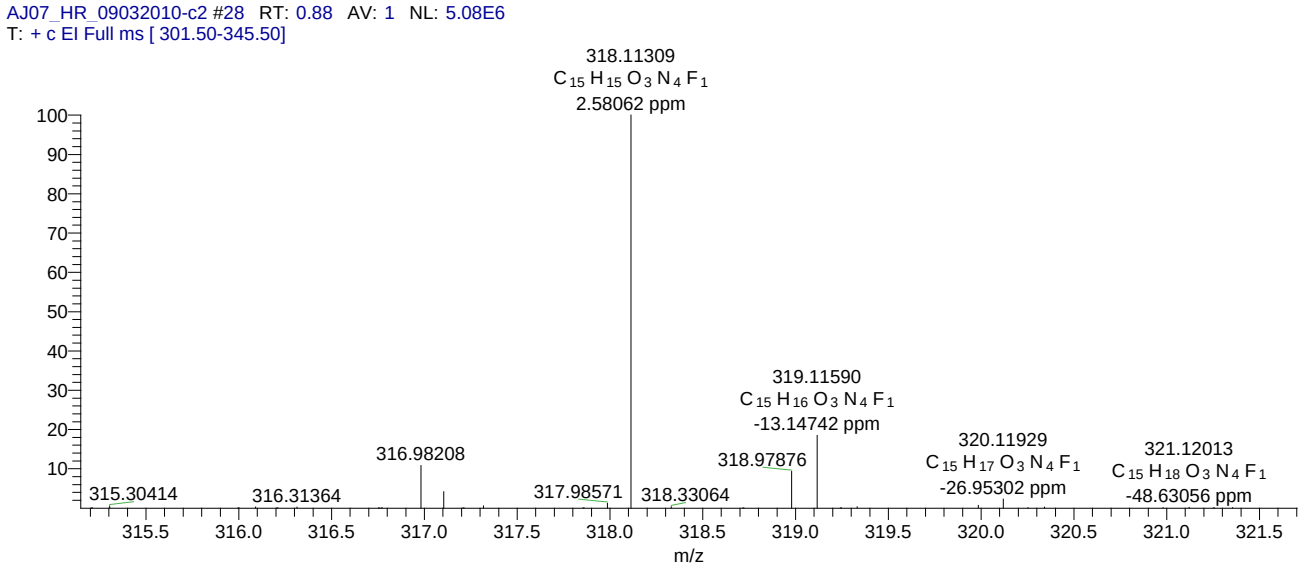

8-(3-Trifluoromethylphenoxymethyl)caffeine (5)

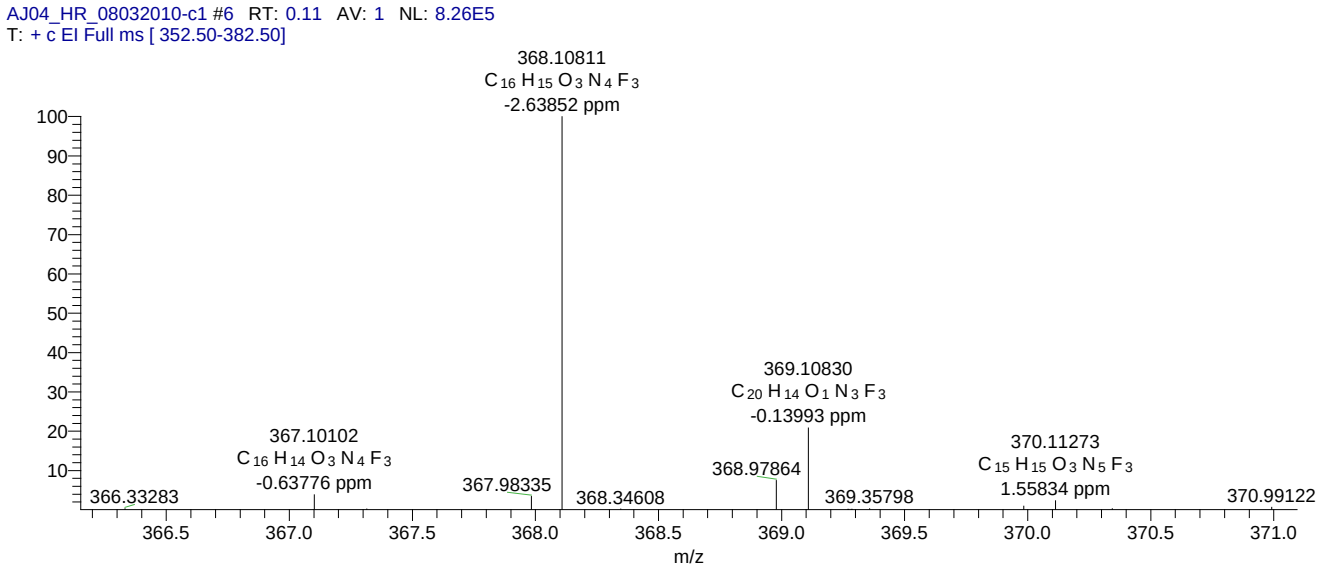

8-(3-Methylphenoxymethyl)caffeine (6)

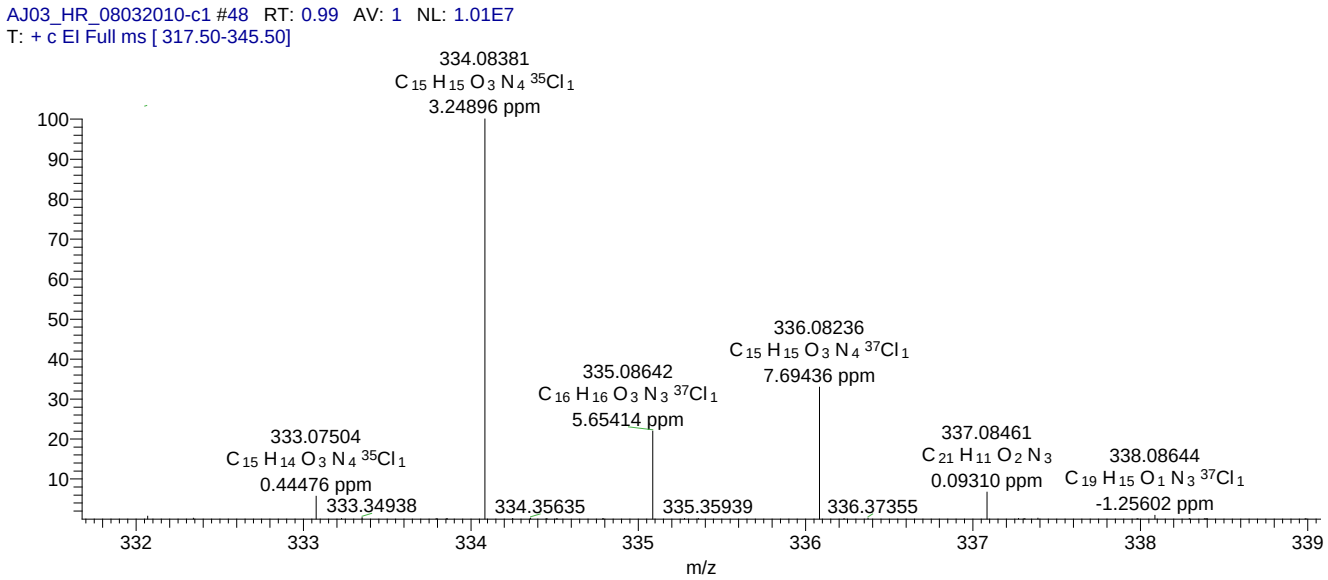

8-(3-Methoxyphenoxymethyl)caffeine (7)

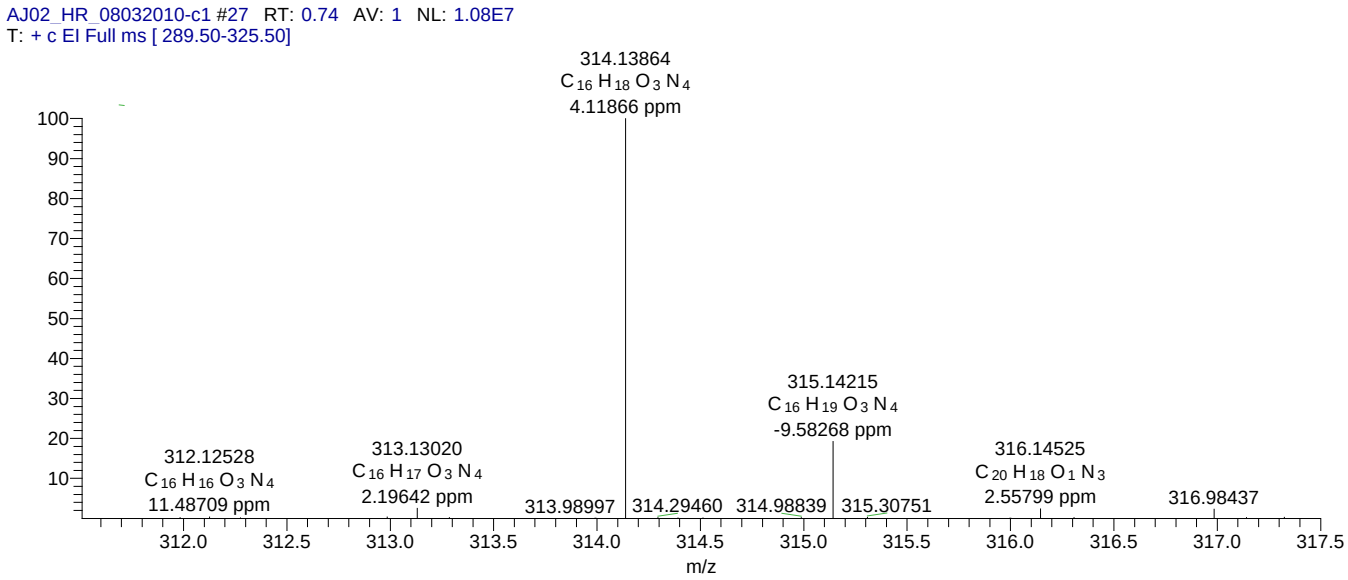

8-(4-Chlorophenoxymethyl)caffeine (8)

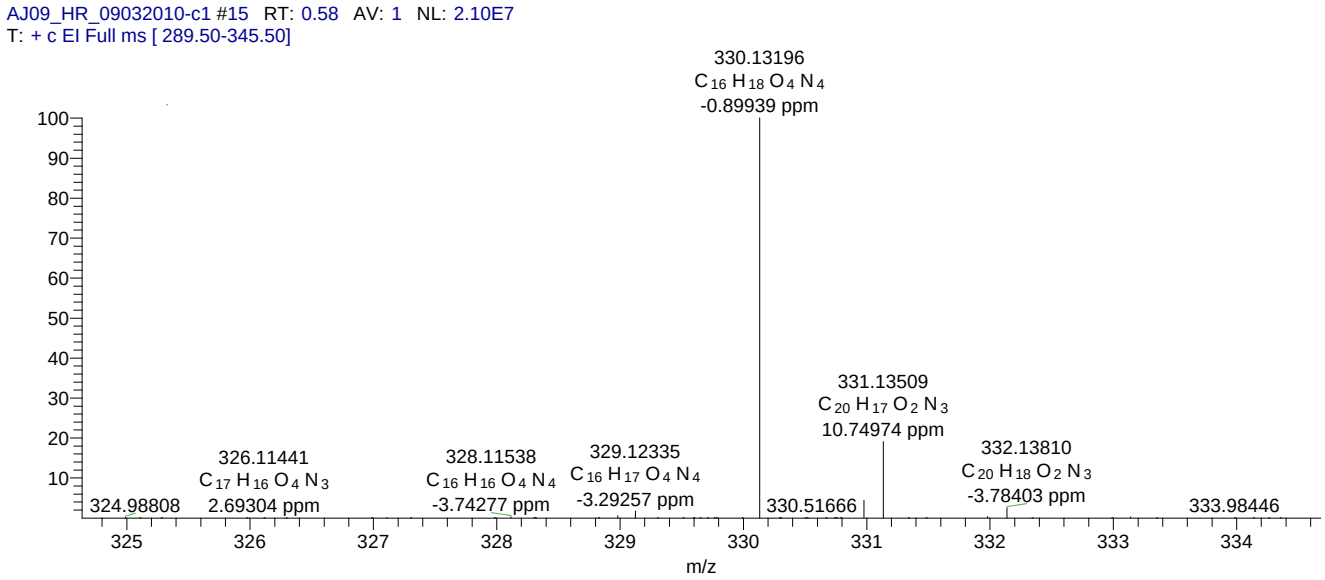

8-(4-Bromophenoxymethyl)caffeine (9)

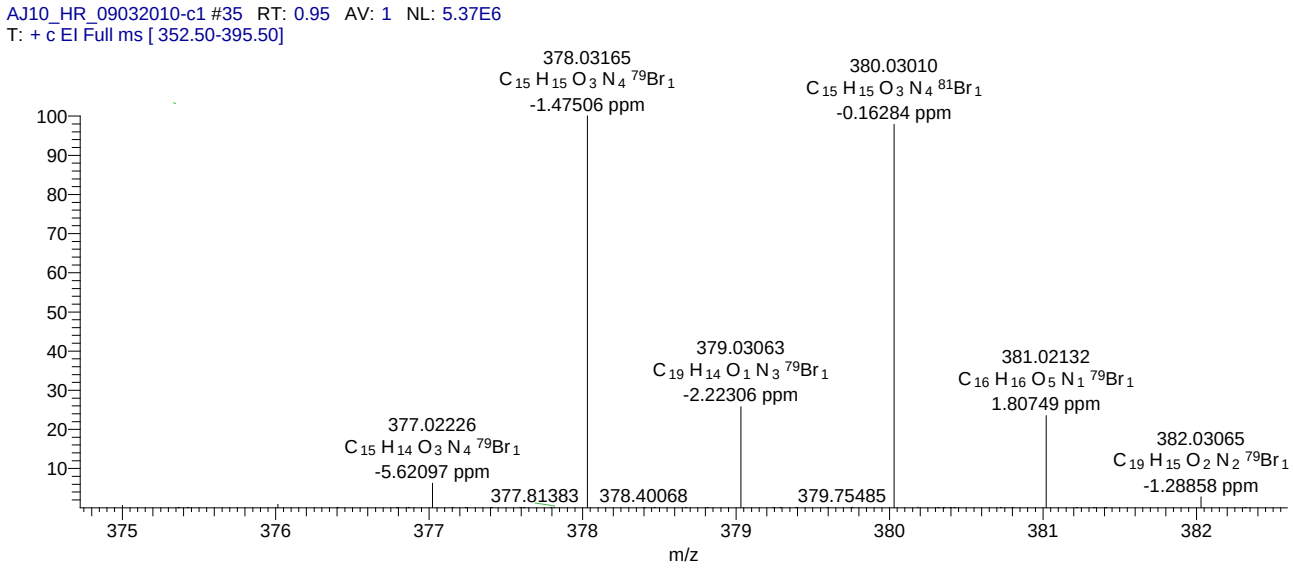

8-(4-Fluorophenoxymethyl)caffeine (10)

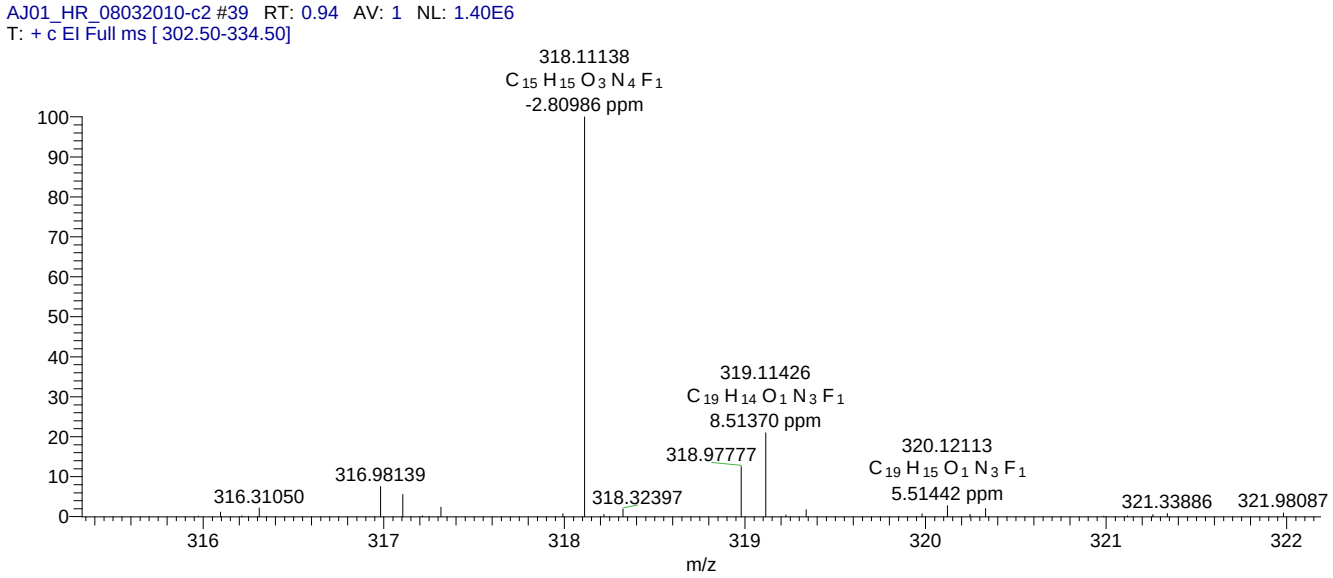

ACKNOWLEGMENTS

This study was carried out at the Department of Pharmaceutical Chemistry, North-West University, Potchefstroom campus.

I would like to express my gratitude to the following people and organizations:

- My Lord and Saviour for the ability and talents He gave me.
- My parents for their financial and moral support.
- My supervisor, Prof Jacques Petzer for all the support, encouragement and late hours.
- Prof. Kobus Bergh for the helping hand when needed.
- Andre Joubert for the NMR experiments and Wits University for the MS measurements.
- All the people in the MAO functional group, for all the help and assistance during all the experimental and enzymology work.
- NRF for the bursaries.